THE INFLUENCE OF SPATIAL VARIABILITY OF HYDROLOGIC PARAMETERS ON SIMULATED OVERLAND FLOW HYDROGRAPHS

LIBRARIES
SEP 1 1989
COLORADO STATE UNIVERSITY

P.Y. Julien and G.E. Moglen

Center for Geosciences

Hydrologic Modeling Group

Colorado State University

CER89-90PYJ-GEM-1

July 1989

THE INFLUENCE OF SPATIAL VARIABILITY OF HYDROLOGIC PARAMETERS ON SIMULATED OVERLAND FLOW HYDROGRAPHS

P.Y. Julien and G.E. Moglen

Center for Geosciences

Hydrologic Modeling Group

Colorado State University

CER89-90PYJ-GEM-1

July 1989

U18401 0077740

FOLIO
TA7
.C6
CER-89/90-1

TABLE OF CONTENTS

COLORADO STATE UNIVERSITY
Fort Collins, Colorado 80523

LIST OF TABLES

TABLE OF FIGURES

LIST OF SYMBOLS

Symbol	Definition
C_v	coefficient of variation
F_r	Froude number
g	gravitational acceleration
h	depth of flow
$\dot{h}$	derivative of depth with respect to time
δh	variation in depth, h, used in the finite element formulation
i	excess rainfall intensity
$\bar{i}$	spatially averaged excess rainfall intensity
j	the j^{th} element of an array
k	parameter used to determine the appropriateness of the kinematic wave approximation
L	length of the overland flow plane
L_g	maximum grid spacing to achieve complete equilibrium within each grid
ΔL	change in horizontal distance along an overland flow plane
m	number of elements in an array
N	the shape function used in the finite element formulation
n	Manning coefficient
$\bar{n}$	average Manning coefficient
q	unit discharge
$q_{k,t}$	the k^{th} perturbed discharge at time t
$q_{np,t}$	the non-perturbed discharge at time t
$R_{s,l}$	relative sensitivity of parameter l

List of Symbols - continued

Symbol	Definition
$\overline{S}$	average slope
S_f	friction slope
S_o	bed slope
t	time
t_d	time at which the discharge hydrograph begins to decline
t_e	time to equilibrium
t_r	duration of rainfall
u	local coordinate system in finite element formulation
v	flow velocity
V	volume of the input excess rainfall
ΔV	volume of the hydrograph envelope for variation ϕ
V^*	ratio of hydrograph envelope volume to excess rainfall volume
X	any arbitrary parameter
x	distance measured along flow plane
Z_j	elevation at node j
α	coefficient of the stage-discharge relationship
β	exponent of the stage-discharge relationship
ϵ	safety factor used to determine L_g
μ	mean of an array of elements
ϕ	model input parameter which determines the maximum node to node variation
σ	standard deviation of an array of elements
σ_t	deviation of discharges at time, t

CHAPTER 1 - INTRODUCTION

Overland flow modeling requires information about numerous hydrologic parameters. Among those parameters most important to simulating overland flow are topography; surface roughness; and the distribution, duration, and intensity of precipitation. These parameters vary continuously in space and, in the case of precipitation, in time as well. Frequently, data describing this variation is scarce or non-existent. Furthermore, hydrologic models tend to simplify the system being modeled, choosing a single value to represent an areal average of a given parameter. As a consequence, hydrologic models are unable to account for variation of input parameter values within a system. The resulting output, therefore, fails to reflect the effects of spatial variability in the input. It would be useful to know what the differences between a constant and a spatially varied system are, and to know under what conditions these differences are large or are negligibly small.

The objectives of this report are to investigate the effects of spatial variability on overland flow hydrographs. Specific areas of interest include:

- Analysis of the differences in model response for the cases of partial and complete equilibrium.
- Comparison of the relative influence of the four spatially varying quantities: slope, Manning's "n", width, and rainfall intensity, on the overland flow discharge.
- Provision of a procedure based upon the results which will be used to determine a grid spacing. This grid spacing will sufficiently describe spatial variability within a system such that error due to spatial variability in a parameter is small.

These objectives will be met by simulating overland flow for several different sets of statistically similar, spatially varied systems. Each set will be characterized by a particular parameter or set of parameters which have been spatially varied. The output from the model, discharge hydrographs, will be used to illustrate the effects of that set of perturbed parameters on the simulated discharge. In all simulations, CASC, an overland flow model capable of handling spatial variability will be used. Use of this model is described extensively in CER 87-88 GEO7, *CASC User's Manual - A Finite Element Model for Spatially Varied Overland Flow Hydrographs*.

The format of this report is as follows. Chapter 2 presents a literature review and background material on overland flow fundamentals. Chapter 3 presents single parameter analyses of the effects of random parameter variation on the discharge hydrograph. This chapter delineates the procedure used to randomly vary the input parameters and the methods developed to quantify the variation in output. Chapter 4 will illustrate some direct applications which follow from the results of these analyses. Chapter 5 will summarize the findings and present conclusions. Following Chapter 5 is a list of references used in various aspects of this research. The appendices provide source code (model routines, control code, and postprocessors) and tabulated output data (appearing in graphical form throughout the text).

CHAPTER 2 - BACKGROUND

Section 2.1 - LITERATURE REVIEW

The literature review presented here is in four subsections. The first subsection, Hydraulics, details some of the literature associated with the fundamentals of overland flow. Section 2.1.2, Numerical Methods, presents a review of some of the available numerical techniques for modeling overland flow. Section 2.1.3, Modeling Spatial Variability, reviews some of the literature involving case studies investigating effects of spatially varied overland flow parameters. Section 2.1.4, Examining Variability in Discharge, presents a number of studies which consider the fluctuations in discharge that may be expected to result from variations in the input parameters.

The intention of this review is to present a concise overview of the current literature and to place the work presented here in its appropriate context.

2.1.1 - Hydraulics

The governing equations for overland flow are St-Venant's momentum and continuity equations. Derivations of these equations may be found in numerous texts. Eagleson (1970) and Lighthill and Whitham (1955) are two good sources for these derivations. The St-Venant equations which account for unsteady, non-uniform flow may be simplified (see Woolhiser and Liggett, 1967) to the kinematic wave approximation which is applicable when k is greater than approximately 20. Where:

$$k = \frac{S_o L}{h F_r^2} \qquad (2.1)$$

where S_o is the bed slope, L is the length of the plane, h is the normal flow depth, and F_r is the Froude number. For a wide range of unsteady free surface flow problems k is large, and therefore, the kinematic wave approximation is valid. Iwagaki (1955) was the first to use the kinematic wave approximation incorporating a continuous lateral inflow. He used the approximation to examine overland flow and streamflow hydrographs in greater detail. The recent studies of spatially varied overland flow by Richardson (1989) indicate that, while the kinematic wave approximation is quite valid under a wide range of applications, the order of significance of the remaining terms of the St-Venant equation is actually reversed from the commonly accepted order for open channel flow.

2.1.2 - Numerical Methods

The modeling of overland flow by numerical techniques has evolved considerably as digital computers have become faster and more common. Originally, the method of characteristics was used to find "the space-time locus of discontinuity in the partial derivatives" (Eagleson, 1970). This method graphically shows the location at which one may expect changes in the value of a partial derivative. A clear discussion of this method may be found in Crandall (1956).

Liggett and Woolhiser (1967) present an extensive analysis of several finite difference schemes applied to the shallow-water equations (i.e. overland flow). These schemes were analyzed for stability, accuracy, and ease of applicability. Their conclusions found both a characteristic scheme and an implicit scheme to work favorably. The strengths and weaknesses of each scheme were demonstrated and discussed.

Kibler and Woolhiser (1970) compared the results from three different schemes: an upstream differencing scheme, a four point implicit scheme, and the Lax-Wendroff explicit scheme, with the results given from the method of characteristics. Their findings indicated the

Lax-Wendroff method yielded the most satisfactory results. Advantages of finite difference algorithms are their ease of programming and conceptual simplicity. However, depending upon the conditions and the method used, failure to converge or oscillation may occur.

The finite element method is the newest numerical technique available to solve the equations of overland flow. Julien et al. (1988) present the fundamentals of the application of this method to solving the kinematic wave approximation to overland flow. A strong advantage of this method is that it allows complex boundary conditions to be handled easily.

2.1.3 - Modeling Spatial Variability

Spatially variability of overland flow parameters is a significant consideration when modeling overland flow. Kibler and Woolhiser (1970) used a kinematic cascade of planes to examine the effect of the spatial distribution of slope on the rising limb of the discharge hydrograph. Their results showed that the shape of the rising limb of the hydrographs were similar to the shapes of the slope profiles. They also examined the effects of varying the width of the flow plane using a converging conical surface. The results were used to verify their model.

Wu et al. (1978) investigated the effects of the spatial distribution of surface roughness on runoff hydrographs. Their investigation involved spatial distributions of two different types of roughness elements in either the flow direction or the transverse direction. Their objective was to quantify the effects of the different spatially distributed systems and develop criteria indicating when varied parameter values may be validly lumped together. Their results showed that for nonuniform roughness in the direction of flow, the lumped parameters could,

> *... be estimated by selecting the values of parameters which can reproduce the equilibrium detention storage equivalent to the equilibrium detention storage produced by the watershed with nonuniform roughness.* [For] *non-uniform roughness in the transverse direction, the hydrographs can be simulated by combining the hydrographs produced by the individual elements.*

Different spatial distributions of the same rainfall pattern have been shown to produce different discharge patterns. Investigations regarding the spatial distribution of rainfall often take the form of a probable maximum storm (PMS) analysis. Shalaby (1989) demonstrated the procedure used to determine the location, orientation, duration, and magnitude of the storm which will generate the probable maximum flood (PMF) for a given watershed. In PMF calculations the isohyetal pattern recommended by the National Weather Service (1982) depends on the geographic location of the watershed in question. As of 1980, five different isohyetal patterns were used for determination of the PMF in the U.S. The isohyetal pattern shows the spatial distribution of the PMS with the intensity diminishing in elliptical isohyets from the storm center to the storm fringes.

Another analysis involving the spatial distribution of rainfall was performed by Wilson et al. (1979). They considered the influence of the spatial distribution of rainfall on storm runoff. Their research used a kinematic wave runoff model in conjunction with a nonstationary time varying multidimensional rainfall generation model. The runoff model was used to simulate and compare hydrographs based on a single rainfall input location with those based on 20 locations. The comparison emphasized differences in the runoff volume, the peak discharge, and the time to peak. Results indicated that the mean absolute error in the runoff volumes of the single location case with respect to the 20 location case was 13 percent. Likewise, there was an 18 percent error in peak discharge and a 13 percent error in the time to peak. Discrepancies as large as 40 to 50 percent were calculated for the peak and time to peak. They finally conclude that,

> *It seems clear from these experiments that the spatial distribution of rainfall has a marked influence on the behavior of the runoff hydrograph. Thus even in cases were the total depth of precipitation is appropriately estimated by the existing* [rainfall gauge] *network, and even when the temporal character is recorded, there may exist serious errors in the total volume, peak, and time-to-peak of the estimated runoff hydrograph when the spatial pattern of rainfall is not appropriately preserved.*

Wood et al. (1988) sought the existence of a representative elementary area (REA) at the catchment scale. As the scale of a catchment increases, local differences in the hydrologic behavior of the catchment tend to cancel with the response of the catchment becoming more simple and more linear. The REA is the smallest area for which this behavior may be observed. In essence, the investigations were searching for the smallest area for which spatial variability within the system was effectively eliminated and lumped parameter values were found to yield good results. Their findings indicated that the REA did exist. The size of the REA was found to be highly sensitive to topography, with a secondary dependence to rainfall inputs. These results are interesting, however, Wood et Al. were working at the macro-scale of hydrology, while the investigation discussed in this thesis is a micro-scale examination of effects on small overland flow elements.

2.1.4 - Examining Variability in Discharge

Many studies have been performed which attempt to quantify the effects of variability in model parameters on the simulated discharge. Wood (1976) considered the effects of uncertainty in model parameters on deterministic hydrologic models. Wood demonstrated the differences in error bounds on the 100 year discharge depending on the probability distribution of one of the model parameters, although his work may be generalized to other models and applications. The results indicated that the error bounds were strongly affected by the input parameter probability distribution. Therefore, the nature of the model parameter distribution is a significant consideration in the design or decision making processes.

Bras and Rodriquez-Iturbe (1976) studied the effects of different rainfall-sampling networks on the accuracy of the predicted discharge from a rainfall-runoff model. In an example, they present a discharge hydrograph based on mean storm input along with error bounds enveloping the hydrograph. The error bounds are shown to be a function of the number

and positioning of the rainfall sampling locations with error in the peak reduced by a factor of five when going from one to eight sampling locations. The largest variances in discharge were shown to occur during the rising limb and peak portions of the hydrograph.

Machado and O'Donnell (1977) developed a physically based, kinematic wave model using a finite differencing scheme. They considered discharge to be a random variable dependent on the variances of several independent variables. Variability in model outflow was estimated as a function of the variance in each model parameter, and partial derivatives of the outflow with respect to each parameter. Their results present mean discharges with confidence intervals describing the simulated variation in discharge. They state that the variation in discharge can be made as small as desired by simply,

> *...dividing the catchment into small homogeneous subcatchments for which the variance of each parameter is small.*

Machado and O'Donnell do not make any distinction of variability in discharge as a function of the degree of equilibrium. Furthermore, all parameters are lumped together with only variation in discharge reported. The effects of variation of any one parameter on discharge are not investigated. The conclusions state that variation in discharge can be reduced by considering smaller more homogeneous areas. However, no methodology is presented on how to determine an appropriate area.

Smith and Hebbert (1979) performed a Monte Carlo analysis on the spatial variability of infiltration to analyze the effects of the random distribution of excess rainfall on the hydrologic performance of catchment areas. The results showed that variability in the infiltration parameter, K_s (saturated hydraulic conductivity), was influential in the behavior of the distributed watershed. Although they used a uniform rainfall rate, they noted that,

> *...the rate and duration of rainfall pattern have been demonstrated to influence the extent of effect that random variations exert on the composite infiltration curve and watershed runoff.*

Duration of rainfall will be studied extensively in this thesis.

Garen and Burges (1981) considered uncertainty in discharge as a function of error in the input parameters. Specifically, they used first-order and Monte Carlo analyses to examine variation in computed discharge using a modified version of the Stanford Watershed Model. Their results presented several simulated discharge hydrographs enclosed by error bounds on the discharge. The results indicate the relative influence of several input parameters on the simulated discharge. They found that the first-order analysis produced good results when the coefficient of variation of the input parameter was no larger than 25 percent for sensitive parameters and maybe a little larger for less sensitive parameters. The Monte Carlo analysis had no such constraints, however, a greater number of simulations were required in order to attain sufficient results.

Section 2.2 - FUNDAMENTALS OF OVERLAND FLOW

The overland flow system is shown in Figure 2.1. Identified are the parameters governing overland flow: L is the length of the horizontal projection of the overland flow plane, h is the depth of flow, v is the average velocity of flow, S_o is the surface gradient, i is the excess rainfall intensity, and q is the discharge per unit width. Two other important quantities which cannot be illustrated are gravitational acceleration, g, and the Manning's roughness of the plane, n.

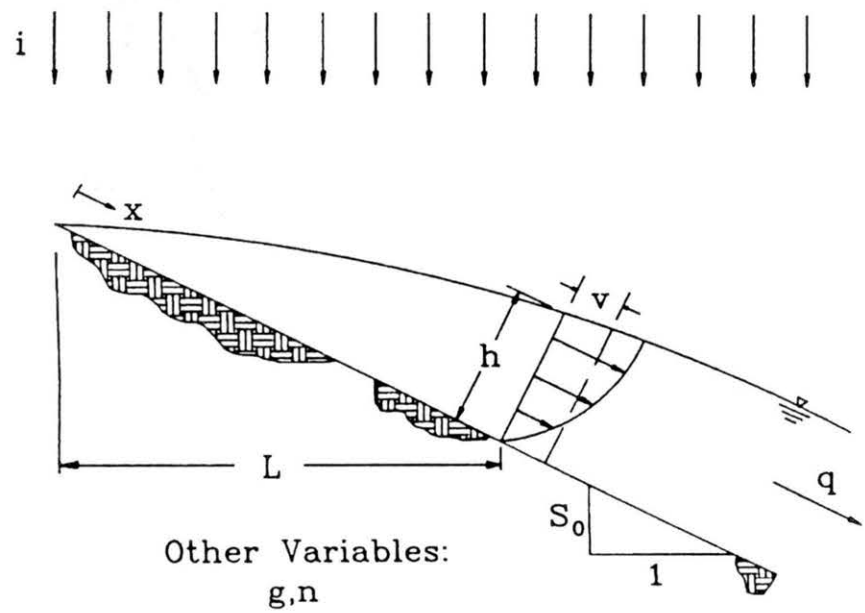

Figure 2.1. Overland Flow Parameters.

The governing equation of overland flow is the St-Venant equation:

$$S_f = S_o - \frac{\partial h}{\partial x} - \frac{v}{g}\frac{\partial v}{\partial x} - \frac{1}{g}\frac{\partial v}{\partial t} \qquad (2.2)$$

where S_f is the friction slope, x is the distance along the direction of flow, and t is time.

For overland flow, the partial derivative terms are very small relative to the friction and bed slopes and therefore the simplification:

$$S_f = S_o \qquad (2.3)$$

is commonly used and referred to as the kinematic wave approximation. This relationship implies that the gravitational forces provided by S_o are balanced by the friction slope, S_f

which is dependent on surface resistance. Conservation of mass yields the continuity equation:

$$\frac{\partial h}{\partial t} + \frac{\partial q}{\partial x} - i = 0 \qquad (2.4)$$

in which q is often expressed by the stage-discharge relationship:

$$q = \alpha h^{\beta} \qquad (2.5)$$

Several resistance equations may be employed to determine S_f (Julien et al., 1988) depending on the nature of flow being modeled (i.e. laminar or turbulent). Table 2.1 below shows values of α, β, and t_e for these equations.

Table 2.1. Values of α, β, and t_e for overland flow

Type of Flow	α	β	t_e
Laminar	$\frac{8gS}{K\nu}$	3	$\left[\frac{K\nu L}{8gSi^2}\right]^{1/3}$
Blasius: Turbulent Smooth Boundary	$\frac{1}{\nu^{1/7}}\left[\frac{8gS}{0.22}\right]^{4/7}$	12/7	$\left[\left(\frac{0.22}{8gS}\right)^{(4/7)}\frac{\nu^{1/7}}{i^{5/7}}L\right]^{7/12}$
Manning: Turbulent Rough Boundary (n constant)	$\frac{S^{1/2}}{n}$	5/3	$\left[\frac{nL}{S^{1/2}i^{2/3}}\right]^{3/5}$
Darcy-Weisbach: Turbulent Rough Boundary (f constant)	$\left[\frac{8gS}{f}\right]^{1/2}$	3/2	$\left[\frac{fL^2}{8gSi}\right]^{1/3}$
Chezy: Turbulent Rough Boundary (C constant)	$CS^{1/2}$	3/2	$\left[\frac{L^2}{C^2Si}\right]^{1/3}$

This analysis focuses on the Manning equation to determine S_f. The Manning equation as applied to overland flow is:

$$q = \frac{S_o^{1/2}}{n} h^{5/3} \tag{2.6}$$

where:

$$\alpha = \frac{S_o^{1/2}}{n} \tag{2.7a}$$

and,

$$\beta = 5/3 \tag{2.7b}$$

from equation (2.5). From equation (2.3) S_f may be substituted for S_o. Therefore, equation (2.6) may be used to express the relationship between unit discharge and friction slope. Substituting (2.5) into (2.4) the following is obtained:

$$\frac{\partial h}{\partial t} + \alpha\beta h^{\beta-1} \frac{\partial h}{\partial x} + h^{\beta} \frac{\partial \alpha}{\partial x} - i = 0 \tag{2.8}$$

where the second and third terms from the left account for the variation in discharge, q with respect to x.

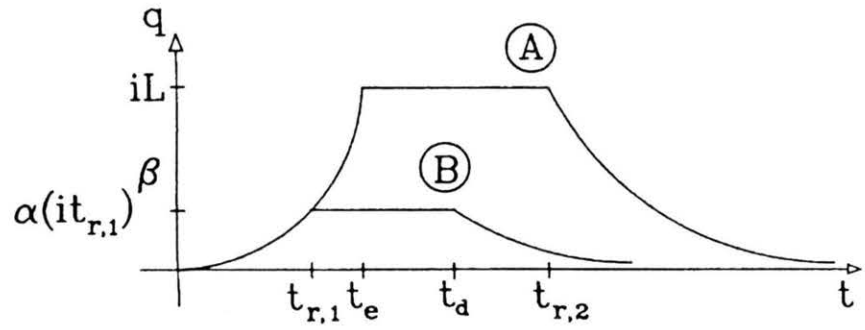

Figure 2.2. The Kinematic Wave Hydrograph.

If the kinematic assumption is applied to a single overland flow plane of constant properties receiving rainfall of a constant intensity, for a duration greater than the time to equilibrium, t_e, then the resulting hydrograph "A" will be obtained as shown in Figure 2.2. The time to equilibrium is the duration of rainfall until the discharge from the system is constant with time.

Note that hydrograph "A" has three distinct sections: the rising limb from $t = 0$ to $t = t_e$ (the time to equilibrium), the equilibrium plateau from $t = t_e$ to $t = t_{r,2}$ (the time at which the rainfall ceases), and the falling limb from $t = t_{r,2}$ to $t = \infty$. The rising limb of the hydrograph results from the second term of equation (2.8) being zero. Therefore, when $t < t_e$,

$$h = it \tag{2.9}$$

At equilibrium, the discharge is simply the area of the overland flow plane, iL. The following relationship involving the time to equilibrium, t_e is then given by:

$$q = \alpha h^{\beta} = \alpha(it_e)^{\beta} = iL \tag{2.10}$$

and then solving for t_e,

$$t_e = \left(\frac{L}{\alpha i^{\beta-1}} \right)^{1/\beta} \qquad (2.11a)$$

or specifically for Manning's equation:

$$t_e = \left(\frac{nL}{S_o^{1/2} i^{2/3}} \right)^{3/5} \qquad (2.11b)$$

If $t_r < t_e$ the result is shown in Figure 2.2 as hydrograph "B". For this hydrograph an equilibrium discharge exists, however this discharge is less than that given for hydrograph "A". At time $t_{r,2}$ partial equilibrium begins with:

$$q = \alpha h^{\beta} = \alpha (i t_{r,1})^{\beta} \qquad (2.12)$$

This discharge condition will persist until the characteristic caused by the cessation of rainfall reaches the downstream end of the system at the time of decline, t_d,:

$$t_d - t_{r,1} = \frac{L}{\alpha h^{\beta}} \qquad (2.13)$$

with a recession observed thereafter.

CHAPTER 3 - EFFECTS OF SPATIALLY VARIED OVERLAND FLOW PARAMETERS

The investigation here will focus on multiple simulations of numerous systems with statistically similar properties. Examination of the discharge hydrographs produced by these systems will indicate the behavior of the variation within the systems as a function of time and the parameters being changed.

Section 3.1 - VARYING THE INPUT DATA

In order to perform a set of analyses several parameters need to be defined. Some parameters will vary while others will be held constant. For purposes of this investigation, the effects of parameter variation on the discharge hydrograph will be investigated for spatially varied slope, Manning's "n", width, and rainfall intensity. In contrast, the time step size, number of nodes defining the systems, and the probability distribution function of the spatially varied parameters will remain the same for all analyses.

Consider for a moment the reasoning for holding some of these parameters constant. The time step size will be set to one-tenth of the time to equilibrium, t_e. This choice has been previously shown (Julien et al., 1988) to more than adequately define the rising limb of the discharge hydrograph. Eleven nodes will be used to define all systems. Preliminary analyses showed that discharge was relatively unaffected by the number of nodes used provided there were a minimum of seven present. Regarding the probability distribution function, a uniform distribution from 0 to 1 will be used. A more realistic, normal distribution used in a test analysis indicated that the general behavior of the results were not changed by the chosen distribution function (See Appendix A). Each of the above parameters was, therefore, found to have little effect on model performance and will be held constant for simplicity.

In order to investigate the effects on discharge caused by variations in the remaining parameters, it is necessary to develop a scheme to vary these parameters. First, base values are selected which will be the mean value about which the parameters will vary. The base values used in this analysis are a 10 percent slope, a Manning's "n" of 0.1, a 10 meter width of the overland flow plane, and an excess rainfall intensity of 1×10^{-5} m/s.

It should be noted that although this analysis incorporates the values cited above, the results are not limited to these particular values. All results will be presented in dimensionless form using equations (2.9) and (2.10b) to non-dimensionalize discharge and time, respectively. Results presented in this manner apply to any set of parameter values, provided that the kinematic wave approximation is valid.

The input perturbation scheme uses a variation factor, ϕ. This parameter describes the maximum allowable variation from the mean value using equation (3.1):

$$\mu_x\left(1 - \frac{\phi - 1}{\phi + 1}\right) \leq X_j \leq \mu_x\left(1 + \frac{\phi - 1}{\phi + 1}\right) \qquad (3.1)$$

where μ_X is the base value of parameter, X, and X_j is the value of parameter, X, at the j^{th} node. Notice that the quantity, $(\phi - 1)/(\phi + 1)$ appearing in equation (3.1) has the property that for very large ϕ, the quantity approaches unity, therefore, the maximum variation from the mean using this scheme is $2\mu_x$. The parameter, ϕ, should always be chosen to be greater than or equal to unity, where $\phi = 1$ indicates no perturbations. A non-perturbed system will be defined as a system which has all parameters held constant (i.e. there are no perturbations to any parameter). A constraint applied to the parameters: Manning's "n", width, and rainfall intensity, is for the spatial average of the parameter to equal the chosen base value, μ_X for that parameter:

$$\frac{X_1 + X_2 + X_3 + \ldots + X_m}{m} = \mu_X \qquad (3.2)$$

where m is the number of nodes describing the system (11 for these analyses). For the parameter, slope, the constraint is:

$$\frac{Z_1 - Z_m}{\Delta L} = S_o \qquad (3.3)$$

where Z_1 and Z_m are the elevations at the top and bottom nodes of the overland flow plane, respectively, and ΔL is the distance over which this change in elevation takes place. S_o is the base slope value.

The above scheme was used to generate 100 perturbed systems for each of the four overland flow parameters. We will define the input parameter envelope by the set of values describing the maximum and minimum of those 100 parameter perturbations at each node. Figures 3.1a-3.1d show the envelopes for each of the input parameters. It should be noted that these are not the actual systems that were used as input to the model, but rather that these envelopes indicate the maximum extent of the variation in each of the parameters about the base value. They have also been non-dimensionalized in space and for the particular parameter being plotted (i.e. x^* is dimensionless space, and z^*, n^*, w^*, and i^* are dimensionless elevation, Manning roughness, width, and excess rainfall intensity, respectively). These figures show how the parameter, ϕ, effects the size of the envelope resulting in small envelopes when $\phi = 2$ and large envelopes when $\phi = 6$.

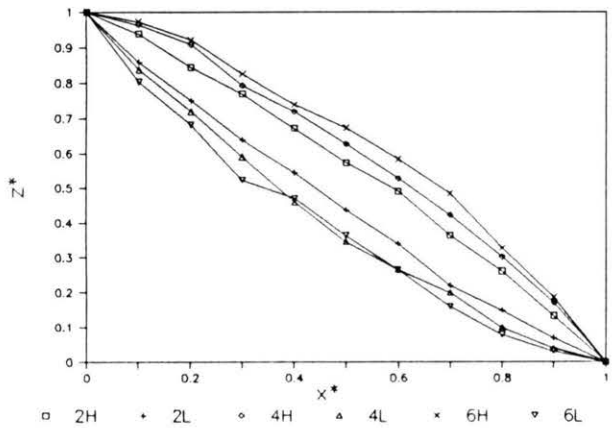

Figure 3.1a. Input Envelopes for Slope.

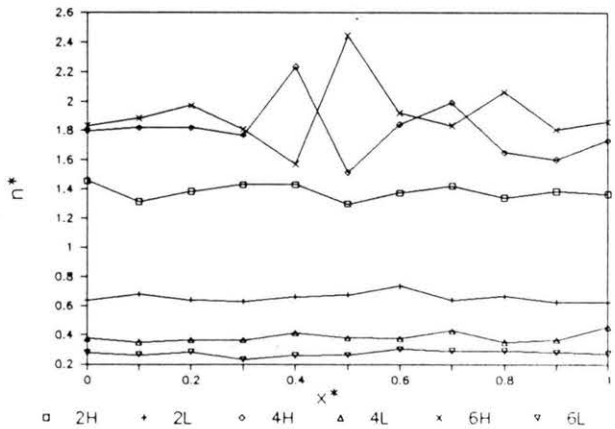

Figure 3.1b. Input Envelopes for Manning's "n".

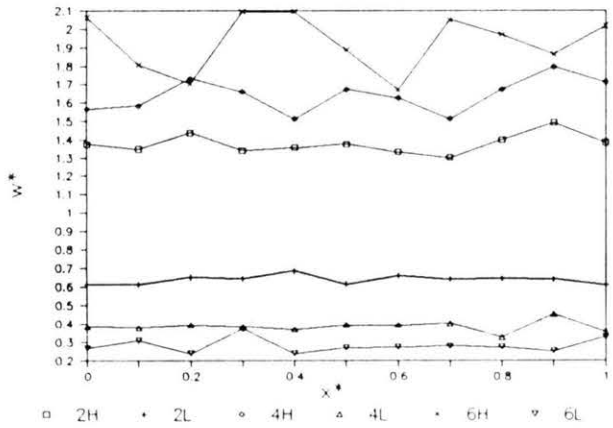

Figure 3.1c. Input Envelopes for Width.

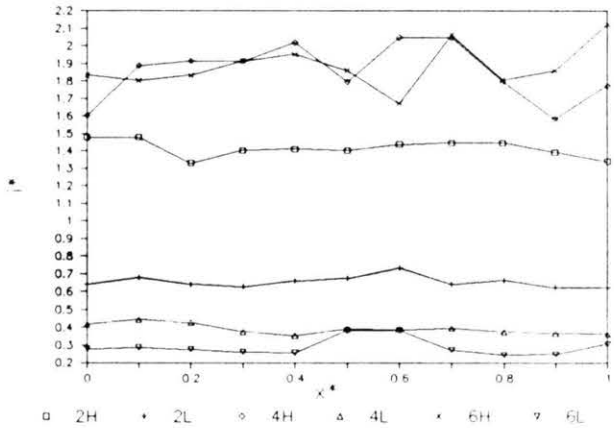

Figure 3.1d. Input Envelopes for Rainfall Intensity.

In order to investigate all possible permutations of the input parameters it is important to recognize that there are three classes of input parameters: the duration of rainfall (partial or complete equilibrium), the magnitude of parameter perturbation (ϕ), and the overland flow parameter to be varied (slope Manning's "n", width, rainfall intensity). It was chosen to perform simulations for three different durations of rainfall: $t_r / t_e = 0.4$, 1.0, and 5.0. These three durations cover the range from partial to complete equilibrium. Similarly, simulations were done for three different values of ϕ: 2, 4, and 6. And of course, the effects of all four overland

flow parameters were investigated. For each permutation of the above conditions, 100 simulations were performed. This number was chosen by trial and error and was found to yield fairly smooth results. This amounts to 3600 hydrographs being simulated over all possible permutations of the above conditions.

Section 3.2 - RESULTS - SINGLE PARAMETER VARIATION

3.2.1 - Hydrograph Envelopes

The large amount of information generated necessitated the reduction of the data into an interpretable form. One procedure was to generate a hydrograph envelope for each set of 100 equivalent systems. The envelope was determined by finding the highest and lowest simulated discharges at each time step over the 100 hydrographs. These envelopes show the maximum variation in discharge as a function of time along the hydrograph.

The hydrograph envelopes are pictured in Figures 3.2a-3.2l. Notice that they have been non-dimensionalized in time by dividing by the time to equilibrium, t_e; and in discharge by the equilibrium discharge iL.

The general shape of these envelopes is primarily a function of the duration of rainfall, t_r, relative to the time to equilibrium, t_e. The degree of variation within a set of hydrographs is quite large for $t_r/t_e=0.4$, decreasing to the point that the different envelopes are difficult to distinguish when $t_r/t_e=5.0$

1) When t_r/t_e is less than unity a partial hydrograph results with the highest simulated discharge occurring at the last time interval experiencing rainfall, and followed by a long recession limb (see Figures 3.2a-3.2d). The region enclosed by the envelopes is much larger than that for $t_r/t_e=1.0$ or 5.0.

2) When $t_r/t_e=1.0$ (see Figures 3.2e-3.2h) a particular case of complete hydrograph is obtained. Notice that these hydrographs exhibit peak discharges near unity at

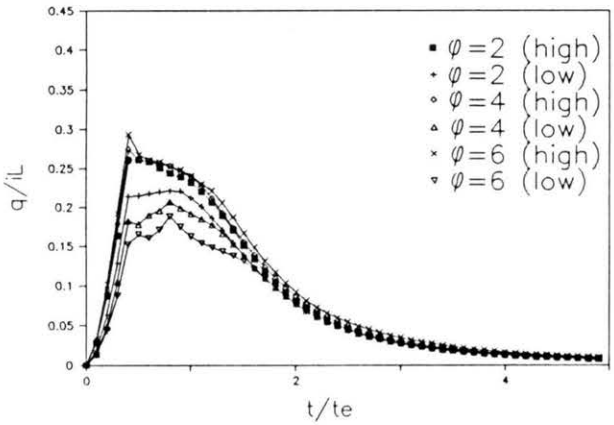

Figure 3.2a. Hydrograph Envelopes for Slope ($t_r / t_e = 0.4$).

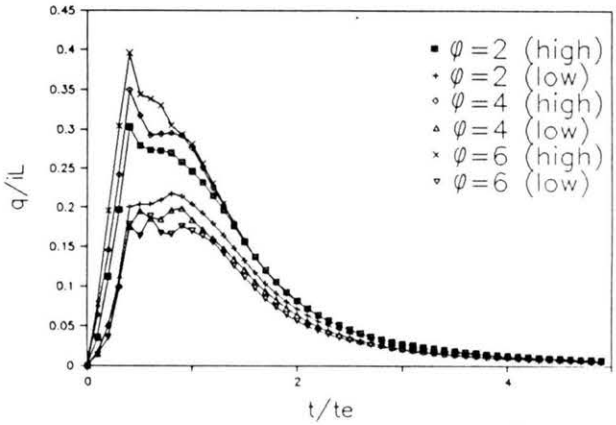

Figure 3.2b. Hydrograph Envelopes for Manning's "n" ($t_r / t_e = 0.4$).

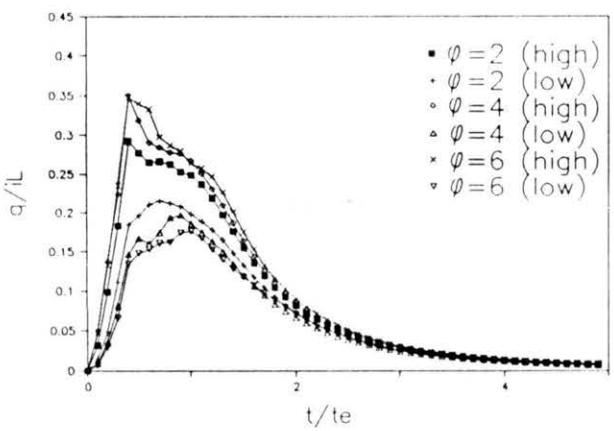

Figure 3.2c. Hydrograph Envelopes for Width ($t_r / t_e = 0.4$).

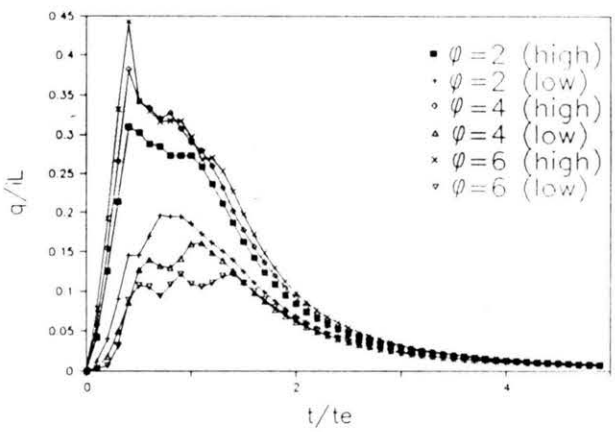

Figure 3.2d. Hydrograph Envelopes for Rainfall Intensity ($t_r / t_e = 0.4$).

$t/t_e = t_r/t_e = 1.0$ and then begin to recede. In essence, these hydrographs are like the complete hydrographs without an equilibrium plateau and like the partial hydrographs in that the peak discharge occurs during the last time interval with rainfall.

3) When $t_r/t_e \gg 1$ (i.e. $t_r/t_e = 5.0$ - see Figures 3.2i-3.2l), then a complete hydrograph results, characterized by an equilibrium plateau region where the non-dimensionalized discharge is unity from $t/t_e \approx 1.0$ to $t/t_e = t_r/t_e$. A non-perturbed system will

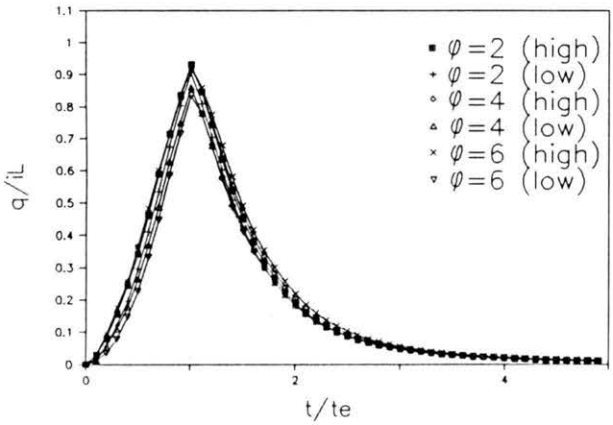

Figure 3.2e. Hydrograph Envelopes for Slope ($t_r / t_e = 1.0$).

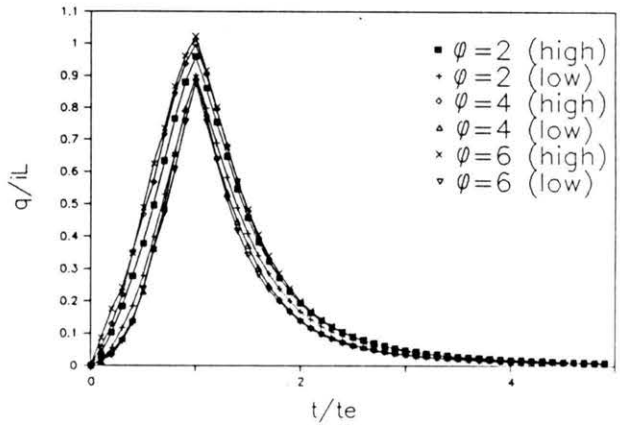

Figure 3.2f. Hydrograph Envelopes for Manning's "n" ($t_r / t_e = 1.0$).

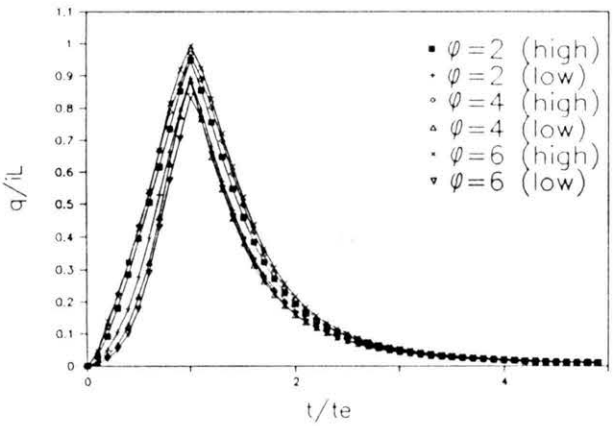

Figure 3.2g. Hydrograph Envelopes for Width ($t_r / t_e = 1.0$).

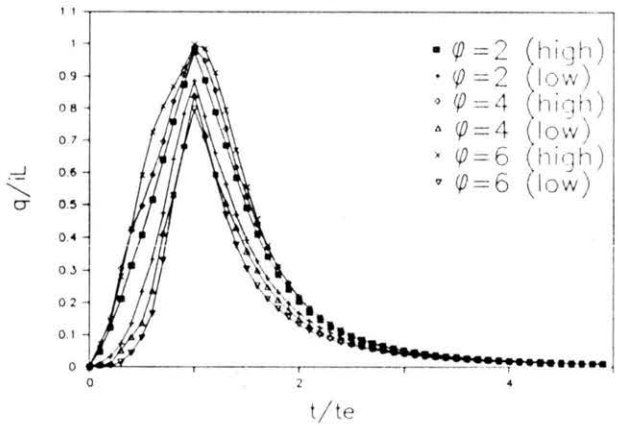

Figure 3.2h. Hydrograph Envelopes for Rainfall Intensity ($t_r / t_e = 1.0$).

demonstrate equilibrium discharge at precisely $t / t_e = 1.0$. As a consequence of the assumptions used to derive equation 2.11a, any perturbation to slope, roughness, width, or rainfall intensity will delay the dimensionless time to equilibrium to a value greater than one. This is why none of the hydrograph envelopes reaches unity at $t / t_e = 1.0$. It is important to observe that regardless of the magnitude or type of perturbation of the system, the non-dimensionalized equilibrium discharge is unity. This value cannot be

exceeded under equilibrium conditions.

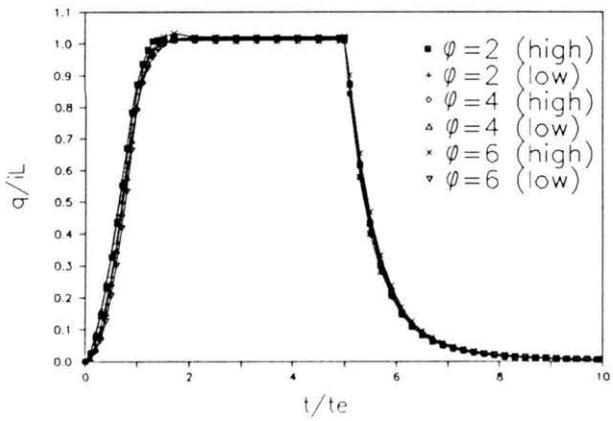

Figure 3.2i. Hydrograph Envelopes for Slope ($t_r / t_o = 5.0$).

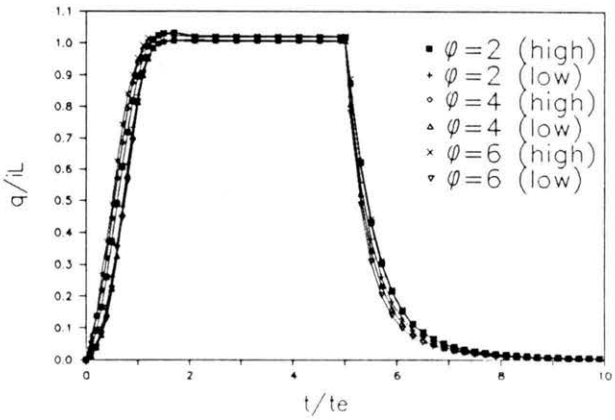

Figure 3.2j. Hydrograph Envelopes for Manning's "n" ($t_r / t_o = 5.0$).

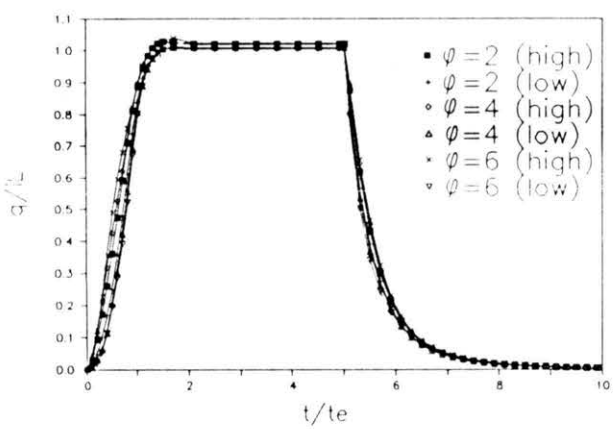

Figure 3.2k. Hydrograph Envelopes for Width ($t_r / t_o = 5.0$).

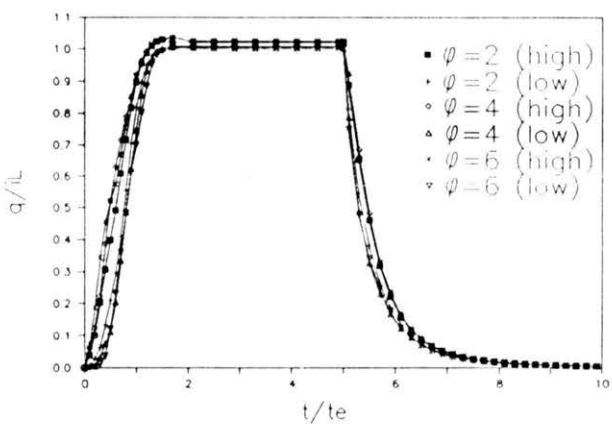

Figure 3.2l. Hydrograph Envelopes for Rainfall Intensity ($t_r / t_o = 5.0$).

4) Examination of the hydrograph envelopes indicates differing model response depending on which parameter has been perturbed. Qualitatively, the model response is most effected by variations in rainfall intensity, followed by Manning's "n" and width which cause comparable variation in output, and finally slope which causes the smallest variation in discharge.

3.2.2 - Deviation Hydrographs

Consider precisely what the effects of parameter perturbation are on the simulated hydrograph. Figure 3.3 shows the discharge hydrographs for two systems: one in which there are no perturbations, and one in which slope is allowed to vary. While the non-perturbed system produces smooth rising and falling limbs, the perturbed system creates fluctuations in discharge about the non-perturbed hydrograph.

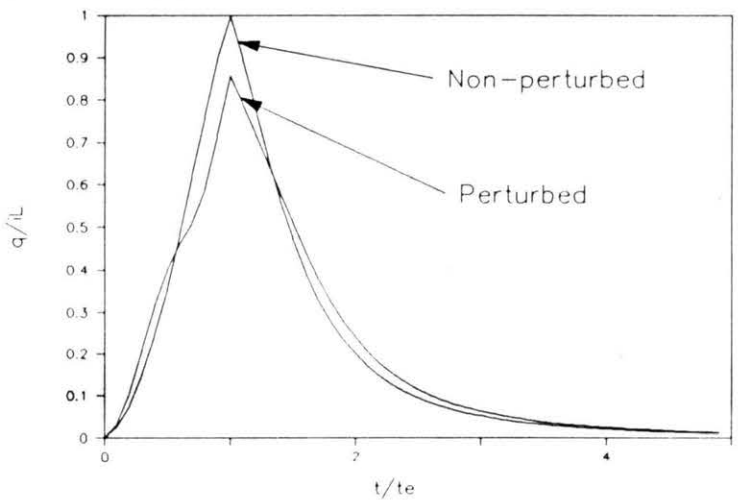

Figure 3.3. Hydrographs for perturbed and non-perturbed overland flow systems.

The discharge from a non-perturbed system at any time may be considered as a base or mean value about which the other perturbed discharges will vary. The deviation hydrograph will be defined as the standard deviation of the discharges about the non-perturbed discharge at each time step. Expressed symbolically, the deviation hydrographs were generated using the formula:

$$\sigma_t = \sqrt{\frac{1}{m-1}\sum_{k=1}^{m}(q_{k,t} - q_{np,t})^2} \qquad (3.4)$$

where σ_t is the deviation in discharges at the outlet at time, t; m is the number of simulated hydrographs (100 in this case); $q_{k,t}$ is the k^{th} perturbed discharge at time, t; and $q_{np,t}$ is the non-perturbed discharge at time, t. The curve traced out by the deviation hydrograph will indicate the magnitude of discharge variation as a function of time.

Shown in figures 3.4a-3.4l are the non-dimensionalized deviation hydrographs, where the deviation has been non-dimensionalized by dividing by the equilibrium discharge, $\alpha(it_r)^{\beta}$ when $t_r/t_e < 1.0$ and iL when $t_r/t_e \geq 1.0$. The resulting value is indicative of the percentage variation in discharge relative to the non-perturbed equilibrium discharge. For example, in Figure 3.4a, the largest variation in discharge is approximately 0.12 at $t/t_e = 0.4$. This means that the deviation of discharges simulated over 100 equivalent systems at $t/t_e = 0.4$ was approximately 12 percent of the partial equilibrium discharge when the perturbed input variable was slope.

Examination of these figures reveals that the general shape of the graphs is primarily dependent on the value of t_r/t_e. Several observations may be made:

1) Figures 3.4a-3.4d exhibit the largest variations in discharge because the duration of rainfall is only $0.4t_e$ indicating partial equilibrium, and therefore the discharge from the system is highly sensitive to any perturbations in input parameters.

2) The region between $t/t_e = 0$ and $t/t_e = 1.0$ in Figures 3.4e-3.4l exhibits a maximum value at $t/t_e = 0.7$. For $t < 0.7t_e$ the deviation increases because the discharges are getting larger. For $0.7t_e < t < t_e$ the deviation decreases with time because the system is approaching equilibrium discharge which, as shown in Figures 3.2i-3.2l, is independent of deviations in the system. Therefore, at $t = 0.7t_e$ a balance seems to exist between the opposing trends of near equilibrium behavior and near peak discharge causing a maximum deviation in discharge.

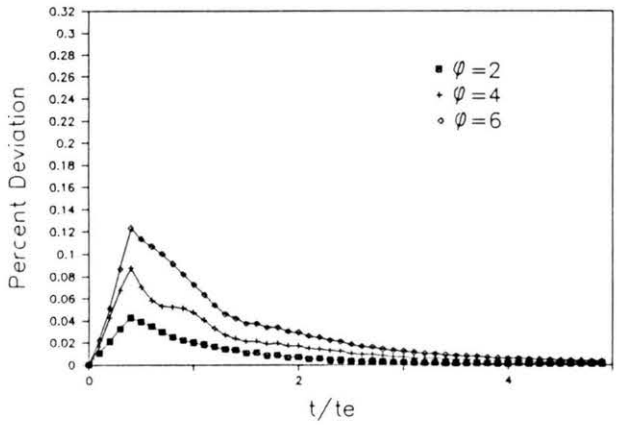

Figure 3.4a. Deviation Hydrographs for Slope ($t_r / t_e = 0.4$).

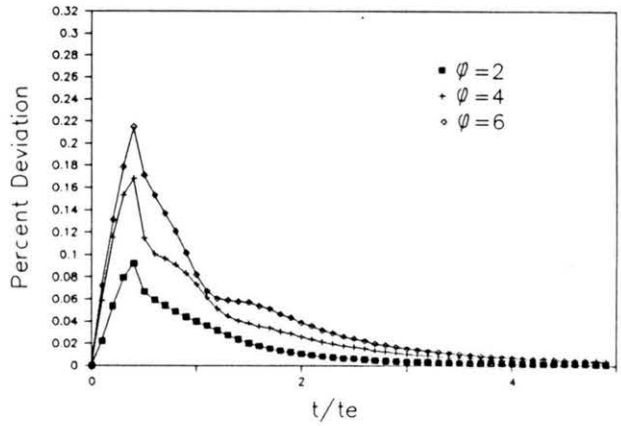

Figure 3.4b. Deviation Hydrographs for Manning's "n" ($t_r / t_e = 0.4$).

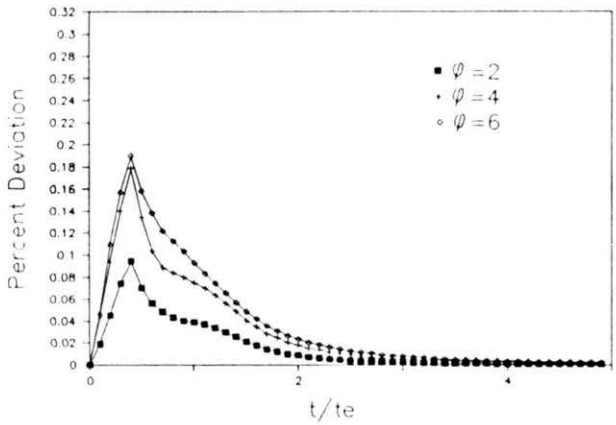

Figure 3.4c. Deviation Hydrographs for Width ($t_r / t_e = 0.4$).

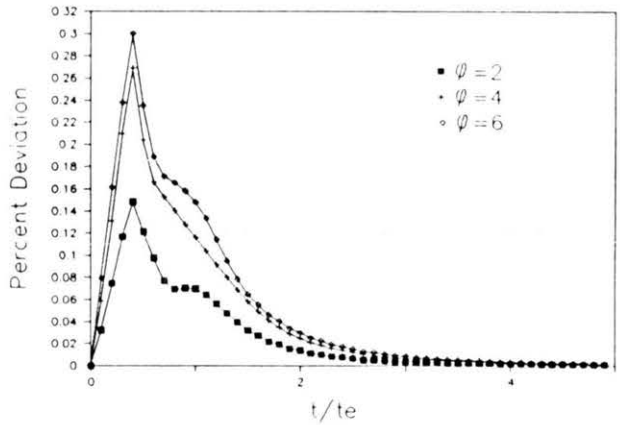

Figure 3.4d. Deviation Hydrographs for Rainfall Intensity ($t_r / t_e = 0.4$).

3) Figures 3.4i-3.4l show the standard deviation in discharge for varying input parameters and $t_r / t_e = 5.0$. Notice again, that the maximum deviations in discharge occur at $t / t_e = 0.7$ as in case for $t_r / t_e = 1.0$. A similar peak is observed for the recession limb caused by a balance in the same two trends as explained in observation 2). The central region exhibiting very small variation corresponds to the equilibrium plateau in Figures 3.2i-3.2l. Theoretically, if mass balances were performed for an infinite simulation time, this

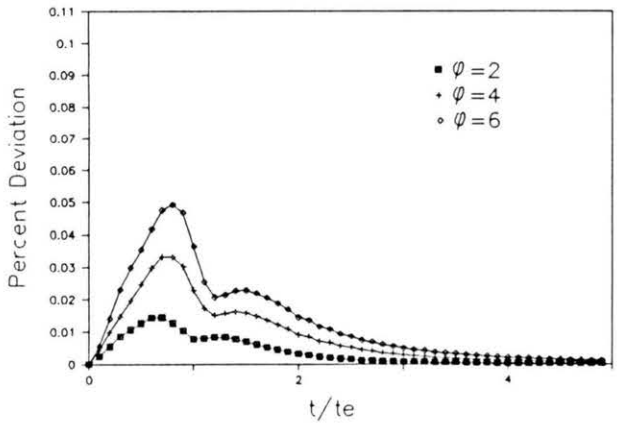

Figure 3.4e. Deviation Hydrographs for Slope ($t_r / t_o = 1.0$).

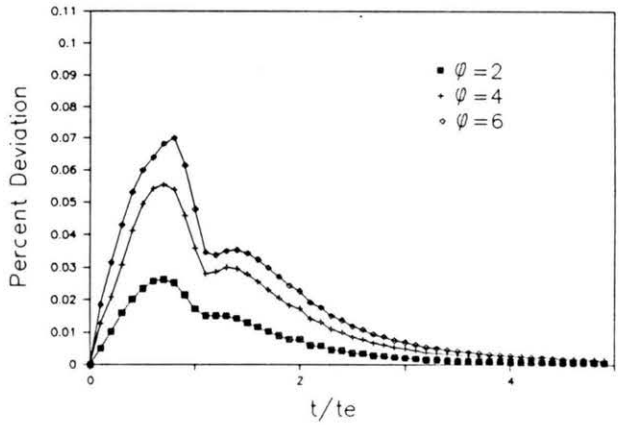

Figure 3.4f. Deviation Hydrographs for Manning's "n" ($t_r / t_o = 1.0$).

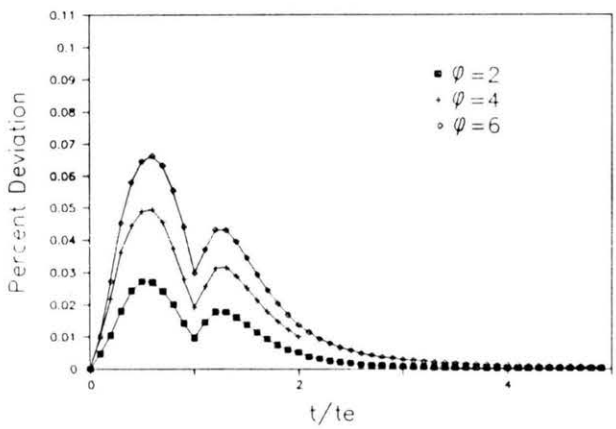

Figure 3.4g. Deviation Hydrographs for Width ($t_r / t_o = 1.0$).

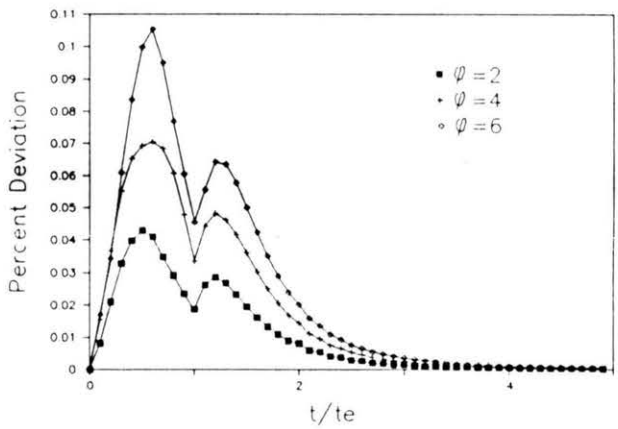

Figure 3.4h. Deviation Hydrographs for Rainfall Intensity ($t_r / t_o = 1.0$).

central region would be identically zero.

4) A qualitative analysis of the deviation hydrographs indicates that the model response is most sensitive to variations in rainfall intensity, followed by Manning's "n", width, and slope. This corroborates the previous findings from the hydrograph envelope analysis.

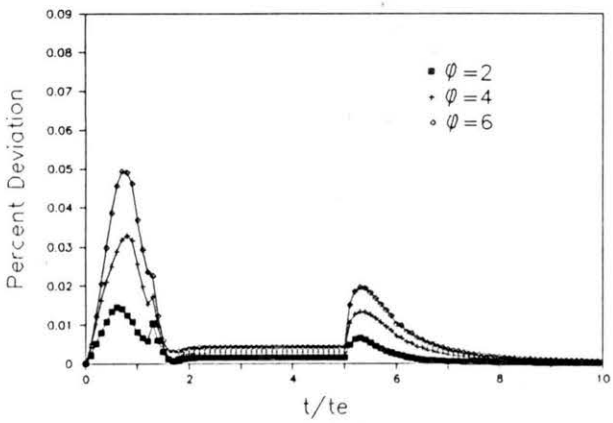

Figure 3.4i. Deviation Hydrographs for Slope ($t_r / t_o = 5.0$).

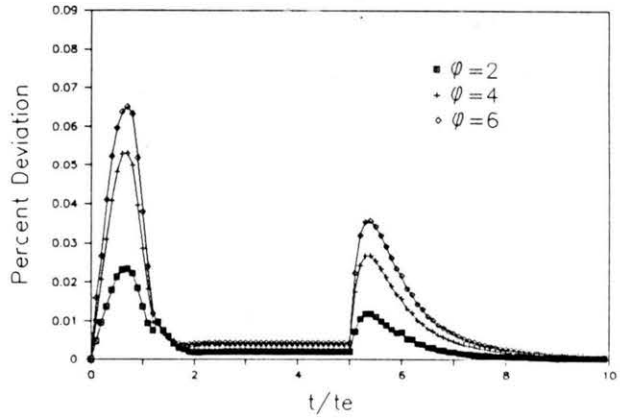

Figure 3.4j. Deviation Hydrographs for Manning's "n" ($t_r / t_o = 5.0$).

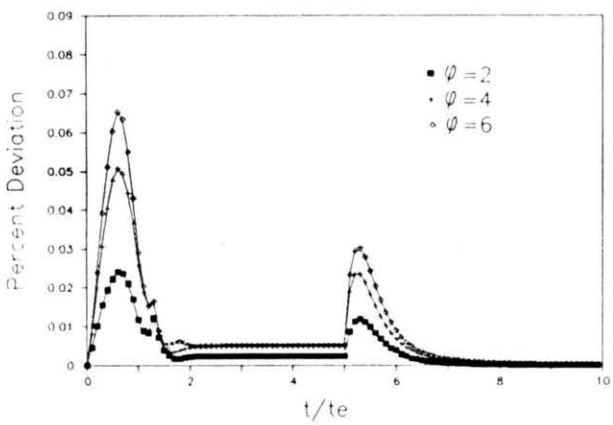

Figure 3.4k. Deviation Hydrographs for Width ($t_r / t_o = 5.0$).

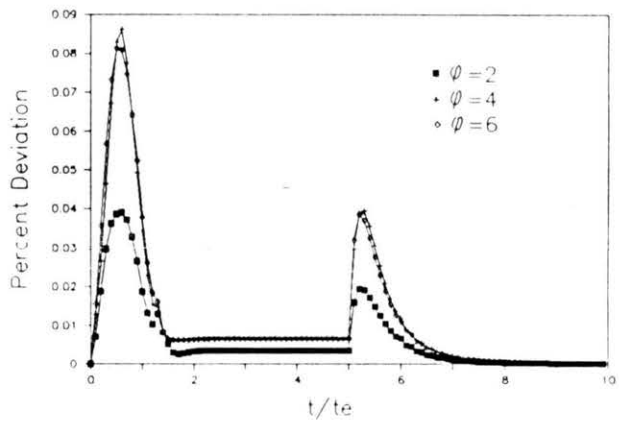

Figure 3.4l. Deviation Hydrographs for Rainfall Intensity ($t_r / t_o = 5.0$).

3.2.3 - Spatial Sensitivity Analysis

Sensitivity, a measure of the model response to change in an input parameter, is used to determine the importance of parameters in a given model, and to optimize parameter values within a model. McCuen (1973) presented a means of analytical sensitivity analysis for simple models through differentiation of the model equation with respect to the parameter of interest. Parameter perturbation numerically achieves the same goal for more complex models.

With an understanding of the general behavior of the model response to input variation, the goal is to quantify the spatial sensitivity of the model output to each parameter, which has only been qualitatively deduced to this point.

From the Figures 3.2a-3.2l presented in the hydrograph envelope section, a logical measure of output variation is the volume of the hydrograph envelopes. As the magnitude of ϕ increases, and therefore the magnitude of the input perturbations increases, the area enclosed by the hydrograph envelopes increases. If this area is integrated over the duration of the hydrograph, a volume is the result. The magnitude of this volume is indicative of the variation in the 100 hydrographs used to generate the envelope. This technique is similar in concept to that used by Wu et al. (1978).

The coefficient of variation is defined as:

$$C_v = \frac{\sigma}{\mu} \tag{3.5}$$

where C_v is the coefficient of variation, σ is the standard deviation of the parameter of interest (i.e. a measure of the parameter variation) and μ is the average value of the parameter (i.e. a measure of a base value of the parameter). Table 3.1 gives the tabulated values of V^* for the hydrograph envelopes where these values were calculated using:

$$V^* = \frac{\Delta V}{V} \tag{3.6}$$

ΔV is the hydrograph envelope volume, and V is the input rainfall volume. These values are not coefficients of variation in the strict statistical sense, however, conceptually they represent the same ratio of a variation divided by a base value. Figure 3.5 illustrates the two volumes ΔV and V.

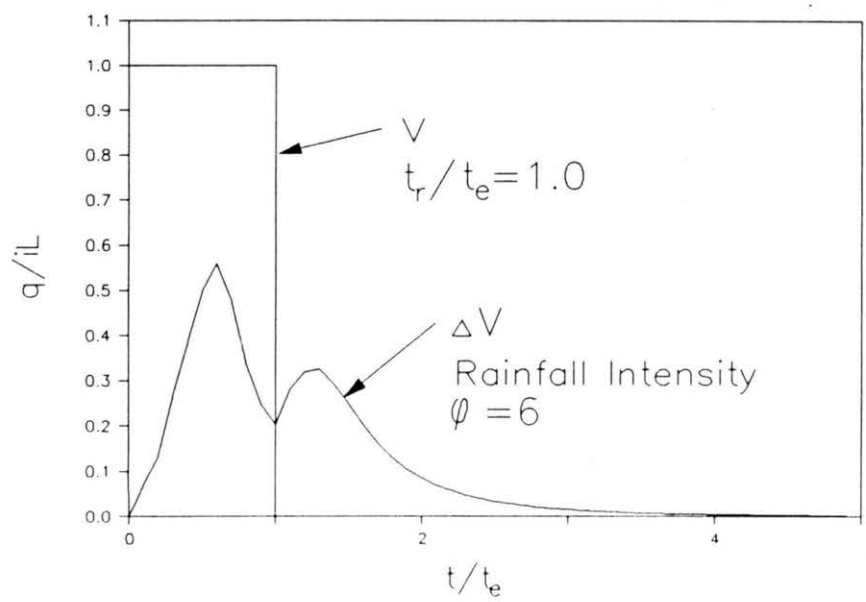

Figure 3.5. Definition sketch of the volumes ΔV and V.

Table 3.1. Values of V^* of the Output Discharge

Parameter	ϕ	$t_r/t_e=0.4$	$t_r/t_e=1.0$	$t_r/t_e=5.0$
Slope	2	0.01126	0.00650	0.00199
"	4	0.02204	0.01372	0.00340
"	6	0.03533	0.02033	0.00496
Manning's "n"	2	0.02322	0.01414	0.00399
"	4	0.04108	0.02937	0.00701
"	6	0.05567	0.03716	0.00909
Width	2	0.02181	0.01352	0.00344
"	4	0.04281	0.02755	0.00621
"	6	0.05145	0.03426	0.00815
Rainfall Intensity	2	0.03824	0.02293	0.00560
"	4	0.06749	0.04400	0.01060
"	6	0.08429	0.05805	0.01098

From Table 3.1, it is clear that the coefficient of variation is a function of the parameter being varied, the chosen value of ϕ and the value of t_r/t_e. These results provide a quantitative basis to the results found earlier regarding the response of the model to variations in the input parameters. Rainfall intensity produces the largest V^* values (up to 10 percent), followed by

Manning's "n" and width which produce very similar variations, and finally, slope which exhibits the smallest variation. Also note that as t_r / t_e increases the variation decreases. There is approximately a factor of ten decrease in V^* as t_r / t_e goes from 0.4 to 5.0.

The discussion to this point only considers variation of the output hydrographs. A more meaningful measure of the variation would be the degree of variation in output per unit variation in input. Such a measure is called the relative sensitivity and may be represented mathematically by (McCuen and Snyder, 1986):

$$R_{s,l} = \frac{V^*}{C_v} \qquad (3.7)$$

where $R_{s,l}$ is the relative sensitivity of the output function, V^* to the input variation of variable, l. This is called the relative sensitivity because the scaling factors μ and V appearing in the denominators of equations (3.6) and (3.7), respectively, are used to make $R_{s,l}$ a dimensionless quantity which is, therefore, independent of the units used to measure μ and V.

Table 3.2. Values of $R_{s,l}$

Parameter	ϕ	t_r / t_e =0.4	t_r / t_e=1.0	t_r / t_e=5.0
Slope	2	0.05536	0.03163	0.01005
"	4	0.06145	0.03846	0.00948
"	6	0.07977	0.04561	0.01161
Manning's "n"	2	0.11648	0.07270	0.02033
"	4	0.11327	0.08260	0.02001
"	6	0.12678	0.08447	0.02048
Width	2	0.10987	0.06707	0.01741
"	4	0.11651	0.07523	0.01666
"	6	0.11697	0.07787	0.01860
Rainfall Intensity	2	0.19591	0.11301	0.02743
"	4	0.18717	0.12124	0.02890
"	6	0.19622	0.12834	0.02522

Table 3.2 presents the values of $R_{s,l}$ values corresponding to the V^* values shown in Table 3.1. The values given in Table 3.2 are similar to those from Table 3.1. Again, rainfall

intensity exhibits the largest sensitivity values, followed by Manning's "n" and width, and finally slope. This behavior is explained by considering the exponents of each of the parameters in the Manning equation. Rewriting equation (2.6) for total discharge:

$$Q = \frac{S_o h^{5/3} w}{n} \tag{3.8}$$

where Q is the total discharge in (L^3/t) and w is the width of the flow plane in (L). From equation (2.8) which shows that at equilibrium, $h = it_e$, the excess rainfall intensity, it_e, may be substituted for h when $t_r / t_e = 1.0$. Using this substitution for conditions at the time to equilibrium:

$$Q = \frac{S_o^{1/2} (it_e)^{5/3} w}{n} \tag{3.9}$$

The qualitative and quantitative rankings of sensitivity given in the sections 3.2.1-3.2.2 and again in this section are corroborated by ranking the parameters according to magnitude of their respective exponents. Rainfall intensity is raised to the largest exponent (power=5/3), followed by Manning's "n" and width (power=1), and finally slope is raised to the smallest exponent (power=1/2). This is the same ranking of variations presented earlier. This ranking would vary according to resistance equation used since different resistance equations place different emphases on the overland flow parameters (See Table 2.1).

Also, the variation in the model output is strongly influenced by t_r / t_e. The relative sensitivity values decrease dramatically as t_r / t_e increases, which is reasonable since we have seen how systems at equilibrium yield the same discharge, iL, regardless of any perturbations in input variables. The columns showing values of variation and relative sensitivity for t_r / t_e =5.0 demonstrate this most clearly since all these values were generated from systems at equilibrium for a duration of five times the time to equilibrium. In contrast to Table 3.1, notice

that the values shown in Table 3.2 are relatively unaffected by the parameter, ϕ. This indicates that the scaling of the output variation to account for the magnitude of input variation essentially removes the effects of ϕ.

More analyses were performed to determine additional values of t_r / t_e especially in the region of $1.0 \leq t_r / t_e \leq 2.0$ in an effort to more precisely determine how relative sensitivity changes as t_r / t_e increases. Figure 3.6 gives this relationship.

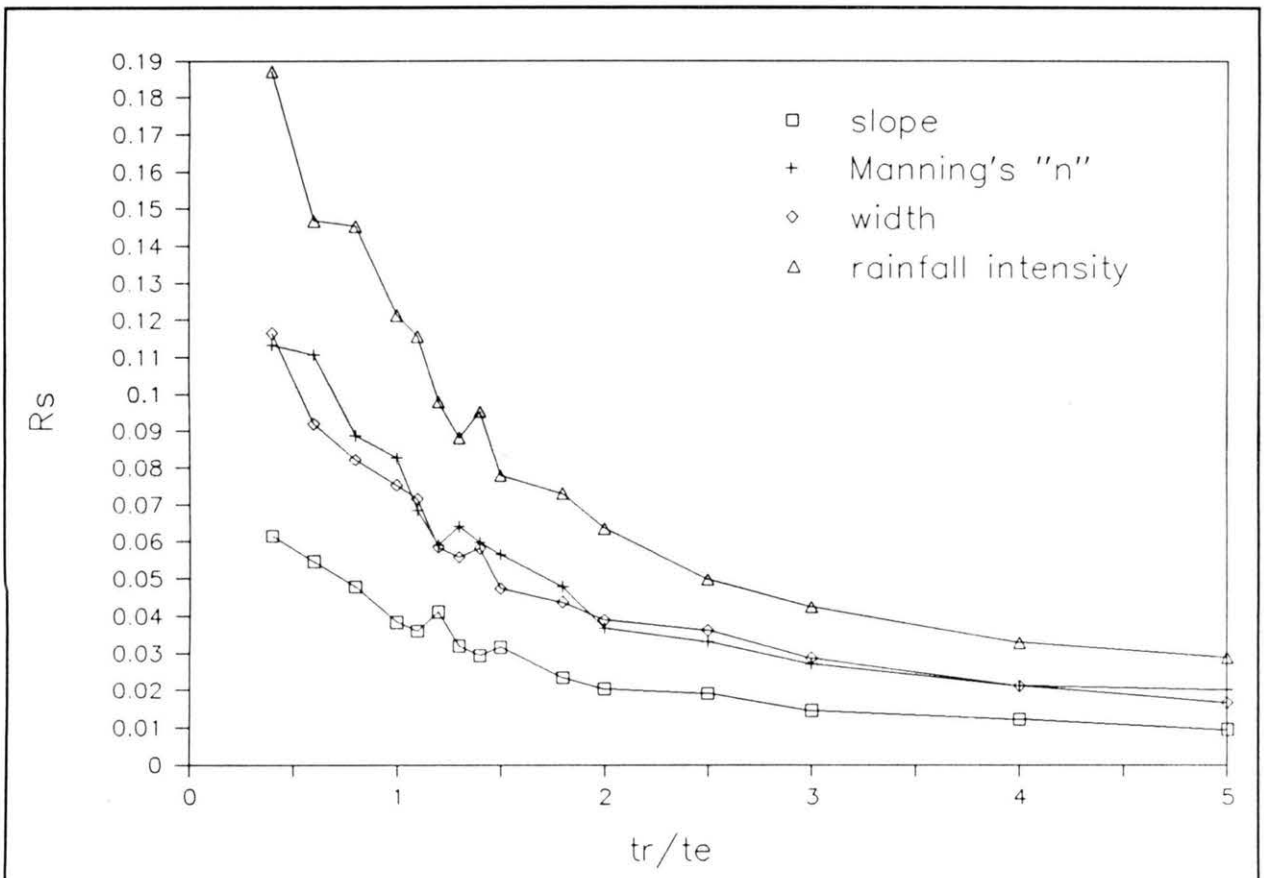

Figure 3.6. Relative sensitivity values for various values of t_r / t_e.

From this figure it is apparent that the magnitude of relative sensitivity decreases rapidly for small values of t_r / t_e and then changes slowly for large values of t_r / t_e. In other words, the

variability in discharge is largest under partial equilibrium conditions and is smallest under complete equilibrium conditions. Since the rainfall intensity curve is the highest and the slope curve is the lowest, this figure shows, in another way, that computed discharge is most sensitive to excess rainfall intensity and least sensitive to slope.

A breakpoint factor, ϵ, may now be determined from Figure 3.6. This factor is defined as the point at which the change in R_s with increasing t_r / t_e becomes small. Therefore, at this point, the effects of variation in the system due to input parameter perturbations must be small as well. The selection of this value is somewhat arbitrary, depending on the degree of certainty desired, however, Figure 3.6 shows that $t_r / t_e = 2.0$ approximately marks the point at which the change in the relative sensitivity of the model output becomes fairly small. That is, for values of t_r / t_e greater than 2.0, the decrease in R_s is slight. Using this reasoning, the selection of $\epsilon = 2.0$ is a logical choice.

The peaks of the hydrographs used to generate Figure 3.6 were also analyzed. Figures 3.7a-3.7d show the non-dimensionalized peak discharges for several values of t_r / t_e for perturbations in each of the input parameters. The discharges were ranked and plotted against their non-exceedance probability. These figures show most dramatically the effect of equilibrium on peak discharge. When $t_r / t_e < 1.0$ the peak discharge may vary over a wide range of values as indicated by the shallow slopes in Figures 3.7a-3.7d. As rainfall duration approaches and exceeds the time to equilibrium, the system is forced to peak closer to or at unity as indicated by the steep lines in Figures 3.7a-3.7d.

Figures 3.6 and 3.7a-3.7d seem to indicate contradictory behavior since Figure 3.6 shows a gradual decrease in relative sensitivity as t_r / t_e increases, while Figures 3.7a-3.7d illustrate a dramatic change in behavior as t_r / t_e approaches 1.0. This is, in fact, not contradictory. Figure 3.6 is based on values which are a function of entire hydrographs, while Figures 3.7a-3.7d

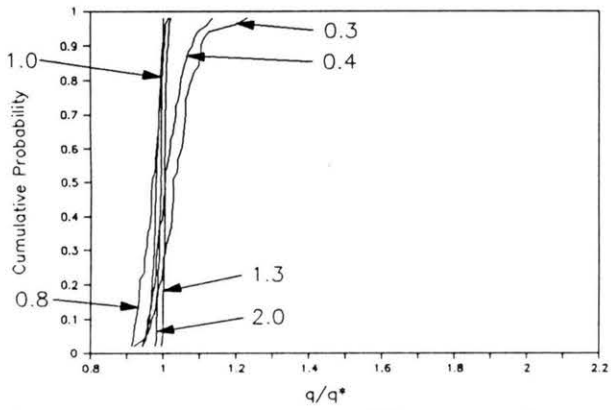

Figure 3.7a. Distribution of Peaks for Slope.

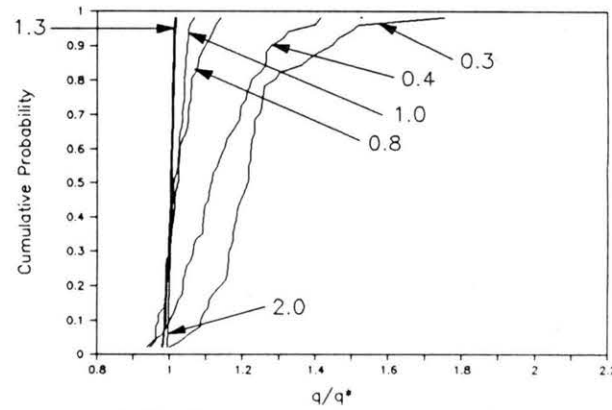

Figure 3.7b. Distribution of Peaks for Manning's "n".

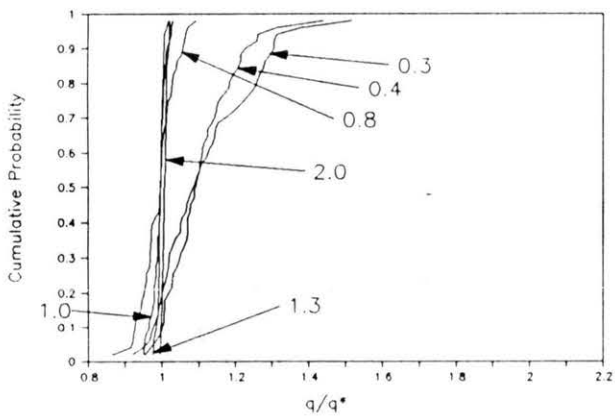

Figure 3.7c. Distribution of Peaks for Width.

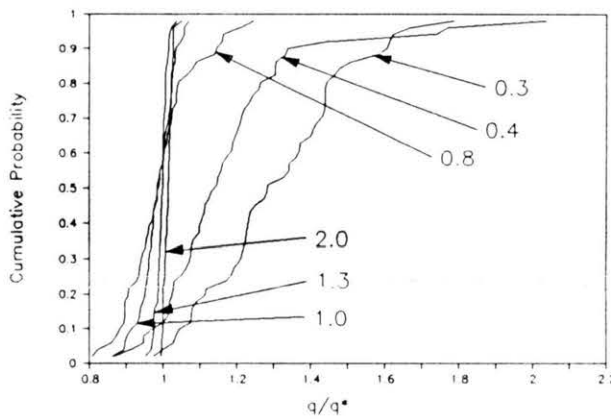

Figure 3.7d. Distribution of Peaks for Rainfall Intensity.

are based only on hydrograph peaks. Therefore, Figure 3.6 is indicative of properties observed over time which creates a smoothing effect. Figures 3.7a-3.7d are generated from single values selected from many hydrographs, in which time has no bearing on the outcome.

CHAPTER 4 - PRACTICAL IMPLICATIONS

The results presented in sections 3.2.1-3.2.3 indicate that variability within a system has little influence on the computed discharge if the duration of rainfall exceeds ϵ times the time to equilibrium. The criteria used to calculate the time to equilibrium may now be reversed and used to determine an appropriate grid size to use in overland flow modeling, given a known input duration of rainfall, t_r, mean excess rainfall intensity, $\bar{i}$, average slope, $\overline{S}$, and average surface roughness, $\bar{n}$. It is instructive to consider the corresponding formulation for the laminar resistance equation, in which the resistance factor, K, is analogous to Manning's "n". The average laminar resistance factor will, therefore, be $\overline{K}$. With these parameters known for a given storm event and location, the appropriate grid size to use is calculated by solving for L in equation (2.11a):

$$L_g = \alpha i^{\beta-1}\left(\frac{t_r}{\epsilon}\right)^{\beta} \tag{4.1}$$

or, specifically for the Manning equation:

$$L_g = \left[\frac{(t_r/\epsilon)^{5/3}\overline{S}^{1/2}\bar{i}^{2/3}}{\bar{n}}\right] \tag{4.2a}$$

and the laminar equation:

$$L_g = \left[8g\overline{S}\frac{(t_r/\epsilon)^3\bar{i}^2}{\overline{K}\nu}\right] \tag{4.2b}$$

where ϵ is the breakpoint factor described in section 3.2.3, the parameter, ν in equation (5.2b) is the kinematic viscosity of water and will be set to $1x10^{-6}$ m^2/s for this discussion, and the bars indicate that mean values are used to estimate each parameter value. Under these conditions mean parameters may be used to simulate overland flow because L_g is chosen such that complete equilibrium will result within each grid and therefore the spatial variability within each grid will have a negligible influence on the computed discharge.

Since the results here are presented for a strictly one-dimensional model, a distinction must be made regarding what is being referred to as the "grid length". Along the direction of flow the grid length would be the maximum node to node spacing required by the model. In the direction transverse to the direction of flow, the watershed would have to be divided into separate flow sections of maximum width equal to the grid length. The model would be applied to each section separately with each resulting discharge routed to the outlet of the basin.

As evidenced by Figure 3.6, there is still relatively large variation in discharge at $t_r / t_e = 1.0$. In section 3.2.3 a value of $\epsilon = 2.0$ provided reasonably small variation in the simulated discharge. If increased accuracy is desired, $\epsilon > 2.0$ could be used. Notice that as ϵ increases, the value of L_g becomes smaller, therefore, as higher accuracy is desired, a smaller grid spacing is indicated by equation (4.1) which would be an expected consequence to obtain greater accuracy. It should be a emphasized that there is a trade-off depending on the chosen value of ϵ. For large values of ϵ, increased accuracy will result but at the expense of more extensive data requirements and more lengthy computation needs. If small values of ϵ are chosen then the converse of the above statement is the result. Therefore, the selection of ϵ should be based upon the best balance of required accuracy, available data, and computer resources. It is possible that equation (4.1) will indicate that a higher degree of resolution is necessary than is available. If this is the case, then data should be collected on a finer scale or it should be noted

that results based on the larger grid spacing are of questionable accuracy.

Figure 4.1 (below) shows the surface describing the Manning resistance equation grid spacing, L_g (in kilometers), as a function of t_r (in hours), and i (in inches per hour), with $\overline{S}$ and $\overline{n}$ held constant at the same base values used in the previous analyses. From equation (4.2a), the grid spacing is most sensitive to the duration of rainfall (since t_r is raised to the 5/3 power), and less sensitive to rainfall intensity (because i is only raised to the 2/3 power). This sensitivity is shown in the figure as well. Note that the curvature of the surface is facing upwards for increasing rainfall duration while the curvature is facing downwards for increasing excess rainfall intensity.

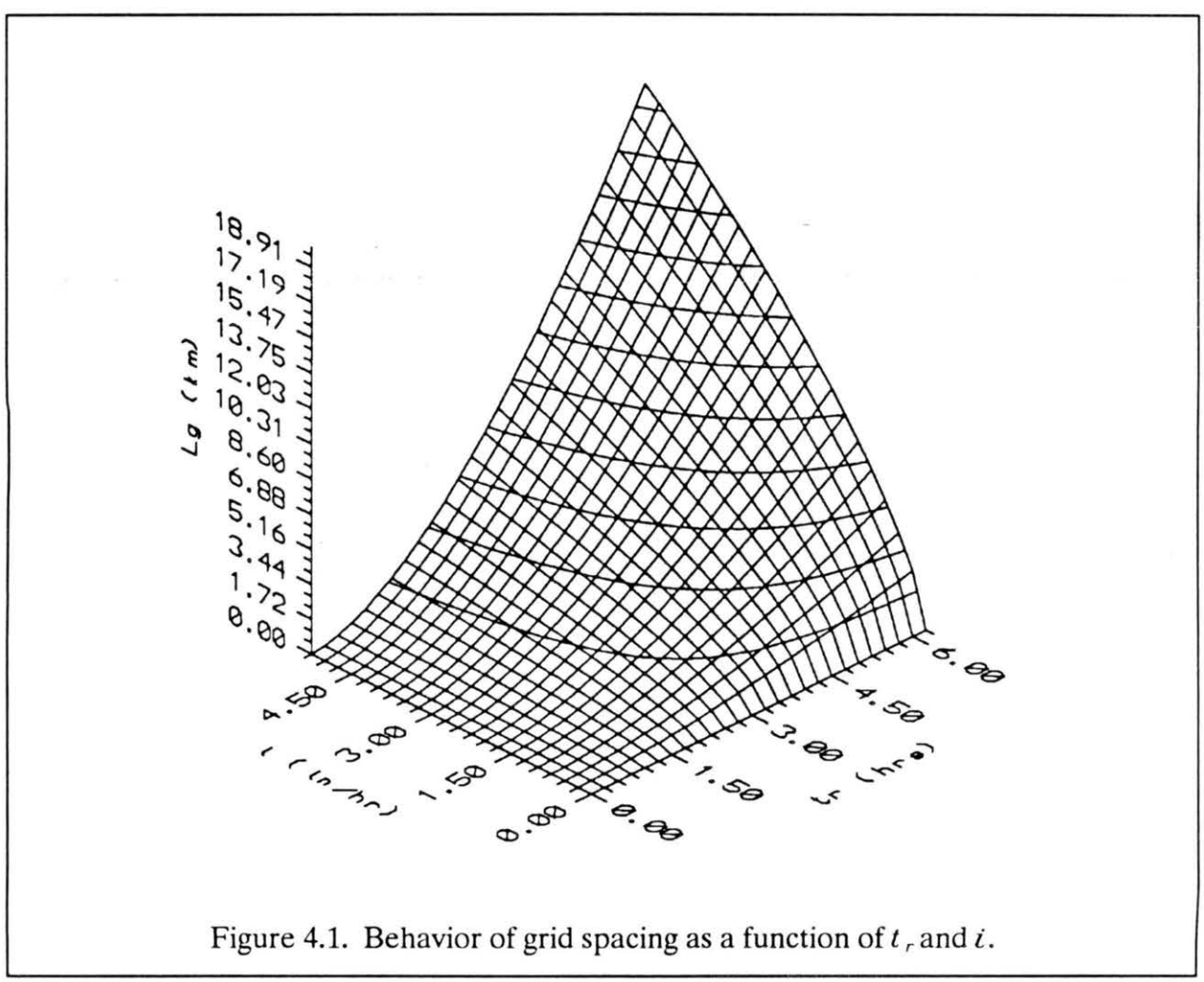

Figure 4.1. Behavior of grid spacing as a function of t_r and i.

Figure 4.1 could be used for a particular watershed. A figure similar to Figure 4.1 could be generated by choosing appropriate values of $\overline{S}$ and $\bar{n}$. Then, depending on the duration and intensity of rainfall being investigated, the figure could be used to determine an appropriate value for the grid spacing.

Considered another way, imaging that the available slope length is set at 1 km. Setting L_g equal to 1 km in equations (4.2a) and (4.2b), a relationship between the rainfall intensity and the duration of rainfall results. This is equivalent to taking a slice parallel to the $i - t_r$ plane at $L_g = 1$ km. The general equation for the grid spacing is:

$$\bar{i} = \left(\frac{L_g}{\left(\frac{t_r}{\epsilon}\right)^{\beta} \alpha} \right)^{1/(\beta-1)} \tag{4.3}$$

The equations for the curves defined by a grid spacing of 1 km are given by:

$$\bar{i} = \left(\frac{1000\bar{n}}{\left(\frac{t_r}{\epsilon}\right)^{5/3} \overline{S}^{1/2}} \right)^{3/2} \tag{4.4a}$$

for the Manning equation, and:

$$\bar{i} = \left(\frac{1000\overline{K}\nu}{\left(\frac{t_r}{\epsilon}\right)^{3} 8g\overline{S}} \right)^{1/2} \tag{4.4b}$$

for the laminar equation. Figures 4.2 and 4.3 show these curves for the Manning and laminar resistance equations, respectively.

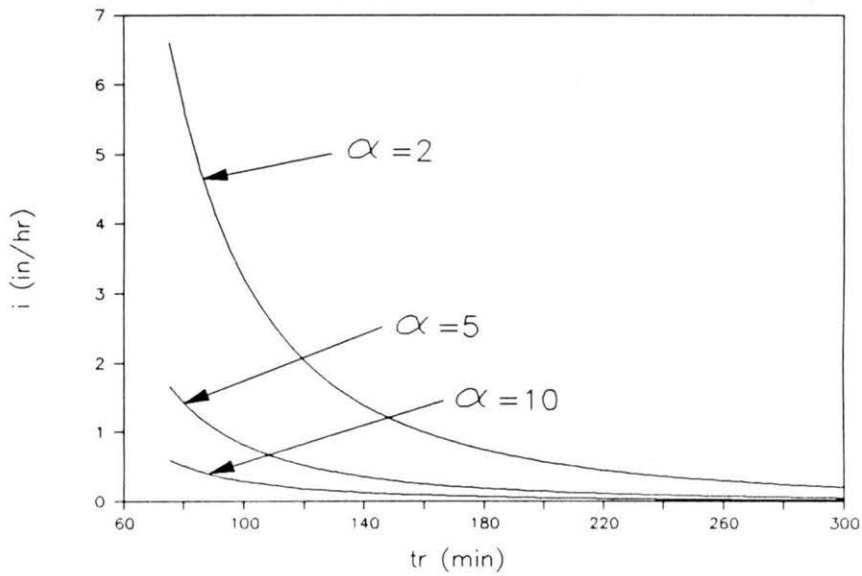

Figure 4.2. Relationship between excess rainfall intensity, i, and duration of rainfall, t_r, for the Manning equation with the grid spacing, L_g, set at 1 km ($\epsilon = 2.0$).

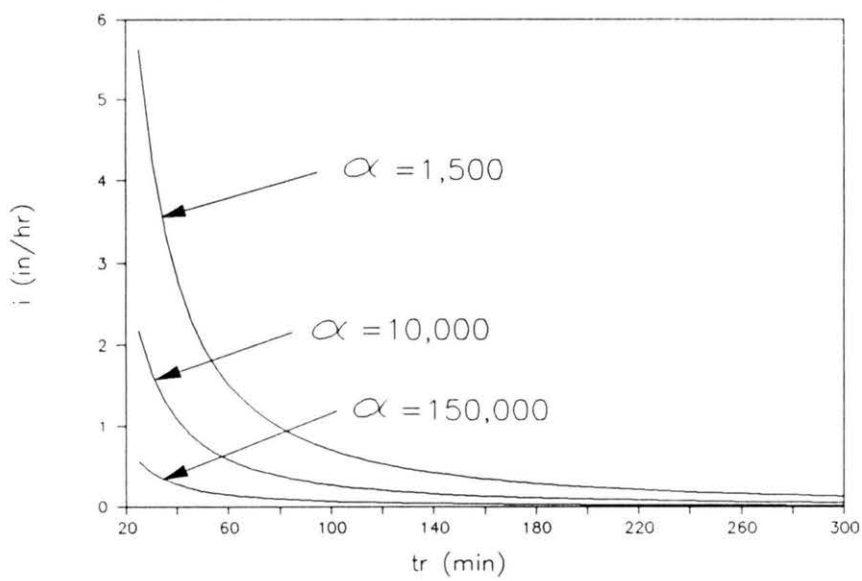

Figure 4.3. Relationship between excess rainfall intensity, i, and duration of rainfall, t_r, for the laminar equation with the grid spacing, L_g, set at 1 km ($\epsilon = 2.0$).

Both of the above figures show the trade-off between rainfall intensity and duration in order to obtain equilibrium. The region above a given α curve indicates complete equilibrium for a 1 km grid size, while the region below indicates partial equilibrium. As α increases the curves shift downwards, indicating that complete equilibrium will result for shorter duration, lower intensity storms. Notice that the general shapes of the curves in the two pictures are the same. The difference is that the laminar equation curves have a higher rate of curvature due to the larger exponent of $\bar{i}$, (2) for the laminar equation as compared to the (2/3) for the Manning equation (see equations (4.4b) and (4.4a), respectively).

As an example, consider a watershed with a mean slope of four percent, and an average Manning's "n" of 0.1. For a three hour duration of rainfall with an average excess intensity of 1.5 in/hr, Figure 4.2 may be used to determine if a 1 km grid spacing is sufficient to describe the spatial variability within the watershed. For these conditions, α is determined by:

$$\alpha = \frac{S^{1/2}}{n} = \frac{(0.04)^{1/2}}{0.1} = 2.0 \qquad (5.5)$$

The point $t_r = 180$ min (3 hours), and $i = 1.5$ in/hr, is located above the curve defining $\alpha = 2$. Therefore, a 1 km spacing will satisfactorily describe the variation within the watershed.

CHAPTER 5 - CONCLUSIONS

In the introduction of this thesis several objectives were outlined. This chapter will state the major conclusions pertaining to each of these objectives.

The degree of variability in overland flow discharge has been shown to be highly dependent on the degree of equilibrium. Figure 3.6, as well as Tables 3.1-3.2 illustrate the differences in model response as a function of t_r / t_o. Regardless of the parameter being varied and regardless of the nature of the distribution function of that parameter, variation in model response has been shown to be large under partial equilibrium conditions and small for complete equilibrium conditions. This difference in variation is due to the constraint that equilibrium discharge is $q = iL$ (see equation (2.10)), which is independent of the hydrologic parameters: slope, Manning's "n", width, and rainfall intensity. In contrast, the discharge under partial equilibrium conditions is highly variable.

Relative variations in computed discharge were shown to differ depending on which overland flow parameter was varied. Using the relative sensitivity, R_s, defined in Section 3.2.3 by equation (3.7), the overland flow hydrographs were shown to be most sensitive to perturbations in rainfall intensity. Manning's "n" and width of the overland flow plane produced comparable sensitivity, but smaller than for rainfall intensity. Output was least sensitive to perturbations in slope (Sections 3.2.1-3.2.3). It was noted in Chapter 3 that this sensitivity ranking ($i > n \approx w > S$) corresponded to the absolute value of the exponents of these parameters in the Manning equation (equations (3.8) and (3.9)). As presented in Section 2.1.3, Wood et al. found that the REA was highly sensitive to topography, with a secondary dependence to rainfall inputs. This may appear to be a contradiction with the findings of this thesis. In fact,

it is not. Wood et al. worked with a model at the catchment scale in which the **overall** parameters were observed to vary from one basin to the next. In this thesis the variability **within** the catchment was examined with no overall variations to the system. Recall in this thesis that variation within the system was constrained such that the mean value of each parameter for each system was set to some chosen base value. There is a profound difference between varying the overall slope of a catchment by say five percent, and allowing the slope within the catchment to vary by five percent. Therefore, their results are not directly comparable with those presented here and no conflict in findings exists.

The results of these analyses were applied to a method to determine a grid spacing which would minimize the effects due to spatial variability in the input parameters (Chapter 4). For a system in which all hydrologic parameters are known, solving for L, in the equation for the time to equilibrium (equation (2.11a) or (2.11b)), yields a length which will ensure complete equilibrium within each grid, thus minimizing the effects of spatial variability within a system. Figures 4.2 and 4.3 show curves which illustrate the relationship between excess rainfall intensity, i, and duration of rainfall, t_r, for several values of α, with the grid spacing, L_g, set to 1 km.

REFERENCES

Bras, R.L. and Rodriguez-Iturbe, 1976, *Rainfall Network Design for Runoff Prediction*, Water Resources Research, Vol. 12, No. 6, pp. 1197-1208.

Crandall, S.H., 1956, Engineering Analysis, McGraw-Hill Book Company, pp. 352-364.

Crawford, N.H. and Linsley, R.K., 1966, Digital Simulation in Hydrology, Stanford Watershed Model IV, Dept. of Civil Engineering, Technical Report No. 39.

Dickinson, W.T., Holland, M.E., and Smith, G.L., 1967, *An Experimental Rainfall Runoff Facility*, Colorado State University, Hydrology Paper No. 25.

Dhatt, G. and Touzot, G., 1984, The Finite Element Method Displayed, English Version, John Wiley & Sons.

Dooge, J.C., 1981, *Parameterization of Hydrologic Processes*, paper presented at the Johnson Space Center Study Conference on Land Surface Processes in Atmospheric General Circulation Models, Greenbelt, USA, January, pp. 243-284.

Eagleson, P.S., 1970, Dynamic Hydrology, McGraw-Hill, Inc.

Garen, D.C. and Burges, S.J., 1977, *Approximate Error Bounds for Simulated Hydrographs*, Proc. Am. Soc. Civil Engrs., J. Hydr. Div., Vol 107, (HY11), pp. 1519-1534.

Iwagaki, Y., 1955, Fundamental Studies on the Runoff Analysis by Characteristics

Julien, P.Y., Moen, C.E., and Sunada, G.U., 1988, *FEM1U User's Manual - A One-Dimensional Finite Element Model for Overland Flow Simulation*, Report CER 87-88 GEO6, Colorado State University, April 1988.

Julien, P.Y., Moglen, G.E., and Sunada, G.U., 1988, *CASC User's Manual - A Finite Element Model for Spatially Varied Overland Flow Simulation*, Report CER 87-88 GEO7, Colorado State University, October 1988.

Keulegan, G.H., 1945, *Spatially Varied Discharge Over a Sloping Plane*, Trans. Amer. Geophys. Union, Part t. pp. 956-969.

Kibler, D.F., and Woolhiser, D.A., 1970, *The Kinematic Cascade as a Hydrologic Model*, Colorado State University, Hydrology Paper No. 39.

Liggett, J.A., and Woolhiser, D.A., 1967, *Difference Solutions of the Shallow-Water Equation*, Proc. Am. Soc. Civil Engrs., J. Mech. Div., Vol. 93, (EM2), pp. 39-71.

Lighthill, M.H. and Whitham, G.B., 1955, *On Kinematic Waves I. Flood Movement in Long Rivers*, Proc. Roy. Soc., Ser. A, Vol. 229, pp. 281-316.

Machado, D. and O'Donnell, T., 1977, *A Stochastic Interpretation of a Lumped Overland Flow Model*, Proc. of the Fort Collins Third International Hydrology Symposium, on Theoretical and Applied Hydrology, Fort Collins, Colorado, pp. 259-269.

McCuen, R.H., 1973, *The Role of Sensitivity Analysis in Hydrologic Modeling*, Journal of Hydrology, Vol. 18, No.1. pp. 37-53.

McCuen, R.H., and Snyder, W.M., 1986, Hydrologic Modeling - Statistical Methods and Applications, Prentice-Hall.

McCuen, R.H., 1989, Hydrologic Analysis and Design, Prentice-Hall.

Moglen, G.E., 1989, On the Effects of Spatial Variability of Overland Flow Parameters, Proceedings - Ninth Annual AGU Front Range Branch Hydrology Days., pp. 1-12.

National Weather Service, 1982, *Hydrometerological Report No. 52, Application of Probable Maximum Precipitation Estimates, United States East of the 105th Meridian*, National Oceanic and Atmospheric Administration, Silver Spring, Maryland.

Richardson, J.R., 1989, *The Influence of Moving Precipitation Fields on Rainfall-Runoff Processes*, Ph.D. dissertation, Dept. of Civil Engineering, Colorado State University, Fort Collins, Colorado.

Rovey, E.W., Woolhiser, D.A., and Smith, R.E., 1977, *A Distributed Kinematic Model of Upland Watersheds*, Colorado State University, Hydrology Paper No. 93.

Shalaby, A.I., 1989, Hydrologic Analysis and Design, (Chapter 13) Prentice-Hall.

Smith, R.E. and Hebbert, R.H.B., 1979, *A Monte Carlo Analysis of the Hydrologic Effects of Spatial Variability of Infiltration*, Water Resources Research, Vol. 15, No. 2. pp. 419-429.

Wilson, C.B., Valdes, J.B., and Rodriguez-Iturbe, I, 1979, *On the Influence of the Spatial Distribution of Rainfall on Storm Runoff*, Water Resources Research, Vol. 15, No. 2, pp. 321-328.

Wood, E.F., 1976, *An Analysis of the Effects of Parameter Uncertainty in Determinisitic Hydrologic Models*, Water Resources Research, Vol. 12, No. 5, pp. 925-932.

Wood, E.F., Sivapalan, M., Beven, K., and Band L., 1988, *Effects of Spatial Variability and Scale with Implications to Hydrologic Modeling*, Journal of Hydrology, Vol. 102, No.1-4, pp. 29-47.

Wooding, R.A., 1965, *A Hydraulic Model for the Catchment-Stream Problem I, Kinematic Wave Theory*, J. Hydrol., Vol. 3, pp. 254-267.

Wooding, R.A., 1965, *A Hydraulic Model for the Catchment-Stream Problem II, Numerical Solutions*, J. Hydrol., Vol. 3, pp. 268-282.

Wooding, R.A., 1966, *A Hydraulic Model for the Catchment-Stream Problem III, Comparison With Runoff Observations*, J. Hydrol., Vol. 4, pp. 21-37.

Woolhiser, D.A. and Liggett, J.A., 1967, *Unsteady, One-dimensional Flow over a Plane: The Rising Hydrograph*, Water Resources Research, Vol 3, No.3, pp. 753-771.

Woolhiser, D.A., 1975, *Simulation of Unsteady Overland Flow*, Chapter 12, Unsteady Flow in Open Channels. (ed. by K. Mahmood and V. Yevjevich), Water Resour. Publ.

Wu, Y.H., Yevjevich, V., And Woolhiser, D.A., 1978, *Effects of Surface Roughness and its Spatial Distribution on Runoff Hydrographs*, Colorado State University, Hydrology Paper No. 96.

APPENDIX A - SOURCE CODE

B-1.1 - CASC, overland flow program

```
    ∇ R←ΔT CASC RI;WG;N;NX;KSI;KSIG;F;W;C;ΔH;CG;I;IT;JAC;MN;MNX;M;WN;RE;
                   DA;CO;IR;IT1;SCY;HP;COL;VIEW;H;S;CTK;K;MH;AL
[1]   VIEW← 0 512 1023 1023
[2]   ⍝
[3]   ⍝ Compute transformation vector
[4]   ⍝
[5]   JAC←0.5×((P-1)↓X)-(-P-1)↓X
[6]   ⍝
[7]   ⍝ Compute slopes for the given X and Y vectors
[8]   ⍝
[9]   S←S[0],S←-(÷(1↓X)-¯1↓X)×(1↓Y)-¯1↓Y
[10]  ⍝
[11]  ⍝ Make a table for identifying nodes for each element
[12]  ⍝
[13]  CG←(⍳P)∘.+⍳⍴Y
[14]  MH←0×RI
[15]  ⍝
[16]  ⍝ Set weighting factor and make local coordinates for Gauss points
[17]  ⍝
[18]  WG←⍎'WG',⍕PG
[19]  KSIG←⍎'KSIG',⍕PG
[20]  MH[;1]←H←RI[;0]×ΔT⍳□←⍎⍕'ΔTE[',(⍕RES),';]',0⍴IR←⌈/,RI ⍝←RI+1E¯10×⌈/,RI
[21]  MN←(KSIG∘.*⍳P)+.×⍸(P,P)⍴(¯1+(2÷P-1)×⍳P)∘.*⍳P
[22]  MNX←((((⍴KSIG),P)⍴⍳P)×KSIG∘.*0⌈¯1+⍳P)+.×⍸(¯1+(2÷P-1)×⍳P)∘.*⍳P
[23]  ⍝
[24]  ⍝ Initialize graphics controls
[25]  ⍝
[26]  INIT
[27]  COL←6
[28]  (SCY←800÷⌈/Y+0.1×(⌈/Y)-⌊/Y)ES80(1,⍴Y)⍴Y-0.01×(⌈/Y)-⌊/Y
[29]  VIEW←□GVIEW VIEW
[30]  COL←3
[31]  (800÷⌈/,RI)ES80(1,⍴RI[;0])⍴RI[;0]
[32]  (800÷⌈/,RI)ES80(1,⍴RI[;0])⍴RI[;1]
[33]  VIEW←□GVIEW VIEW
[34]  ' OF 50' □GWRITE 75 750 7
[35]  (⍕ITER+1)□GWRITE 0 750 7
[36]  ' D:HH:MM:SS' □GWRITE 75 850 7
[37]  IT←1
[38] AA:IT←IT+1 ⍝ Start of AA loop
[39]  ⍝
[40]  ⍝ Display time and iteration number on the screen
[41]  ⍝
[42]  (⍕IT)□GWRITE 0 850 7
[43]  (TIME(IT×ΔT))□GWRITE 75 950 7
[44]  ⍝
[45]  ⍝ Program will iterate until rainfall greater than 1E¯10 is encountered
[46]  ⍝
[47]  →(((⌈/RI[;IT1←IT])<1E¯10)/AA ⍝ End of AA loop
[48]  ⍝
[49]  ⍝ Large number sets upstream boundary to zero depth
[50]  ⍝
[51] A:K←((⍴Y),⍴Y)⍴10000000000⋄M←0 ⍝ Start of A loop
[52]  HP←,MH[;IT-1]
[53]  ⍝
[54]  ⍝ Display most recent iteration that the K matrix was rebuilt
[55]  ⍝
[56]  (⍕IT)□GWRITE 0 950 7
[57]  →(IT>IT1)/E ⍝ Go to E
[58]  C←F←((⍴Y),⍴Y)⍴0
```

CASC, overland flow program - continued

```
[59] E:I←0 ⍝ Start of E loop
[60]  KSI←KSIG[M]
[61]  W←WG[M]
[62]  WN←W×⍉N←(1,P)⍴MN[M;]
[63]  NX←(1,P)⍴MNX[M;]
[64] B:CO←CG[;I] ⍝ Start of B loop
[65]  →(IT>IT1)/BB ⍝ Go to BB
[66] ⍝
[67] ⍝ Build the F, C, and K matrices
[68] ⍝
[69]  F[CO;CO]←F[CO;CO]+(W×JAC[I])×(⍉N)+.×N
[70]  C[CO;CO]←C[CO;CO]+WN+.×N×(N+.×(P,1)⍴WI[CO])×JAC[I]
[71] BB:K[CO;CO]←K[CO;CO]+WN+.×⍉⍤1⊢KDA ⍝ Start of BB
[72]  →((⍴X)>(P-1)+I←I+P-1)/B ⍝ End of B loop
[73]  →((⍴WG)>M←M+1)/E ⍝ End of E loop
[74]  CTK←⌹C+ΔT×K
[75] ⍝
[76] ⍝ Iterations will start here if K matrix isn't rebuilt
[77] ⍝
[78] DD:MH[;IT]←H←0⌈H+ΔH←CTK+.×(ΔT×(F+.×RI[;IT-1]×WI)-K+.×H)
              +C+.×MH[;IT-1]-H←0⌈H ⍝ Start of DD loop
[79] ⍝
[80] ⍝ Check to see if change in depths is sufficiently small - if not,
[81] ⍝ then go to DD
[82] ⍝
[83]  →(0.2<(+/ΔH*2)÷+/H*2)/DD
[84]  COL←1+8×RI[;IT]≠0
[85]  SCY ES80(1,⍴Y)⍴Y+0⌈H×SC
[86]  VIEW←⎕GVIEW VIEW
[87]  COL←3
[88]  (800÷⌈/,RI)ES80(1,⍴RI[;0])⍴RI[;IT]
[89]  VIEW←⎕GVIEW VIEW
[90] ⍝
[91] ⍝ Display time and iteration number on the screen
[92] ⍝
[93]  (⍕IT←IT+1)⎕GWRITE 0 850 7
[94]  (TIME(IT×ΔT))⎕GWRITE 75 950 7
[95] ⍝
[96] ⍝ Loop back to DD - K matrix will not be rebuilt - End of DD loop
[97] ⍝
[98]  →(((1.1>(÷0.999⌊1E¯10⌈(1↓HP⌈H)÷1↓HP⌈H)*ΔEXP[RES]))∧(¯1↑⍴RI)>IT)/DD
[99] ⍝
[100] ⍝ Loop back to A - K matrix will be rebuilt - End of A loop
[101] ⍝
[102]  →((¯1↑⍴RI)>IT)/A
[103]  COL←1
[104]  CLOSE
[105] ⍝
[106] ⍝ Store hydrographs in matrix, R
[107] ⍝
[108]  MHTEMP←MH[ORDER-1;]
[109]  R←(MH[ORDER-1;]*1.67)×(S[ORDER-1]*0.5)×WI[ORDER-1]÷MAN[ORDER-1]
[110]
    ∇
```

B-1.2 - CASC related programs

```
    ∇ INIT
[1]  ⍝
[2]  ⍝ This function initializes the graphics display
[3]  ⍝
[4]   0 0 ⍴(⎕GCARD, 0 0)⎕GINIT 'IBMCOLOR'
[5]   0 ⎕GSHADE 0 0 1023 1023
[6]   0 0 ⍴⎕GVIEW 0 0 1023 511
    ∇
    ∇ DISP80 M;VIEW
[1]  ⍝
[2]  ⍝ This function displays the results of a calculation stored in M
[3]  ⍝
[4]  ⍝ Initializes the  graphics mode and clears the screen
[5]  ⍝
[6]   0.0⍴((⎕GCARD,0.0)⎕GINIT 'IBMCOLOR')
[7]   0 ⎕GSHADE 0 0 1023 1023
[8]   COL←7
[9]  ⍝
[10] ⍝ Sets the viewport for the upper half of the screen and display
[11] ⍝ the spatial hydrograph
[12] ⍝
[13]  VIEW←⎕GVIEW 0 0 1023 511
[14]  (800÷⌈/,M)ES80⍉M
[15] ⍝
[16] ⍝ Annotates the spatial hydrograph
[17] ⍝
[18]  'DISCHARGE' ⎕GWRITE 0 0 ,COL
[19]  'DISTANCE' ⎕GWRITE 450 950 ,COL
[20] ⍝
[21] ⍝ Sets the viewport to the lower half of the screen and display the
[22] ⍝ temporal hydrograph
[23] ⍝
[24]  VIEW←⎕GVIEW 0 512 1023 1023
[25]  (800÷⌈/,M)ES80 M
[26] ⍝
[27] ⍝ Annotates the temporal hydrograph
[28] ⍝
[29]  'DISCHARGE' ⎕GWRITE 0 0 ,COL
[30]  'TIME' ⎕GWRITE 470 950 ,COL
[31]  0 0 ⍴⎕INKEY
[32]  0 0 ⍴3 ⎕INT 16
    ∇
    ∇ SC ES80 M;I
[1]  ⍝
[2]  ⍝ This function does the actual plotting of the water surface
[3]  ⍝ profiles and hydrographs
[4]  ⍝
[5]   I←⎕IO
[6]  ⍝10⍴⎕AV[10]
[7]  A:COL ⎕GLINE(1,(1↓⍴M),2)⍴(100+800×(⍳1↓⍴M)÷1↓⍴M),[0.1]900-SC×M[I;]
[8]   →((1↑⍴M)>I←I+1)/A
    ∇

    ∇ CLOSE
[1]   0 0 ⍴3 ⎕INT 16
    ∇
```

CASC related programs - continued

```
    ∇ M←TIME T;VV;SEC;MIN;HRS;DAY
[1]   ⍝
[2]   ⍝ This function reads in the time, T, in seconds and returns a vector
[3]   ⍝ of days, hours, minutes, and seconds for the CASC program
[4]   ⍝
[5]    VV← 31 24 60 60 ⊤T
[6]    SEC←(⍕('I2' ⎕FMT VV[3]))
[7]    MIN←(⍕('I2' ⎕FMT VV[2]))
[8]    HRS←(⍕('I2' ⎕FMT VV[1]))
[9]    DAY←(⍕('I2' ⎕FMT VV[0]))
[10]   →(SEC[0;0]=' ')/LSEC
[11]  ⍝
[12]  ⍝ The remaining statements put in leading zeros if needed
[13]  ⍝
[14]  BACK1:→(MIN[0;0]=' ')/LMIN
[15]  BACK2:→(HRS[0;0]=' ')/LHRS
[16]  BACK3:M←DAY,':',HRS,':',MIN,':',SEC
[17]   →EXIT
[18]  LSEC:SEC[0;0]←'0' ⋄ →BACK1
[19]  LMIN:MIN[0;0]←'0' ⋄ →BACK2
[20]  LHRS:HRS[0;0]←'0' ⋄ →BACK3
[21]  EXIT:
    ∇
```

B-1.3 - CASC related variables

```
∆RES
LAMINAR
BLASIUS
MANNING
DARCY-WEISBACH
CHEZY

∆ALP
((P,1)ρWI[CO]×8×G×S[CO]+KK[CO]×NU)
((P,1)ρWI[CO]×((8×G×S[CO]+.316)*.57)+NU*.14)
((P,1)ρWI[CO]×(S[CO]*.5)+MAN[CO])
((P,1)ρWI[CO]×(8×G×S[CO]+DWF[CO])*.5)
((P,1)ρWI[CO]×CHE[CO]×(S[CO]+3.28)*.5)

∆EXP
2
0.72
0.67
0.5
0.5

∆KDA
((N+.×(0⌈H[CO])*∆EXP[RES])×((N+.×AL×1+∆EXP[RES])+.×NX)+
                              (NX+.×(AL+⍉∆ALP[RES;])+.×N))

∆Q
8×G×(⍟(ΦρMH)ρS)×(⍟(1ΦρMH)ρWI+KK)×(MH*3)+NU
(((8×G×(⍟(ΦρMH)ρS)+.22)*.57)+(NU*.14))×(⍟(1ΦρMH)ρWI)×MH*1.72
((⍟(ΦρMH)ρS)*.5)×(⍟(1ΦρMH)ρWI+MAN)×MH*1.67
((8×G×⍟(ΦρMH)ρS)*.5)×(⍟(1ΦρMH)ρWI+DWF*.5)×MH*1.5
(((⍟(ΦρMH)ρS)+3.28)*.5)×(⍟(1ΦρMH)ρWI×CHE)×MH*1.5

∆TE
(KK×NU×X+8×G×S×IR*2)*÷3
(((.22÷8×G×S)*.57)×(NU*.14)×X+IR*.72)*.58
(MAN×X+(S*.5)×IR*.67)*.6
(DWF×(X*2)+8×G×S×IR)*÷3
(((X+CHE)*2)×3.28+S×IR)*÷3
```

B-1.4 - RANDOM, spatially uncorrelated/spatially correlated random simulation function

```
    ∇ LA RANDOM AM;DIS;Y;MAN;WI;ITER
[1]  ⍝
[2]  ⍝ This is the controller function for the random perturbation
[3]  ⍝ analysis
[4]  ⍝
[5]   □←×/(¯1↓AM)* 0.5 1 1
[6]   AM←(AM-1)÷1↑AM
[7]   DIS←(PATTERN3[COUNTR3],1)⍴0
[8]  ⍝
[9]  ⍝ Build perturbed input matrix
[10] ⍝
[11]  MY←MEL AM[0]
[12]  MANNING←MMAN AM[1]
[13]  MW←MWI AM[2]
[14]  MRI←MVP AM[3]
[15]  ITER←0
[16] A:Y←MY[;ITER]
[17]  MAN←MANNING[;ITER]
[18]  WI←MW[;ITER]
[19] ⍝
[20] ⍝ Call DCASC
[21] ⍝
[22]  DIS←DIS,[1],(PATTERN3[COUNTR3])↑R←LA DCASC VP←MRI[;ITER]
[23]  →(50>ITER←ITER+1)/A
[24]  CLEARFILES
[25]  MDIS←((RANK),50)↑ 0 1 ↓DIS
[26]
    ∇


    ∇ LA RANDOM AM;DIS;Y;MAN;WI;ITER
[1]  ⍝
[2]  ⍝ This function is used specifically for the spectral analysis
[3]  ⍝ as the random control code (see below)
[4]  ⍝
[5]   □←×/(¯1↓AM)* 0.5 1 1
[6]   AM←(AM-1)÷1↑AM
[7]   DIS←(PATTERN3[COUNTR3],1)⍴0
[8]   MANNING←MMAN AM[1]
[9]   MW←MWI AM[2]
[10]  MRI←MVP AM[3]
[11]  ITER←0
[12] ⍝
[13] ⍝ MY1 and MY2 are matrices containing the spectral slope profiles
[14] ⍝
[15] A:Y←⍎('MY',(⍕NLOOP),'[;ITER]')
[16]  MAN←MANNING[;ITER]
[17]  WI←MW[;ITER]
[18]  DIS←DIS,[1],(PATTERN3[COUNTR3])↑R←LA DCASC VP←MRI[;ITER]
[19]  →(50>ITER←ITER+1)/A
[20]  CLEARFILES
[21] ⍝DISP80 MY
[22]  MDIS←((RANK),50)↑ 0 1 ↓DIS
[23] ⍝DISP80 MDIS
[24]
    ∇
```

B-1.5 - RANDOM related functions

```
    ∇ R←MEL AM;I
[1]  ⍝
[2]  ⍝ This function generates the pertubed slope profiles using the
[3]  ⍝ function NEWY
[4]  ⍝
[5]   R←(11÷ORDER)×⍉(50,ORDER)⍴ORDER-⍳ORDER
[6]   I←1
[7]  A:R[;I]←NEWY AM
[8]   →(50>I←I+1)/A
    ∇

    ∇ R←NEWY AM;RA
[1]  ⍝
[2]  ⍝  This function computes a single perturbed slope profile and returns
[3]  ⍝  the value to function MEL
[4]   RA←0,(1-AM)+2×AM×0.1×?(ORDER-1)⍴11
[5]   R←Y←11-(10÷+/RA)×+\RA
    ∇

    ∇ R←MMAN AM;I;DMAN
[1]  ⍝
[2]  ⍝ This function generates the perturbed Manning's 'n' values
[3]  ⍝
[4]   R←(ORDER,50)⍴0.1
[5]   DMAN←0.1×AM
[6]   I←1
[7]  A:R[;I]←(0.1-DMAN)+2×DMAN×0.1×?ORDER⍴11
[8]   R[;I]←R[;I]×0.1÷(+/R[;I]÷ORDER)
[9]   →(50>I←I+1)/A
    ∇

    ∇ R←MWI AM;I;DWI
[1]  ⍝
[2]  ⍝ This function generates the perturbed overland flow widths
[3]  ⍝
[4]   R←(ORDER,50)⍴10
[5]   DWI←10×AM
[6]   I←1
[7]  A:R[;I]←(10-DWI)+2×DWI×0.1×?ORDER⍴11
[8]   R[;I]←R[;I]×10÷(+/R[;I]÷ORDER)
[9]   →(50>I←I+1)/A
[10]
    ∇

    ∇ R←MVP AM;I
[1]  ⍝
[2]  ⍝ This function generates the spatially perturbed rainfall intensity
[3]  ⍝ matrix
[4]  ⍝
[5]   R←(ORDER,50)⍴1
[6]   I←1
[7]  A:R[;I]←(1-AM)+2×AM×0.1×?ORDER⍴11
[8]   R[;I]←R[;I]×1÷(+/R[;I]÷ORDER)
[9]   →(50>I←I+1)/A
    ∇
```

RANDOM related functions - continued

```
    ∇ R←LA DCASC VR;RI0;RI
[1]  ⍝
[2]  ⍝ This function is called from RANDOM and is used to initialize the
[3]  ⍝ parameters used by CASC, set the time step, and create the
[4]  ⍝ rainfall intensity matrix
[5]  ⍝
[6]   ⎕IO←0
[7]   RES←2
[8]   SC←100
[9]   X←10×(11÷ORDER)×⍳ORDER
[10]  RI←VR∘.×(PATTERN3[COUNTR3])↑(10×LA)⍴RI0←1E¯5
[11] ⍝
[12] ⍝ Determine time step
[13] ⍝
[14]  TE←(0.1×100÷(((⌈/Y)-⌊/Y)÷(⌈/X)-⌊/X)*0.5)×(1E¯5)*2÷3)*0.6
[15] ⍝ ΔT←0.1×(2×(⌈/TE)×LA)⌊⌈/TE
[16]  ΔT←0.1×TE
[17] ⍝
[18] ⍝ Call CASC
[19] ⍝
[20]  R←ΔT CASC RI
[21] ⍝MQ←ΔT CASC RI
[22] ⍝R←MQ[(ORDER-1);]
    ∇
```

B-1.6 - Control Code, functions used to drive the RANDOM code

B-1.6.1 - MASTER, primary rainfall durations random control code

```
    ∇ MASTER;AM;COUNTR1;COUNTR2;COUNTR3;COUNTR4;COUNTR5;COUNTR6;HYD;ROW;
            PATTERN1;PATTERN2;PATTERN3;RANK;PEAK;FILE1;FILE2;COL;ORDER;
            FILE3;STATS;STEMP;S2;LENPLANE;LA;YTEMP;SUMQ;SUMR;ENV
[1]  ⍝
[2]  ⍝ This function performs the random perturbation data analysis
[3]  ⍝ for Chapter 3
[4]  ⍝
[5]   PATTERN1← 2 4 6
[6]   PATTERN2← 0.4 1 5
[7]   PATTERN3← 50 50 100
[8]  ⍝
[9]  ⍝ Initialize all variables
[10] ⍝
[11]  COUNTR1←0 ⋄ COUNTR2←0 ⋄ COUNTR3←0 ⋄ COUNTR4←0 ⋄ COUNTR5←1
                ⋄ ORDER←11 ⋄ NLOOP←1
[12]  AM← 1 1 1 1
[13] ⍝
[14] ⍝ Set patterns for RANDOM
[15] ⍝
[16] NEWLA:LA←PATTERN2[COUNTR3]
[17]  RANK←PATTERN3[COUNTR3]
[18]  PEAK←(RANK,12)⍴0
[19]  HYD←(RANK,50)⍴0
[20]  ENV←(ORDER,50)⍴0
[21] NEWAM:AM[COUNTR1]←PATTERN1[COUNTR2]
[22] ⍝
[23] ⍝ Execute RANDOM
[24] ⍝
[25]  LA RANDOM AM
[26] ⍝
[27] ⍝ Perform mass balance on all 50 hydrographs
[28] ⍝
[29]  COLUMN←0
[30] MASS:SUMQ←+/MDIS[;COLUMN]
[31]  LENPLANE←(110÷ORDER)×(ORDER-1)
[32]  MDIS[;COLUMN]←MDIS[;COLUMN]×1E¯3×LA×LENPLANE÷SUMQ
[33]  COLUMN←COLUMN+1
[34]  →(COLUMN≤49)/MASS
[35] ⍝
[36] ⍝ Save largest and smallest values at each time step over 50 hydrographs
[37] ⍝
[38]  ROW←0
[39] MAKEHYD:HYD[ROW;COUNTR4]←⌈/MDIS[ROW;]
[40]  HYD[ROW;COUNTR5]←⌊/MDIS[ROW;]
[41]  ROW←ROW+1
[42]  →(ROW≤(RANK-1))/MAKEHYD
[43] ⍝
[44] ⍝ Save input parameter envelope
[45] ⍝
[46]  ROW←0
[47] MAKENV:ENV[;COUNTR4]←⌈/⍎'ΔENV[',(⍕COUNTR1),';]'
[48]  ENV[;COUNTR5]←⌊/⍎'ΔENV[',(⍕COUNTR1),';]'
[49]  ROW←ROW+1
[50]  →(ROW≤ORDER-1)/MAKENV
[51] ⍝
[52] ⍝ Create standard deviation hydrographs
[53] ⍝
[54]  ROW←0 ⋄ COUNTR6←COUNTR4÷2
[55] SDEV:PEAK[ROW;COUNTR6]←(((+/((MDIS[ROW;]-MDIS[ROW;0])*2)÷49))
                            *0.5)÷MDIS[ROW;0]
```

MASTER, primary rainfall durations random control code - continued

```
[56]  ROW←ROW+1
[57]  →(ROW≤(RANK-1))/SDEV
[58] ⍝
[59] ⍝ Collect statistics on input variables
[60] ⍝
[61]  →(COUNTR1≠0)/MAKESTATS
[62]  S2←(ORDER,50)⍴0
[63]  ITER←0
[64] MAKES:YTEMP←MY[;ITER]
[65]  STEMP←-(÷(1↓X)-¯1↓X)×(1↓YTEMP)-¯1↓YTEMP
[66]  S2[;ITER]←STEMP[0],STEMP
[67]  ITER←ITER+1
[68]  →(ITER<50)/MAKES
[69] MAKESTATS:STATS←STAT,⍕'⍙STAT[',(⍕COUNTR1),';]'
[70]  FILE3←'D:\GEM\ST',(⍕NLOOP),(⍕ORDER),(⍕COUNTR1),(⍕COUNTR2),
          (⍕(COUNTR3+1)),'.DAT'
[71]  FILE3 EXPORT STATS
[72] ⍝
[73] ⍝ Reset values to be used by RANDOM
[74] ⍝
[75]  COUNTR4←COUNTR4+2 ⋄ COUNTR5←COUNTR5+2
[76]  COUNTR2←COUNTR2+1
[77]  →(COUNTR2≤2)/NEWAM
[78]  COUNTR1←COUNTR1+1
[79]  COUNTR2←0 ⋄ AM← 1 1 1 1
[80]  →(COUNTR1≤3)/NEWAM
[81] ⍝
[82] ⍝ Export output data files
[83] ⍝
[84]  FILE1←'D:\GEM\HYD',(⍕NLOOP),(⍕(COUNTR3+1)),(⍕ORDER),'.DAT'
[85]  FILE1 EXPORT,&HYD
[86]  FILE2←'D:\GEM\PEAK',(⍕NLOOP),(⍕(COUNTR3+1)),(⍕ORDER),'.DAT'
[87]  FILE2 EXPORT,&PEAK
[88]  FILE3←'D:\GEM\ENV',(⍕NLOOP),(⍕(COUNTR3+1)),(⍕ORDER),'.DAT'
[89]  FILE3 EXPORT,&ENV
[90]  COUNTR1←0 ⋄ COUNTR3←COUNTR3+1 ⋄ COUNTR4←0 ⋄ COUNTR5←1
[91]  (COUNTR3≤2)/NEWLA
[92]  NLOOP←NLOOP+1 ⋄ COUNTR3←0
[93]  →(NLOOP≤2)/NEWLA
[94]
    ∇
```

B-1.6.2 - NEWMASTER, multiple rainfall durations random control code

```
    ∇ NEWMASTER;AM;COUNTR1;COUNTR3;COUNTR4;COUNTR5;COUNTR6;HYD;ROW;PATTERN2;
                PATTERN3;RANK;PEAK;FILE1;FILE2;COL;ORDER;FILE3;STATS;STEMP;
                S2;LENPLANE;LA;YTEMP;SUMQ;SUMR;ENV
[1]   ⍝
[2]   ⍝ This function performs the analysis required to determine
[3]   ⍝ the Rs vs tr/te relationship
[4]   ⍝
[5]    PATTERN2← 0.6 0.8 1.1 1.2 1.3 1.4 1.5 1.8 2 2.5 3 4 7 10
[6]    PATTERN3← 50 50 50 50 50 50 50 50 50 100 100 100 120 150
[7]   ⍝
[8]   ⍝ Initialize all variables
[9]   ⍝
[10]   COUNTR1←0 ⋄ COUNTR3←0 ⋄ COUNTR4←0 ⋄ COUNTR5←1 ⋄ ORDER←11 ⋄ NLOOP←1
[11]   AM← 1 1 1 1
[12]  ⍝
[13]  ⍝ Set patterns for RANDOM
[14]  ⍝
[15]  NEWLA:LA←PATTERN2[COUNTR3]
[16]   RANK←PATTERN3[COUNTR3]
[17]   PEAK←(RANK,4)⍴0
[18]   HYD←(RANK,8)⍴0
[19]   ENV←(ORDER,8)⍴0
[20]  NEWAM:AM[COUNTR1]←4
[21]  ⍝
[22]  ⍝ Execute RANDOM
[23]  ⍝
[24]   LA RANDOM AM
[25]  ⍝
[26]  ⍝ Perform mass balance on all 50 hydrographs
[27]  ⍝
[28]   COLUMN←0
[29]  MASS:SUMQ←+/MDIS[;COLUMN]
[30]   LENPLANE←(110÷ORDER)×(ORDER-1)
[31]   MDIS[;COLUMN]←MDIS[;COLUMN]×1E¯3×LA×LENPLANE÷SUMQ
[32]   COLUMN←COLUMN+1
[33]   →(COLUMN≤49)/MASS
[34]  ⍝
[35]  ⍝ Save largest and smallest values at each time step over 50 hydrographs
[36]  ⍝
[37]   ROW←0
[38]  MAKEHYD:HYD[ROW;COUNTR4]←⌈/MDIS[ROW;]
[39]   HYD[ROW;COUNTR5]←⌊/MDIS[ROW;]
[40]   ROW←ROW+1
[41]   →(ROW≤(RANK-1))/MAKEHYD
[42]  ⍝
[43]  ⍝ Save input parameter envelope
[44]  ⍝
[45]   ROW←0
[46]  MAKENV:ENV[;COUNTR4]←⌈/⍎'⍙ENV[',(⍕COUNTR1),';]'
[47]   ENV[;COUNTR5]←⌊/⍎'⍙ENV[',(⍕COUNTR1),';]'
[48]   ROW←ROW+1
[49]   →(ROW≤ORDER-1)/MAKENV
[50]  ⍝
[51]  ⍝ Create standard deviation hydrographs
[52]  ⍝
[53]   ROW←0 ⋄ COUNTR6←COUNTR4÷2
[54]  SDEV:PEAK[ROW;COUNTR6]←(((+/((MDIS[ROW;]-MDIS[ROW;0])*2)÷49))
                            *0.5)÷MDIS[ROW;0]
[55]   ROW←ROW+1
[56]   →(ROW≤(RANK-1))/SDEV
```

NEWMASTER, multiple rainfall durations random control code - continued

```
[57] ⍝
[58] ⍝ Collect statistics on input variables
[59] ⍝
[60]  →(COUNTR1≠0)/MAKESTATS
[61]  S2←(ORDER,50)⍴0
[62]  ITER←0
[63] MAKES:YTEMP←MY[;ITER]
[64]  STEMP←-(÷(1↓X)-¯1↓X)×(1↓YTEMP)-¯1↓YTEMP
[65]  S2[;ITER]←STEMP[0],STEMP
[66]  ITER←ITER+1
[67]  →(ITER<50)/MAKES
[68] MAKESTATS:STATS←STAT,⍎⍎'⍙STAT[',(⍕COUNTR1),';]'
[69]  FILE3←'C:\GEM\ST',(⍕NLOOP),(⍕COUNTR1),(⍕(COUNTR3+1)),'.DAT'
[70]  FILE3 EXPORT STATS
[71] ⍝
[72] ⍝ Reset values to be used by RANDOM
[73] ⍝
[74]  COUNTR4←COUNTR4+2 ⋄ COUNTR5←COUNTR5+2
[75]  COUNTR1←COUNTR1+1
[76]  AM← 1 1 1 1
[77]  →(COUNTR1≤3)/NEWAM
[78] ⍝
[79] ⍝ Export data to output data files
[80] ⍝
[81]  FILE1←'C:\GEM\',(⍕NLOOP),'HYD',(⍕(COUNTR3+1)),(⍕ORDER),'.DAT'
[82]  FILE1 EXPORT,&HYD
[83]  FILE2←'C:\GEM\',(⍕NLOOP),'PEK',(⍕(COUNTR3+1)),(⍕ORDER),'.DAT'
[84]  FILE2 EXPORT,&PEAK
[85]  FILE3←'C:\GEM\',(⍕NLOOP),'ENV',(⍕(COUNTR3+1)),(⍕ORDER),'.DAT'
[86]  FILE3 EXPORT,&ENV
[87]  COUNTR1←0 ⋄ COUNTR3←COUNTR3+1 ⋄ COUNTR4←0 ⋄ COUNTR5←1
[88]  →(COUNTR3≤1)/NEWLA
[89]  NLOOP←NLOOP+1 ⋄ COUNTR3←0
[90]  →(NLOOP≤2)/NEWLA
[91]
    ∇
```

B-1.6.3 - PEAK, multiple rainfall duration peaks random control code

```
    ∇ PEAK;AM;COUNTR1;COUNTR3;COUNTR4;COUNTR5;COUNTR6;HYD;ROW;PATTERN2;
          PATTERN3;RANK;PEAK;FILE1;FILE2;COL;ORDER;FILE3;STATS;STEMP;
          S2;LENPLANE;LA;YTEMP;SUMQ;SUMR;ENV
[1]   ⍝
[2]   ⍝ This function collects the peaks observed over 50
[3]   ⍝ systems and shown in Chapter 3
[4]   ⍝
[5]    PATTERN2← 0.3 0.4 0.6 0.8 1 1.1 1.2 1.3 1.4 1.5 2
[6]    PATTERN3← 50 50 50 50 50 50 50 50 50 50 50
[7]   ⍝
[8]   ⍝ Initialize all variables
[9]   ⍝
[10]   COUNTR1←0 ⋄ COUNTR3←0 ⋄ ORDER←11
[11]   AM← 1 1 1 1
[12]  ⍝
[13]  ⍝ Set patterns for RANDOM
[14]  ⍝
[15]  NEWLA:LA←PATTERN2[COUNTR3]
[16]   RANK←PATTERN3[COUNTR3]
[17]   PEAK←RANK⍴0
[18]  NEWAM:AM[COUNTR1]←4
[19]  ⍝
[20]  ⍝ Execute RANDOM
[21]  ⍝
[22]   LA RANDOM AM
[23]  ⍝
[24]  ⍝ Perform mass balance on all 50 hydrographs
[25]  ⍝
[26]   COLUMN←0
[27]  MASS:SUMQ←+/MDIS[;COLUMN]
[28]   LENPLANE←(110÷ORDER)×(ORDER-1)
[29]   MDIS[;COLUMN]←MDIS[;COLUMN]×1E¯3×LA×LENPLANE÷SUMQ
[30]   COLUMN←COLUMN+1
[31]   →(COLUMN≤49)/MASS
[32]  ⍝
[33]  ⍝ Save hydrograph peaks observed over 50 systems
[34]  ⍝
[35]   COLUMN←0
[36]  SDEV:PEAK[COLUMN]←(⌈/MDIS[;COLUMN])+(⌈/MDIS[;0])
[37]   COLUMN←COLUMN+1
[38]   →(COLUMN≤49)/SDEV
[39]  ⍝
[40]  ⍝ Reset values to be used by RANDOM and export output data
[41]  ⍝
[42]   FILE2←'D:\GEM\DATA\PEAK',(⍕COUNTR1+1),(⍕(COUNTR3+1)),'.DAT'
[43]   FILE2 EXPORT,PEAK
[44]   COUNTR3←COUNTR3+1
[45]   →(COUNTR3≤10)/NEWLA
[46]   COUNTR1←COUNTR1+1
[47]   COUNTR3←0
[48]   →(COUNTR1≤3)/NEWLA
    ∇
```

B-1.7 - Miscellaneous Functions

B-1.7.1 - EXPORT, function used to send data from the APL environment

```
    ∇ FNAME EXPORT VALUES;STRING;I
[1]  ⍝
[2]  ⍝ This function enables the user to export data from an APL workspace
[3]  ⍝ to an ASCII file.
[4]  ⍝
[5]  ⍝ FNAME is the name of the ASCII file you wish to export the data to.
[6]  ⍝ FNAME must be placed in single quotes and must not already exist.
[7]  ⍝
[8]  ⍝ VALUES is a vector of values you wish to export.  If the user wishes
[9]  ⍝ to export a matrix of values the matrix must first be raveled by
[10] ⍝ placing a comma in front of the matrix name.
[11] ⍝
[12] ⍝ Example statement:
[13] ⍝       'B:MYDATA.DAT' EXPORT ,MATRIX
[14] ⍝
[15]  FNAME ⎕NCREATE ¯1
[16]  I←⎕IO
[17] L1:STRING←,'E12.4' ⎕FMT VALUES[I]
[18]  STRING[((⍳⍴STRING)×' '≤STRING)~0]←'-'
[19]  (STRING,⎕TCNL,⎕TCLF)⎕NAPPEND ¯1
[20]  →((⍴VALUES)>I←I+1)/L1
[21]  ⎕NUNTIE ¯1
    ∇
```

B-1.7.2 - GAUSSE, function used to create normally distributed parameter values

```
    ∇ R←GAUSSE V;I;COL
[1]  ⍝
[2]  ⍝ This function inputs a vector, V, of uniform probabilities and outputs
[3]  ⍝ a vector, R, of normally distributed probabilities
[4]  ⍝
[5]   R←(⍴V)⍴0
[6]   COL←0
[7]  B:I←¯1
[8]  A:I←I+1
[9]   →((PROB[I]<V[COL])∧(I<698))/A
[10]  →(I=0)/ZERO
[11]  →(I=698)/INFINITY
[12]  R[COL]←(1+I-(V[COL]-PROB[I])+(PROB[I-1]-PROB[I]))÷700
[13]  →END
[14] ZERO:R[COL]←0
[15]  →END
[16] INFINITY:R[COL]←1
[17] END:COL←COL+1
[18]  →(COL<⍴V)/B
    ∇

    ∇ R←NEWY AM;RA
[1]  ⍝
[2]  ⍝ This function gives an example of how function GAUSSE is used
[3]  ⍝ with the random perturbation scheme to produce normally
[4]  ⍝ distributed random values
[5]  ⍝
[6]   →(AM=0)/NOPERT
[7]   RA←0,(1-AM)+2×AM×(GAUSSE(1E¯4×?10⍴10000)) ⋄ →END
[8]  NOPERT:RA←0,(1-AM)+2×AM×0.1×?(ORDER-1)⍴11
[9]  END:R←Y←11-(10÷+/RA)×+\RA
    ∇
```

B-1.7.3 - STAT, function which returns the mean, standard deviation, and coefficient of variation of a vector of numbers

```
    ∇ R←STAT X;SD;X2;XBAR
[1]   ⍝
[2]   ⍝ This function inputs a vector of values in X, and returns a vector
[3]   ⍝ containing the mean, standard deviation, and coefficient of
[4]   ⍝ variation
[5]   ⍝
[6]    X2←+/X*2
[7]    XBAR←+/X÷⍴X
[8]    SD←(((X2-((+/X)*2)÷⍴X))÷((⍴X)-1))*0.5
[9]    R←XBAR,SD,(SD÷XBAR)
    ∇
```

B-1.1 - Post-Processors, programs which were used to put raw exported output data in interpretable form for use by Lotus 123

B-1.1.1 - Envproc.Bas, creates spreadsheet ready input parameter envelope files

```
    def FNn$(a)
       a$=str$(a)
       fnn$=right$(a$,len(a$)-1)
    end def
'
'
'
   dim env(4000)
   w=10:intensity=0.00001:order=11
   width 80:color 7,1:cls
   for nloop=1 to 2
      for countr3=0 to 13
         inputfile$="c:\gem\data\env"+FNn$(nloop)_
                    +FNn$(countr3+1)+FNn$(order)_
                    +".dat"
         open inputfile$ for input as #1
         cls:print "Working on ",inputfile$
         for i=1 to order*2*4
           input#1, env(i)
         next i
         close #1
         outputfile$="c:\gem\data\env"+FNn$(nloop)_
                     +FNn$(countr3+1)+fnn$(order)_
                     +".prn"
         open outputfile$ for output as #1
         F8.5$="##.#####"
         for j=0 to order-1
           for i=1 to order*2*4 step order
              print#1,using F8.5$; env(i+j);
              print#1," ";
           next i
           print#1,
         next j
         close #1
      next countr3
   next nloop
   end
```

B-1.1.2 - Hydproc.Bas, creates spreadsheet ready hydrograph envelope files

```
def fnn$(a)
   a$=str$(a)
   fnn$=right$(a$,len(a$)-1)
end def
'
'
'
dim hyd(4000),lenhyd(20)
w=10:intensity=0.00001:order=11
lenhyd(0)=50:lenhyd(1)=50:lenhyd(2)=50:lenhyd(3)=50
lenhyd(4)=50:lenhyd(5)=50:lenhyd(6)=50:lenhyd(7)=50
lenhyd(8)=50:lenhyd(9)=100lenhyd(10)=100
lenhyd(11)=100:lenhyd(12)=120:lenhyd(13)=150
width 80:color 7,1:cls
for nloop=1 to 2
   for countr3=0 to 1
      inputfile$="c:\gem\"+fnn$(nloop)_
                 +"hyd"+fnn$(countr3+1)_
                 +fnn$(order)+".dat"
      open inputfile$ for input as #1
      cls:print "Working on ",inputfile$
      for i=1 to lenhyd(countr3)*2*4
        input#1, hyd(i)
      next i
      close #1
      outputfile$="c:\gem\"+fnn$(nloop)_
                  +"hyd"+fnn$(countr3+1)_
                  +fnn$(order)+".prn"
      open outputfile$ for output as #1
      F8.5$="##.#####"
      lenplane=(110/order)*(order-1)
      for j=0 to lenhyd(countr3)-1
        for i=1 to lenhyd(countr3)*2*4 step_
                   lenhyd(countr3)
           print#1,using F8.5$; hyd(i+j)_
           /(lenplane*w*intensity);
           print#1," ";
        next i
        print#1,
      next j
      close #1
   next countr3
next nloop
end
'
'
'
sub pause static
do
```

```
   a$=inkey$
loop until a$<>""
end sub
```

B-1.1.3 - Devproc.Bas, creates spreadsheet ready deviation hydrograph files

```
    def FNn$(a)
       a$=str$(a)
       fnn$=right$(a$,len(a$)-1)
    end def
'
'
'
   dim peak(2000),lenhyd(20)
   lenhyd(0)=50:lenhyd(1)=50:lenhyd(2)=50:lenhyd(3)=50
   lenhyd(4)=50:lenhyd(5)=50:lenhyd(6)=50:lenhyd(7)=50
   lenhyd(8)=50:lenhyd(9)=100:lenhyd(10)=100
   lenhyd(11)=100:lenhyd(12)=120:lenhyd(13)=150
   width 80:color 7,1:cls
   order=11
   for nloop=1 to 2
      for countr3=0 to 0
         inputfile$="a:\peak"+FNn$(nloop)_
                   +FNn$(countr3+1)+FNn$(order)_
                   +".dat"
         open inputfile$ for input as #1
         cls:print "Working on ",inputfile$
         for i=1 to lenhyd(countr3)*4*3
           input#1, peak(i)
         next i
         close #1
         outputfile$="g:\peak"+FNn$(nloop)_
                     +FNn$(countr3+1)+FNn$(order)_
                     +".prn"
         open outputfile$ for output as #1
         F9.7$="#.#######"
         for j=0 to lenhyd(countr3)-1
           for i=1 to lenhyd(countr3)*4*3 step
                      lenhyd(countr3)
              print#1,using F9.7$; peak(i+j);
              print#1,"  ";
           next i
           print#1,
         next j
         close #1
      next countr3
   next nloop
   end
```

B-1.1.4 - Statproc.Bas, creates spreadsheet ready input parameter statistic files

```
     def FNn$(a)
        a$=str$(a)
        fnn$=right$(a$,len(a$)-1)
     end def
'
'
'
    dim avg(13),std(13),cv(13)
    color 7,1:width 80
    order=11
    for nloop=1 to 2
       for countr3=0 to 1
          counter=1
          for am=0 to 3
            inputfile$="c:\gem\st"+FNn$(nloop)_
                       +FNn$(am)+FNn$(countr3+1)+".dat"
            cls:print "Working on: ";inputfile$
            open inputfile$ for input as #1
            input#1,avg(counter),std(counter),_
                    cv(counter)
            counter=counter+1
            close #1
          next am
          outputfile$="c:\gem\st"+FNn$(nloop)_
                      +FNn$(countr3+1)+FNn$(order)_
                      +".prn"
          open outputfile$ for output as #1
          F9.6$="##.######"
          for i=1 to 4
            print#1,using F9.6$; avg(i);
            print#1,"  ";
          next i
          print#1, ''
          for i=1 to 4
            print #1,using F9.6$; std(i);
            print#1,"  ";
          next i
          print#1, ''
          for i=1 to 4
            print#1,using F9.6$; cv(i);
            print#1,"  ";
          next i
          print#1, ''
          close#1
       next countr3
    next nloop
    end
```

APPENDIX B - TABULATED OUTPUT DATA

Dimensionless Hydrograph Envelopes for Slope($t_r / t_e = 0.4$)

t/t_e	$\phi=2$ (High)	$\phi=2$ (Low)	$\phi=4$ (High)	$\phi=4$ (Low)	$\phi=6$ (High)	$\phi=6$ (Low)
0.0	0.0000	0.0000	0.0000	0.0000	0.0000	0.0000
0.1	0.0287	0.0187	0.0313	0.0144	0.0334	0.0126
0.2	0.0874	0.0631	0.0945	0.0483	0.1016	0.0436
0.3	0.1640	0.1283	0.1785	0.1041	0.1915	0.0871
0.4	0.2608	0.2140	0.2742	0.1825	0.2932	0.1527
0.5	0.2608	0.2147	0.2606	0.1782	0.2674	0.1653
0.6	0.2586	0.2173	0.2585	0.1901	0.2607	0.1606
0.7	0.2502	0.2199	0.2567	0.1958	0.2583	0.1708
0.8	0.2434	0.2210	0.2534	0.2067	0.2523	0.1883
0.9	0.2386	0.2208	0.2460	0.1990	0.2485	0.1746
1.0	0.2317	0.2120	0.2396	0.1916	0.2405	0.1625
1.1	0.2201	0.2011	0.2281	0.1849	0.2297	0.1542
1.2	0.2064	0.1866	0.2116	0.1774	0.2211	0.1484
1.3	0.1892	0.1710	0.1928	0.1663	0.2058	0.1433
1.4	0.1706	0.1544	0.1742	0.1524	0.1873	0.1379
1.5	0.1512	0.1387	0.1557	0.1377	0.1672	0.1311
1.6	0.1340	0.1232	0.1392	0.1227	0.1487	0.1208
1.7	0.1176	0.1097	0.1236	0.1096	0.1315	0.1084
1.8	0.1039	0.0969	0.1099	0.0974	0.1169	0.0971
1.9	0.0913	0.0861	0.0972	0.0865	0.1033	0.0863
2.0	0.0809	0.0760	0.0865	0.0768	0.0918	0.0768
2.1	0.0716	0.0678	0.0767	0.0683	0.0814	0.0683
2.2	0.0639	0.0603	0.0686	0.0607	0.0728	0.0607
2.3	0.0569	0.0542	0.0612	0.0544	0.0656	0.0544
2.4	0.0512	0.0486	0.0551	0.0487	0.0597	0.0487
2.5	0.0460	0.0435	0.0495	0.0439	0.0543	0.0440
2.6	0.0412	0.0394	0.0445	0.0397	0.0493	0.0397
2.7	0.0375	0.0357	0.0404	0.0358	0.0452	0.0358
2.8	0.0340	0.0324	0.0367	0.0326	0.0413	0.0326
2.9	0.0309	0.0296	0.0335	0.0297	0.0378	0.0297
3.0	0.0283	0.0271	0.0306	0.0271	0.0348	0.0271
3.1	0.0259	0.0248	0.0281	0.0249	0.0321	0.0249
3.2	0.0238	0.0228	0.0259	0.0229	0.0296	0.0229
3.3	0.0220	0.0211	0.0238	0.0211	0.0275	0.0211
3.4	0.0203	0.0195	0.0221	0.0195	0.0255	0.0195
3.5	0.0188	0.0180	0.0205	0.0181	0.0236	0.0181
3.6	0.0174	0.0167	0.0190	0.0167	0.0219	0.0167
3.7	0.0162	0.0155	0.0177	0.0155	0.0205	0.0155
3.8	0.0151	0.0145	0.0165	0.0145	0.0192	0.0145
3.9	0.0141	0.0135	0.0154	0.0135	0.0179	0.0135
4.0	0.0132	0.0126	0.0144	0.0126	0.0167	0.0126
4.1	0.0123	0.0118	0.0135	0.0118	0.0158	0.0118
4.2	0.0116	0.0111	0.0127	0.0111	0.0148	0.0111
4.3	0.0109	0.0104	0.0119	0.0104	0.0139	0.0104
4.4	0.0103	0.0098	0.0112	0.0098	0.0131	0.0098
4.5	0.0097	0.0092	0.0106	0.0092	0.0124	0.0092
4.6	0.0091	0.0087	0.0100	0.0087	0.0117	0.0087
4.7	0.0087	0.0083	0.0095	0.0083	0.0111	0.0083
4.8	0.0082	0.0078	0.0090	0.0078	0.0105	0.0078
4.9	0.0077	0.0074	0.0085	0.0074	0.0099	0.0074

Dimensionless Hydrograph Envelopes for Manning's "n" ($t_r / t_e = 0.4$)

t/t_e	$\phi=2$ (High)	$\phi=2$ (Low)	$\phi=4$ (High)	$\phi=4$ (Low)	$\phi=6$ (High)	$\phi=6$ (Low)
0.0	0.0000	0.0000	0.0000	0.0000	0.0000	0.0000
0.1	0.0356	0.0173	0.0644	0.0149	0.0779	0.0145
0.2	0.1121	0.0505	0.1457	0.0520	0.1963	0.0358
0.3	0.1972	0.1102	0.2417	0.1011	0.3045	0.0971
0.4	0.3030	0.2006	0.3498	0.1755	0.3964	0.1780
0.5	0.2790	0.2043	0.3176	0.1955	0.3440	0.1634
0.6	0.2735	0.2042	0.2924	0.1855	0.3384	0.1884
0.7	0.2729	0.2093	0.2941	0.1849	0.3304	0.1671
0.8	0.2697	0.2175	0.2953	0.1968	0.3049	0.1655
0.9	0.2581	0.2141	0.2921	0.1987	0.2934	0.1760
1.0	0.2462	0.2043	0.2761	0.1840	0.2813	0.1697
1.1	0.2322	0.1927	0.2509	0.1716	0.2564	0.1635
1.2	0.2148	0.1793	0.2248	0.1600	0.2311	0.1557
1.3	0.1964	0.1644	0.2030	0.1477	0.2047	0.1413
1.4	0.1763	0.1481	0.1800	0.1341	0.1782	0.1254
1.5	0.1554	0.1325	0.1579	0.1206	0.1571	0.1112
1.6	0.1370	0.1166	0.1368	0.1060	0.1376	0.0974
1.7	0.1197	0.1031	0.1193	0.0938	0.1209	0.0840
1.8	0.1053	0.0907	0.1042	0.0826	0.1056	0.0735
1.9	0.0922	0.0804	0.0911	0.0722	0.0930	0.0641
2.0	0.0816	0.0710	0.0804	0.0636	0.0816	0.0566
2.1	0.0719	0.0633	0.0711	0.0559	0.0723	0.0499
2.2	0.0641	0.0563	0.0634	0.0497	0.0639	0.0445
2.3	0.0570	0.0506	0.0565	0.0441	0.0571	0.0396
2.4	0.0511	0.0453	0.0508	0.0395	0.0509	0.0357
2.5	0.0458	0.0406	0.0456	0.0354	0.0458	0.0320
2.6	0.0411	0.0368	0.0410	0.0317	0.0412	0.0288
2.7	0.0373	0.0334	0.0372	0.0287	0.0372	0.0262
2.8	0.0338	0.0302	0.0338	0.0260	0.0337	0.0238
2.9	0.0307	0.0275	0.0307	0.0236	0.0306	0.0217
3.0	0.0282	0.0252	0.0281	0.0216	0.0281	0.0198
3.1	0.0258	0.0231	0.0258	0.0198	0.0257	0.0182
3.2	0.0237	0.0211	0.0236	0.0181	0.0236	0.0166
3.3	0.0219	0.0195	0.0218	0.0167	0.0218	0.0152
3.4	0.0202	0.0180	0.0202	0.0154	0.0201	0.0141
3.5	0.0187	0.0167	0.0186	0.0142	0.0186	0.0130
3.6	0.0174	0.0155	0.0173	0.0132	0.0173	0.0120
3.7	0.0162	0.0144	0.0161	0.0123	0.0161	0.0112
3.8	0.0150	0.0134	0.0150	0.0114	0.0150	0.0104
3.9	0.0140	0.0124	0.0139	0.0106	0.0139	0.0097
4.0	0.0131	0.0117	0.0131	0.0100	0.0130	0.0090
4.1	0.0123	0.0109	0.0123	0.0093	0.0122	0.0084
4.2	0.0115	0.0102	0.0115	0.0087	0.0114	0.0079
4.3	0.0108	0.0096	0.0108	0.0082	0.0107	0.0074
4.4	0.0102	0.0091	0.0101	0.0077	0.0101	0.0069
4.5	0.0096	0.0085	0.0096	0.0073	0.0095	0.0066
4.6	0.0091	0.0080	0.0090	0.0069	0.0090	0.0062
4.7	0.0085	0.0076	0.0085	0.0065	0.0085	0.0058
4.8	0.0081	0.0072	0.0080	0.0061	0.0080	0.0055
4.9	0.0076	0.0068	0.0076	0.0058	0.0076	0.0052

Dimensionless Hydrograph Envelopes for Width ($t_r / t_e = 0.4$)

t/t_e	$\phi=2$ (High)	$\phi=2$ (Low)	$\phi=4$ (High)	$\phi=4$ (Low)	$\phi=6$ (High)	$\phi=6$ (Low)
0.0	0.0000	0.0000	0.0000	0.0000	0.0000	0.0000
0.1	0.0322	0.0146	0.0499	0.0090	0.0479	0.0072
0.2	0.0988	0.0484	0.1372	0.0362	0.1328	0.0298
0.3	0.1834	0.1115	0.2240	0.0812	0.2352	0.0657
0.4	0.2919	0.1846	0.3503	0.1467	0.3474	0.1341
0.5	0.2771	0.1965	0.3184	0.1670	0.3395	0.1481
0.6	0.2647	0.2105	0.2901	0.1605	0.3327	0.1531
0.7	0.2660	0.2151	0.2842	0.1747	0.2976	0.1611
0.8	0.2623	0.2121	0.2779	0.1939	0.2870	0.1624
0.9	0.2528	0.2081	0.2763	0.1970	0.2790	0.1743
1.0	0.2484	0.1982	0.2666	0.1862	0.2639	0.1764
1.1	0.2366	0.1888	0.2505	0.1749	0.2570	0.1673
1.2	0.2186	0.1781	0.2308	0.1629	0.2468	0.1528
1.3	0.1975	0.1650	0.2097	0.1501	0.2262	0.1398
1.4	0.1759	0.1481	0.1870	0.1343	0.2016	0.1282
1.5	0.1552	0.1327	0.1639	0.1201	0.1758	0.1179
1.6	0.1358	0.1178	0.1438	0.1064	0.1534	0.1077
1.7	0.1194	0.1048	0.1251	0.0946	0.1326	0.0982
1.8	0.1047	0.0925	0.1100	0.0837	0.1158	0.0889
1.9	0.0921	0.0823	0.0966	0.0746	0.1023	0.0802
2.0	0.0814	0.0729	0.0857	0.0662	0.0902	0.0710
2.1	0.0719	0.0651	0.0758	0.0593	0.0800	0.0635
2.2	0.0641	0.0580	0.0677	0.0530	0.0713	0.0567
2.3	0.0571	0.0521	0.0603	0.0477	0.0636	0.0510
2.4	0.0513	0.0467	0.0543	0.0429	0.0572	0.0459
2.5	0.0461	0.0422	0.0487	0.0388	0.0513	0.0412
2.6	0.0415	0.0381	0.0437	0.0352	0.0461	0.0373
2.7	0.0375	0.0344	0.0397	0.0318	0.0418	0.0340
2.8	0.0341	0.0314	0.0361	0.0291	0.0380	0.0309
2.9	0.0310	0.0287	0.0328	0.0265	0.0346	0.0281
3.0	0.0283	0.0261	0.0300	0.0242	0.0316	0.0258
3.1	0.0260	0.0241	0.0275	0.0223	0.0289	0.0237
3.2	0.0239	0.0221	0.0252	0.0206	0.0267	0.0218
3.3	0.0220	0.0204	0.0233	0.0189	0.0246	0.0201
3.4	0.0203	0.0189	0.0216	0.0176	0.0227	0.0186
3.5	0.0188	0.0175	0.0199	0.0163	0.0211	0.0172
3.6	0.0175	0.0162	0.0185	0.0151	0.0196	0.0160
3.7	0.0162	0.0150	0.0173	0.0140	0.0182	0.0149
3.8	0.0151	0.0140	0.0160	0.0131	0.0169	0.0139
3.9	0.0141	0.0131	0.0149	0.0122	0.0158	0.0129
4.0	0.0132	0.0123	0.0140	0.0114	0.0148	0.0121
4.1	0.0123	0.0115	0.0131	0.0107	0.0139	0.0114
4.2	0.0116	0.0108	0.0123	0.0101	0.0130	0.0107
4.3	0.0109	0.0101	0.0115	0.0095	0.0122	0.0100
4.4	0.0103	0.0095	0.0109	0.0089	0.0115	0.0094
4.5	0.0097	0.0090	0.0103	0.0084	0.0109	0.0089
4.6	0.0091	0.0085	0.0097	0.0079	0.0102	0.0084
4.7	0.0086	0.0080	0.0091	0.0075	0.0097	0.0079
4.8	0.0082	0.0076	0.0086	0.0071	0.0092	0.0075
4.9	0.0077	0.0072	0.0082	0.0067	0.0087	0.0071

Dimensionless Hydrograph Envelopes for Rainfall Intensity ($t_r / t_e = 0.4$)

t/t_e	$\phi=2$ (High)	$\phi=2$ (Low)	$\phi=4$ (High)	$\phi=4$ (Low)	$\phi=6$ (High)	$\phi=6$ (Low)
0.0	0.0000	0.0000	0.0000	0.0000	0.0000	0.0000
0.1	0.0422	0.0120	0.0579	0.0042	0.0780	0.0027
0.2	0.1257	0.0403	0.1541	0.0185	0.1925	0.0067
0.3	0.2141	0.0902	0.2663	0.0499	0.3317	0.0315
0.4	0.3103	0.1457	0.3831	0.0855	0.4435	0.0887
0.5	0.3024	0.1450	0.3419	0.1268	0.3426	0.1073
0.6	0.2879	0.1696	0.3342	0.1398	0.3295	0.1053
0.7	0.2848	0.1962	0.3204	0.1316	0.3164	0.0934
0.8	0.2732	0.1951	0.3277	0.1300	0.3176	0.1082
0.9	0.2733	0.1950	0.3076	0.1412	0.3174	0.1217
1.0	0.2733	0.1860	0.2901	0.1600	0.2971	0.1090
1.1	0.2588	0.1728	0.2800	0.1610	0.2679	0.1055
1.2	0.2367	0.1615	0.2599	0.1489	0.2708	0.1104
1.3	0.2118	0.1506	0.2322	0.1388	0.2534	0.1192
1.4	0.1871	0.1394	0.2021	0.1261	0.2272	0.1214
1.5	0.1630	0.1248	0.1783	0.1114	0.1980	0.1104
1.6	0.1426	0.1109	0.1567	0.0980	0.1724	0.0998
1.7	0.1239	0.0990	0.1364	0.0869	0.1486	0.0891
1.8	0.1087	0.0875	0.1195	0.0770	0.1294	0.0795
1.9	0.0949	0.0779	0.1043	0.0687	0.1122	0.0714
2.0	0.0838	0.0692	0.0920	0.0613	0.0986	0.0638
2.1	0.0739	0.0619	0.0809	0.0551	0.0864	0.0564
2.2	0.0658	0.0553	0.0719	0.0494	0.0766	0.0504
2.3	0.0585	0.0498	0.0638	0.0447	0.0678	0.0450
2.4	0.0525	0.0447	0.0572	0.0403	0.0607	0.0401
2.5	0.0471	0.0402	0.0512	0.0364	0.0543	0.0363
2.6	0.0422	0.0365	0.0459	0.0332	0.0485	0.0329
2.7	0.0383	0.0332	0.0416	0.0302	0.0439	0.0297
2.8	0.0348	0.0301	0.0377	0.0275	0.0398	0.0272
2.9	0.0315	0.0276	0.0342	0.0253	0.0360	0.0249
3.0	0.0289	0.0253	0.0313	0.0233	0.0330	0.0227
3.1	0.0265	0.0232	0.0287	0.0214	0.0302	0.0210
3.2	0.0242	0.0214	0.0262	0.0198	0.0276	0.0194
3.3	0.0224	0.0198	0.0242	0.0183	0.0255	0.0179
3.4	0.0207	0.0182	0.0224	0.0169	0.0235	0.0166
3.5	0.0191	0.0170	0.0206	0.0158	0.0217	0.0154
3.6	0.0177	0.0158	0.0192	0.0147	0.0202	0.0143
3.7	0.0165	0.0147	0.0178	0.0137	0.0188	0.0133
3.8	0.0153	0.0136	0.0166	0.0127	0.0174	0.0125
3.9	0.0143	0.0128	0.0154	0.0119	0.0162	0.0117
4.0	0.0134	0.0120	0.0144	0.0112	0.0152	0.0110
4.1	0.0125	0.0112	0.0135	0.0105	0.0142	0.0103
4.2	0.0117	0.0105	0.0127	0.0098	0.0133	0.0097
4.3	0.0110	0.0099	0.0119	0.0093	0.0125	0.0091
4.4	0.0104	0.0093	0.0112	0.0088	0.0118	0.0086
4.5	0.0098	0.0088	0.0106	0.0083	0.0111	0.0081
4.6	0.0092	0.0083	0.0100	0.0078	0.0104	0.0077
4.7	0.0087	0.0078	0.0094	0.0074	0.0098	0.0073
4.8	0.0082	0.0074	0.0088	0.0070	0.0093	0.0069
4.9	0.0078	0.0070	0.0084	0.0066	0.0088	0.0065

Dimensionless Hydrograph Envelopes for Slope ($t_r / t_e = 1.0$)

t/t_e	$\phi=2$ (High)	$\phi=2$ (Low)	$\phi=4$ (High)	$\phi=4$ (Low)	$\phi=6$ (High)	$\phi=6$ (Low)
0.0	0.0000	0.0000	0.0000	0.0000	0.0000	0.0000
0.1	0.0272	0.0177	0.0305	0.0136	0.0320	0.0114
0.2	0.0808	0.0574	0.0895	0.0536	0.0936	0.0346
0.3	0.1561	0.1200	0.1664	0.1092	0.1759	0.0776
0.4	0.2451	0.1966	0.2565	0.1789	0.2540	0.1475
0.5	0.3430	0.2952	0.3659	0.2652	0.3654	0.2269
0.6	0.4616	0.4113	0.4754	0.3710	0.4847	0.3322
0.7	0.5895	0.5354	0.5963	0.4891	0.6011	0.4488
0.8	0.7143	0.6734	0.7186	0.6273	0.7116	0.5843
0.9	0.8355	0.8042	0.8338	0.7485	0.8280	0.7139
1.0	0.9308	0.9070	0.9280	0.8598	0.9242	0.8352
1.1	0.8460	0.8098	0.8478	0.7789	0.8587	0.7758
1.2	0.7422	0.7040	0.7526	0.6773	0.7748	0.6743
1.3	0.6356	0.6017	0.6517	0.5824	0.6790	0.5737
1.4	0.5378	0.5093	0.5551	0.4979	0.5820	0.4858
1.5	0.4529	0.4275	0.4715	0.4235	0.4928	0.4113
1.6	0.3798	0.3587	0.3982	0.3565	0.4180	0.3490
1.7	0.3184	0.3016	0.3357	0.3001	0.3543	0.2971
1.8	0.2674	0.2544	0.2832	0.2533	0.3016	0.2540
1.9	0.2255	0.2154	0.2396	0.2148	0.2569	0.2155
2.0	0.1911	0.1811	0.2036	0.1811	0.2193	0.1831
2.1	0.1613	0.1549	0.1725	0.1553	0.1860	0.1561
2.2	0.1385	0.1319	0.1485	0.1326	0.1601	0.1340
2.3	0.1185	0.1141	0.1274	0.1146	0.1373	0.1147
2.4	0.1029	0.0985	0.1109	0.0987	0.1194	0.0997
2.5	0.0893	0.0862	0.0964	0.0863	0.1036	0.0865
2.6	0.0784	0.0754	0.0848	0.0754	0.0911	0.0760
2.7	0.0689	0.0667	0.0746	0.0666	0.0800	0.0667
2.8	0.0612	0.0589	0.0663	0.0588	0.0710	0.0592
2.9	0.0543	0.0526	0.0588	0.0525	0.0630	0.0526
3.0	0.0487	0.0470	0.0528	0.0468	0.0565	0.0471
3.1	0.0436	0.0422	0.0473	0.0422	0.0506	0.0422
3.2	0.0393	0.0378	0.0424	0.0378	0.0453	0.0378
3.3	0.0354	0.0343	0.0384	0.0341	0.0411	0.0343
3.4	0.0322	0.0311	0.0349	0.0311	0.0372	0.0311
3.5	0.0294	0.0282	0.0316	0.0282	0.0337	0.0282
3.6	0.0267	0.0258	0.0290	0.0257	0.0309	0.0258
3.7	0.0246	0.0237	0.0265	0.0237	0.0284	0.0237
3.8	0.0226	0.0217	0.0243	0.0217	0.0261	0.0217
3.9	0.0208	0.0200	0.0224	0.0200	0.0241	0.0200
4.0	0.0193	0.0185	0.0207	0.0185	0.0223	0.0185
4.1	0.0178	0.0171	0.0191	0.0171	0.0207	0.0171
4.2	0.0165	0.0159	0.0178	0.0159	0.0191	0.0159
4.3	0.0153	0.0147	0.0166	0.0147	0.0179	0.0148
4.4	0.0143	0.0138	0.0154	0.0137	0.0167	0.0138
4.5	0.0134	0.0128	0.0144	0.0128	0.0156	0.0128
4.6	0.0125	0.0120	0.0134	0.0120	0.0146	0.0120
4.7	0.0117	0.0112	0.0126	0.0112	0.0137	0.0112
4.8	0.0110	0.0105	0.0118	0.0105	0.0129	0.0105
4.9	0.0103	0.0099	0.0111	0.0099	0.0121	0.0099

Dimensionless Hydrograph Envelopes for Manning's "n" ($t_r / t_e = 1.0$)

t/t_e	$\phi=2$ (High)	$\phi=2$ (Low)	$\phi=4$ (High)	$\phi=4$ (Low)	$\phi=6$ (High)	$\phi=6$ (Low)
0.0	0.0000	0.0000	0.0000	0.0000	0.0000	0.0000
0.1	0.0346	0.0152	0.0563	0.0129	0.0858	0.0134
0.2	0.1025	0.0557	0.1285	0.0417	0.1763	0.0308
0.3	0.1828	0.1162	0.2195	0.0831	0.2420	0.0761
0.4	0.2777	0.1852	0.3527	0.1411	0.3494	0.1329
0.5	0.3789	0.2790	0.4681	0.2294	0.4892	0.2369
0.6	0.4965	0.3991	0.5676	0.3625	0.6250	0.3570
0.7	0.6334	0.5304	0.7173	0.4952	0.7358	0.4712
0.8	0.7658	0.6600	0.8460	0.6566	0.8663	0.6059
0.9	0.8791	0.7922	0.9366	0.7957	0.9619	0.7543
1.0	0.9597	0.9009	0.9996	0.8946	1.0230	0.8803
1.1	0.8606	0.7992	0.9042	0.7812	0.9160	0.7549
1.2	0.7547	0.6893	0.7973	0.6442	0.8011	0.6360
1.3	0.6474	0.5816	0.6791	0.5341	0.6758	0.5150
1.4	0.5462	0.4881	0.5706	0.4463	0.5693	0.4174
1.5	0.4573	0.4091	0.4774	0.3728	0.4835	0.3415
1.6	0.3831	0.3423	0.3966	0.3034	0.4068	0.2821
1.7	0.3220	0.2847	0.3290	0.2487	0.3407	0.2351
1.8	0.2711	0.2381	0.2734	0.2055	0.2853	0.1975
1.9	0.2290	0.2003	0.2282	0.1712	0.2394	0.1636
2.0	0.1943	0.1675	0.1923	0.1418	0.2017	0.1360
2.1	0.1638	0.1427	0.1617	0.1200	0.1709	0.1125
2.2	0.1405	0.1212	0.1384	0.1012	0.1441	0.0952
2.3	0.1201	0.1046	0.1184	0.0870	0.1236	0.0803
2.4	0.1042	0.0901	0.1026	0.0746	0.1057	0.0690
2.5	0.0903	0.0788	0.0889	0.0650	0.0919	0.0592
2.6	0.0793	0.0688	0.0780	0.0566	0.0797	0.0516
2.7	0.0695	0.0608	0.0684	0.0499	0.0701	0.0450
2.8	0.0617	0.0538	0.0606	0.0440	0.0616	0.0397
2.9	0.0547	0.0480	0.0538	0.0392	0.0547	0.0350
3.0	0.0490	0.0428	0.0482	0.0349	0.0486	0.0313
3.1	0.0438	0.0382	0.0432	0.0314	0.0436	0.0279
3.2	0.0392	0.0346	0.0387	0.0282	0.0391	0.0251
3.3	0.0356	0.0313	0.0351	0.0254	0.0351	0.0226
3.4	0.0322	0.0283	0.0318	0.0231	0.0318	0.0203
3.5	0.0292	0.0257	0.0288	0.0210	0.0289	0.0185
3.6	0.0267	0.0236	0.0264	0.0191	0.0263	0.0169
3.7	0.0245	0.0216	0.0242	0.0176	0.0241	0.0154
3.8	0.0224	0.0197	0.0221	0.0161	0.0220	0.0141
3.9	0.0207	0.0182	0.0205	0.0148	0.0203	0.0130
4.0	0.0191	0.0168	0.0189	0.0137	0.0188	0.0119
4.1	0.0176	0.0155	0.0174	0.0127	0.0173	0.0111
4.2	0.0164	0.0144	0.0162	0.0118	0.0161	0.0103
4.3	0.0153	0.0134	0.0151	0.0109	0.0150	0.0095
4.4	0.0142	0.0125	0.0140	0.0102	0.0140	0.0088
4.5	0.0132	0.0116	0.0130	0.0095	0.0130	0.0082
4.6	0.0124	0.0109	0.0122	0.0089	0.0122	0.0077
4.7	0.0116	0.0102	0.0114	0.0083	0.0114	0.0072
4.8	0.0108	0.0095	0.0107	0.0078	0.0107	0.0067
4.9	0.0102	0.0089	0.0100	0.0073	0.0100	0.0063

Dimensionless Hydrograph Envelopes for Width ($t_r / t_e = 1.0$)

t/t_e	$\phi=2$ (High)	$\phi=2$ (Low)	$\phi=4$ (High)	$\phi=4$ (Low)	$\phi=6$ (High)	$\phi=6$ (Low)
0.0	0.0000	0.0000	0.0000	0.0000	0.0000	0.0000
0.1	0.0308	0.0138	0.0419	0.0084	0.0459	0.0062
0.2	0.0918	0.0502	0.1215	0.0343	0.1385	0.0218
0.3	0.1802	0.1056	0.2243	0.0659	0.2182	0.0519
0.4	0.2851	0.1780	0.3229	0.1264	0.3240	0.1007
0.5	0.3964	0.2777	0.4342	0.2172	0.4273	0.1769
0.6	0.5052	0.3973	0.5350	0.3225	0.5403	0.2899
0.7	0.6160	0.5290	0.6669	0.4624	0.6691	0.4308
0.8	0.7344	0.6613	0.7872	0.6253	0.8138	0.5738
0.9	0.8530	0.7919	0.8739	0.7742	0.9189	0.7048
1.0	0.9492	0.8929	0.9694	0.8862	0.9937	0.8364
1.1	0.8554	0.7943	0.8890	0.7654	0.9246	0.7652
1.2	0.7543	0.6799	0.8010	0.6469	0.8272	0.6559
1.3	0.6471	0.5719	0.6979	0.5466	0.7208	0.5497
1.4	0.5476	0.4799	0.5942	0.4580	0.6167	0.4612
1.5	0.4601	0.4024	0.4991	0.3782	0.5215	0.3880
1.6	0.3850	0.3377	0.4166	0.3140	0.4374	0.3274
1.7	0.3224	0.2842	0.3472	0.2626	0.3655	0.2736
1.8	0.2707	0.2400	0.2900	0.2212	0.3056	0.2277
1.9	0.2283	0.2036	0.2432	0.1878	0.2566	0.1912
2.0	0.1932	0.1718	0.2051	0.1588	0.2178	0.1621
2.1	0.1632	0.1473	0.1739	0.1366	0.1835	0.1370
2.2	0.1397	0.1259	0.1478	0.1172	0.1572	0.1180
2.3	0.1196	0.1092	0.1274	0.1020	0.1341	0.1015
2.4	0.1036	0.0945	0.1096	0.0886	0.1162	0.0886
2.5	0.0900	0.0828	0.0957	0.0780	0.1005	0.0772
2.6	0.0789	0.0726	0.0835	0.0685	0.0882	0.0682
2.7	0.0694	0.0641	0.0737	0.0608	0.0772	0.0602
2.8	0.0614	0.0568	0.0650	0.0539	0.0685	0.0537
2.9	0.0546	0.0506	0.0580	0.0483	0.0609	0.0478
3.0	0.0488	0.0454	0.0517	0.0433	0.0543	0.0430
3.1	0.0439	0.0407	0.0465	0.0391	0.0489	0.0387
3.2	0.0395	0.0365	0.0419	0.0352	0.0440	0.0348
3.3	0.0355	0.0331	0.0376	0.0318	0.0396	0.0316
3.4	0.0323	0.0301	0.0343	0.0290	0.0360	0.0287
3.5	0.0294	0.0273	0.0312	0.0264	0.0328	0.0261
3.6	0.0268	0.0250	0.0284	0.0241	0.0298	0.0240
3.7	0.0246	0.0229	0.0261	0.0222	0.0274	0.0220
3.8	0.0226	0.0210	0.0240	0.0204	0.0252	0.0202
3.9	0.0208	0.0194	0.0221	0.0188	0.0232	0.0187
4.0	0.0192	0.0179	0.0204	0.0174	0.0215	0.0173
4.1	0.0178	0.0166	0.0189	0.0161	0.0199	0.0160
4.2	0.0165	0.0154	0.0176	0.0150	0.0184	0.0149
4.3	0.0153	0.0143	0.0163	0.0139	0.0170	0.0139
4.4	0.0143	0.0133	0.0152	0.0130	0.0159	0.0129
4.5	0.0133	0.0124	0.0142	0.0121	0.0149	0.0120
4.6	0.0125	0.0116	0.0133	0.0113	0.0139	0.0113
4.7	0.0117	0.0109	0.0124	0.0106	0.0130	0.0106
4.8	0.0110	0.0102	0.0117	0.0099	0.0122	0.0099
4.9	0.0103	0.0096	0.0110	0.0094	0.0115	0.0093

Dimensionless Hydrograph Envelopes for Rainfall Intensity ($t_r / t_e = 1.0$)

t/t_e	$\phi=2$ (High)	$\phi=2$ (Low)	$\phi=4$ (High)	$\phi=4$ (Low)	$\phi=6$ (High)	$\phi=6$ (Low)
0.0	0.0000	0.0000	0.0000	0.0000	0.0000	0.0000
0.1	0.0467	0.0111	0.0630	0.0045	0.0721	0.0026
0.2	0.1225	0.0313	0.1534	0.0095	0.1363	0.0028
0.3	0.2117	0.0717	0.3061	0.0507	0.2799	0.0137
0.4	0.3149	0.1343	0.4218	0.0926	0.4274	0.0426
0.5	0.4083	0.2335	0.4954	0.1352	0.5915	0.0910
0.6	0.5152	0.3336	0.5927	0.2375	0.7256	0.1660
0.7	0.6396	0.4742	0.6969	0.4137	0.8071	0.3309
0.8	0.7579	0.6408	0.8211	0.5314	0.8682	0.5292
0.9	0.8739	0.7820	0.9038	0.6845	0.9271	0.6775
1.0	0.9759	0.8847	0.9883	0.8414	0.9991	0.7969
1.1	0.8865	0.7750	0.9481	0.7217	0.9855	0.7047
1.2	0.7880	0.6617	0.8560	0.5954	0.9100	0.5896
1.3	0.6847	0.5634	0.7366	0.5051	0.7944	0.4684
1.4	0.5830	0.4706	0.6159	0.4312	0.6704	0.3771
1.5	0.4907	0.3929	0.5250	0.3599	0.5553	0.3054
1.6	0.4107	0.3288	0.4426	0.3010	0.4565	0.2524
1.7	0.3432	0.2761	0.3708	0.2497	0.3752	0.2121
1.8	0.2871	0.2331	0.3103	0.2090	0.3096	0.1804
1.9	0.2410	0.1978	0.2601	0.1765	0.2573	0.1532
2.0	0.2033	0.1670	0.2189	0.1486	0.2170	0.1318
2.1	0.1705	0.1433	0.1832	0.1276	0.1826	0.1131
2.2	0.1456	0.1226	0.1563	0.1093	0.1564	0.0986
2.3	0.1240	0.1064	0.1329	0.0951	0.1334	0.0857
2.4	0.1073	0.0922	0.1149	0.0827	0.1156	0.0755
2.5	0.0927	0.0809	0.0992	0.0728	0.0999	0.0665
2.6	0.0812	0.0708	0.0868	0.0641	0.0875	0.0591
2.7	0.0711	0.0627	0.0759	0.0570	0.0766	0.0525
2.8	0.0630	0.0554	0.0672	0.0507	0.0678	0.0471
2.9	0.0557	0.0496	0.0594	0.0455	0.0600	0.0422
3.0	0.0499	0.0443	0.0531	0.0408	0.0537	0.0381
3.1	0.0446	0.0399	0.0475	0.0366	0.0480	0.0345
3.2	0.0399	0.0360	0.0424	0.0332	0.0429	0.0311
3.3	0.0361	0.0324	0.0384	0.0302	0.0388	0.0284
3.4	0.0327	0.0295	0.0348	0.0274	0.0351	0.0259
3.5	0.0296	0.0269	0.0315	0.0251	0.0318	0.0236
3.6	0.0271	0.0245	0.0288	0.0230	0.0291	0.0218
3.7	0.0248	0.0225	0.0264	0.0211	0.0266	0.0200
3.8	0.0227	0.0207	0.0241	0.0195	0.0243	0.0184
3.9	0.0210	0.0191	0.0223	0.0180	0.0225	0.0171
4.0	0.0194	0.0177	0.0205	0.0166	0.0207	0.0158
4.1	0.0179	0.0164	0.0190	0.0155	0.0191	0.0147
4.2	0.0166	0.0152	0.0176	0.0144	0.0178	0.0136
4.3	0.0155	0.0140	0.0164	0.0134	0.0165	0.0127
4.4	0.0144	0.0131	0.0152	0.0125	0.0153	0.0119
4.5	0.0134	0.0123	0.0141	0.0117	0.0143	0.0111
4.6	0.0125	0.0115	0.0132	0.0109	0.0133	0.0104
4.7	0.0117	0.0107	0.0124	0.0103	0.0125	0.0098
4.8	0.0110	0.0101	0.0116	0.0096	0.0117	0.0092
4.9	0.0103	0.0095	0.0109	0.0091	0.0110	0.0087

Dimensionless Hydrograph Envelopes for Slope ($t_r / t_e = 5.0$)

t/t_e	$\phi=2$ (High)	$\phi=2$ (Low)	$\phi=4$ (High)	$\phi=4$ (Low)	$\phi=6$ (High)	$\phi=6$ (Low)
0.0	0.0000	0.0000	0.0000	0.0000	0.0000	0.0000
0.1	0.0246	0.0168	0.0283	0.0131	0.0312	0.0106
0.2	0.0770	0.0527	0.0849	0.0384	0.0872	0.0285
0.3	0.1447	0.1056	0.1545	0.0804	0.1569	0.0640
0.4	0.2305	0.1789	0.2433	0.1515	0.2374	0.1250
0.5	0.3273	0.2642	0.3340	0.2458	0.3417	0.2051
0.6	0.4345	0.3707	0.4400	0.3485	0.4547	0.3016
0.7	0.5524	0.4969	0.5565	0.4675	0.5642	0.4186
0.8	0.6704	0.6264	0.6729	0.5790	0.6702	0.5333
0.9	0.7845	0.7473	0.7800	0.6965	0.7788	0.6641
1.0	0.8730	0.8450	0.8682	0.7994	0.8672	0.7887
1.1	0.9369	0.9113	0.9341	0.8846	0.9341	0.8738
1.2	0.9806	0.9559	0.9790	0.9409	0.9790	0.9227
1.3	1.0070	0.9834	1.0070	0.9730	1.0070	0.9576
1.4	1.0130	0.9990	1.0120	0.9926	1.0120	0.9811
1.5	1.0150	1.0070	1.0140	1.0040	1.0240	0.9962
1.6	1.0150	1.0110	1.0150	1.0090	1.0300	1.0050
1.7	1.0170	1.0120	1.0180	1.0120	1.0330	1.0110
1.8	1.0180	1.0120	1.0190	1.0120	1.0240	1.0120
1.9	1.0180	1.0120	1.0190	1.0120	1.0220	1.0120
2.0	1.0180	1.0120	1.0200	1.0120	1.0220	1.0110
2.1	1.0180	1.0120	1.0200	1.0120	1.0220	1.0110
2.2	1.0180	1.0120	1.0200	1.0120	1.0220	1.0110
2.3	1.0180	1.0120	1.0200	1.0120	1.0220	1.0110
2.4	1.0180	1.0120	1.0200	1.0110	1.0220	1.0110
2.5	1.0180	1.0120	1.0200	1.0110	1.0220	1.0110
2.6	1.0180	1.0120	1.0200	1.0110	1.0220	1.0110
2.7	1.0180	1.0120	1.0200	1.0110	1.0220	1.0110
2.8	1.0180	1.0120	1.0200	1.0110	1.0220	1.0110
2.9	1.0180	1.0120	1.0200	1.0110	1.0220	1.0110
3.0	1.0180	1.0120	1.0200	1.0110	1.0220	1.0110
3.1	1.0180	1.0120	1.0200	1.0110	1.0220	1.0110
3.2	1.0180	1.0120	1.0200	1.0110	1.0220	1.0110
3.3	1.0180	1.0120	1.0200	1.0110	1.0220	1.0110
3.4	1.0180	1.0120	1.0200	1.0110	1.0220	1.0110
3.5	1.0180	1.0120	1.0200	1.0110	1.0220	1.0110
3.6	1.0180	1.0120	1.0200	1.0110	1.0220	1.0110
3.7	1.0180	1.0120	1.0200	1.0110	1.0220	1.0110
3.8	1.0180	1.0120	1.0200	1.0110	1.0220	1.0110
3.9	1.0180	1.0120	1.0200	1.0110	1.0220	1.0110
4.0	1.0180	1.0120	1.0200	1.0110	1.0220	1.0110
4.1	1.0180	1.0120	1.0200	1.0110	1.0220	1.0110
4.2	1.0180	1.0120	1.0200	1.0110	1.0220	1.0110
4.3	1.0180	1.0120	1.0200	1.0110	1.0220	1.0110
4.4	1.0180	1.0120	1.0200	1.0110	1.0220	1.0110
4.5	1.0180	1.0120	1.0200	1.0110	1.0220	1.0110
4.6	1.0180	1.0120	1.0200	1.0110	1.0220	1.0110
4.7	1.0180	1.0120	1.0200	1.0110	1.0220	1.0110
4.8	1.0180	1.0120	1.0200	1.0110	1.0220	1.0110
4.9	1.0180	1.0120	1.0200	1.0110	1.0220	1.0110

Dimensionless Hydrograph Envelopes for
Slope ($t_r / t_e = 5.0$) - continued

t/t_e	$\phi=2$ (High)	$\phi=2$ (Low)	$\phi=4$ (High)	$\phi=4$ (Low)	$\phi=6$ (High)	$\phi=6$ (Low)
5.0	1.0180	1.0120	1.0200	1.0110	1.0220	1.0110
5.1	0.8717	0.8456	0.8806	0.8449	0.9009	0.8416
5.2	0.7338	0.7046	0.7460	0.6995	0.7706	0.6978
5.3	0.6146	0.5833	0.6265	0.5795	0.6531	0.5771
5.4	0.5141	0.4840	0.5246	0.4815	0.5522	0.4796
5.5	0.4292	0.4028	0.4417	0.4006	0.4680	0.4008
5.6	0.3584	0.3364	0.3726	0.3348	0.3951	0.3368
5.7	0.2999	0.2820	0.3144	0.2811	0.3331	0.2844
5.8	0.2518	0.2375	0.2656	0.2372	0.2810	0.2413
5.9	0.2124	0.2010	0.2249	0.2013	0.2377	0.2050
6.0	0.1801	0.1691	0.1913	0.1698	0.2019	0.1739
6.1	0.1518	0.1446	0.1617	0.1457	0.1705	0.1468
6.2	0.1302	0.1233	0.1389	0.1246	0.1464	0.1260
6.3	0.1113	0.1067	0.1190	0.1078	0.1256	0.1078
6.4	0.0967	0.0921	0.1036	0.0936	0.1093	0.0937
6.5	0.0838	0.0807	0.0899	0.0812	0.0951	0.0812
6.6	0.0736	0.0705	0.0791	0.0714	0.0835	0.0714
6.7	0.0646	0.0624	0.0695	0.0627	0.0741	0.0627
6.8	0.0574	0.0551	0.0618	0.0557	0.0657	0.0557
6.9	0.0509	0.0492	0.0548	0.0494	0.0588	0.0494
7.0	0.0456	0.0439	0.0492	0.0443	0.0527	0.0443
7.1	0.0410	0.0396	0.0441	0.0397	0.0471	0.0397
7.2	0.0369	0.0355	0.0396	0.0355	0.0427	0.0355
7.3	0.0332	0.0321	0.0359	0.0322	0.0387	0.0322
7.4	0.0303	0.0292	0.0325	0.0292	0.0351	0.0292
7.5	0.0276	0.0265	0.0297	0.0265	0.0321	0.0265
7.6	0.0251	0.0242	0.0272	0.0243	0.0294	0.0243
7.7	0.0231	0.0222	0.0249	0.0222	0.0269	0.0222
7.8	0.0212	0.0203	0.0230	0.0204	0.0249	0.0204
7.9	0.0195	0.0188	0.0212	0.0188	0.0229	0.0188
8.0	0.0181	0.0173	0.0196	0.0174	0.0212	0.0174
8.1	0.0168	0.0160	0.0182	0.0161	0.0197	0.0161
8.2	0.0155	0.0149	0.0169	0.0149	0.0183	0.0149
8.3	0.0144	0.0138	0.0157	0.0139	0.0170	0.0139
8.4	0.0134	0.0129	0.0146	0.0129	0.0158	0.0129
8.5	0.0126	0.0120	0.0137	0.0120	0.0148	0.0120
8.6	0.0117	0.0112	0.0128	0.0113	0.0139	0.0113
8.7	0.0110	0.0105	0.0120	0.0106	0.0130	0.0105
8.8	0.0103	0.0098	0.0112	0.0099	0.0122	0.0099
8.9	0.0097	0.0092	0.0106	0.0093	0.0115	0.0093
9.0	0.0091	0.0087	0.0100	0.0087	0.0108	0.0087
9.1	0.0086	0.0082	0.0094	0.0082	0.0102	0.0082
9.2	0.0081	0.0077	0.0089	0.0078	0.0096	0.0078
9.3	0.0077	0.0073	0.0084	0.0073	0.0091	0.0073
9.4	0.0073	0.0069	0.0080	0.0069	0.0086	0.0069
9.5	0.0069	0.0065	0.0075	0.0066	0.0082	0.0066
9.6	0.0065	0.0062	0.0071	0.0062	0.0078	0.0062
9.7	0.0062	0.0059	0.0068	0.0059	0.0074	0.0059
9.8	0.0059	0.0056	0.0065	0.0056	0.0070	0.0056
9.9	0.0056	0.0053	0.0061	0.0053	0.0067	0.0053

Dimensionless Hydrographs Envelopes for Manning's "n" ($t_r / t_e = 5.0$)

t/t_e	$\phi=2$ (High)	$\phi=2$ (Low)	$\phi=4$ (High)	$\phi=4$ (Low)	$\phi=6$ (High)	$\phi=6$ (Low)
0.0	0.0000	0.0000	0.0000	0.0000	0.0000	0.0000
0.1	0.0318	0.0148	0.0571	0.0133	0.0770	0.0116
0.2	0.0921	0.0488	0.1389	0.0400	0.1404	0.0379
0.3	0.1657	0.1035	0.2207	0.0780	0.2687	0.0794
0.4	0.2606	0.1711	0.3214	0.1458	0.3727	0.1291
0.5	0.3720	0.2615	0.4453	0.2234	0.4877	0.2239
0.6	0.4909	0.3592	0.5710	0.3276	0.6259	0.3503
0.7	0.6072	0.4802	0.6862	0.4588	0.7427	0.4454
0.8	0.7185	0.6154	0.7942	0.5826	0.8394	0.5598
0.9	0.8180	0.7339	0.8764	0.7050	0.9014	0.6914
1.0	0.8967	0.8359	0.9384	0.8140	0.9535	0.8147
1.1	0.9543	0.9148	0.9815	0.9010	0.9930	0.9018
1.2	0.9901	0.9584	1.0090	0.9529	1.0160	0.9568
1.3	1.0110	0.9836	1.0140	0.9840	1.0150	0.9847
1.4	1.0240	0.9984	1.0270	1.0010	1.0260	0.9971
1.5	1.0300	1.0070	1.0310	1.0070	1.0320	1.0030
1.6	1.0320	1.0090	1.0340	1.0090	1.0320	1.0060
1.7	1.0330	1.0100	1.0240	1.0090	1.0330	1.0070
1.8	1.0330	1.0110	1.0200	1.0090	1.0240	1.0070
1.9	1.0240	1.0110	1.0200	1.0090	1.0230	1.0070
2.0	1.0190	1.0110	1.0210	1.0080	1.0230	1.0070
2.1	1.0190	1.0110	1.0210	1.0080	1.0230	1.0060
2.2	1.0190	1.0110	1.0210	1.0080	1.0230	1.0060
2.3	1.0190	1.0100	1.0210	1.0080	1.0230	1.0060
2.4	1.0190	1.0100	1.0210	1.0080	1.0230	1.0060
2.5	1.0190	1.0100	1.0210	1.0080	1.0230	1.0060
2.6	1.0190	1.0100	1.0210	1.0080	1.0230	1.0060
2.7	1.0190	1.0100	1.0210	1.0080	1.0230	1.0060
2.8	1.0190	1.0100	1.0210	1.0080	1.0230	1.0060
2.9	1.0190	1.0100	1.0210	1.0080	1.0230	1.0060
3.0	1.0190	1.0100	1.0210	1.0080	1.0230	1.0060
3.1	1.0190	1.0100	1.0210	1.0080	1.0230	1.0060
3.2	1.0190	1.0100	1.0210	1.0080	1.0230	1.0060
3.3	1.0190	1.0100	1.0210	1.0080	1.0230	1.0060
3.4	1.0190	1.0100	1.0210	1.0080	1.0230	1.0060
3.5	1.0190	1.0100	1.0210	1.0080	1.0230	1.0060
3.6	1.0190	1.0100	1.0210	1.0080	1.0230	1.0060
3.7	1.0190	1.0100	1.0210	1.0080	1.0230	1.0060
3.8	1.0190	1.0100	1.0210	1.0080	1.0230	1.0060
3.9	1.0190	1.0100	1.0210	1.0080	1.0230	1.0060
4.0	1.0190	1.0100	1.0210	1.0080	1.0230	1.0060
4.1	1.0190	1.0100	1.0210	1.0080	1.0230	1.0060
4.2	1.0190	1.0100	1.0210	1.0080	1.0230	1.0060
4.3	1.0190	1.0100	1.0210	1.0080	1.0230	1.0060
4.4	1.0190	1.0100	1.0210	1.0080	1.0230	1.0060
4.5	1.0190	1.0100	1.0210	1.0080	1.0230	1.0060
4.6	1.0190	1.0100	1.0210	1.0080	1.0230	1.0060
4.7	1.0190	1.0100	1.0210	1.0080	1.0230	1.0060
4.8	1.0190	1.0100	1.0210	1.0080	1.0230	1.0060
4.9	1.0190	1.0100	1.0210	1.0080	1.0230	1.0060

Dimensionless Hydrograph Envelopes for Manning's "n" ($t_r / t_e = 5.0$) - continued

t/t_e	$\phi=2$ (High)	$\phi=2$ (Low)	$\phi=4$ (High)	$\phi=4$ (Low)	$\phi=6$ (High)	$\phi=6$ (Low)
5.0	1.0190	1.0100	1.0210	1.0080	1.0230	1.0060
5.1	0.8737	0.8308	0.8803	0.8081	0.8869	0.7807
5.2	0.7379	0.6798	0.7493	0.6488	0.7510	0.6231
5.3	0.6199	0.5575	0.6300	0.5216	0.6243	0.4879
5.4	0.5179	0.4590	0.5247	0.4223	0.5260	0.3857
5.5	0.4308	0.3799	0.4392	0.3443	0.4418	0.3084
5.6	0.3610	0.3162	0.3690	0.2825	0.3692	0.2494
5.7	0.3033	0.2621	0.3098	0.2334	0.3098	0.2038
5.8	0.2553	0.2185	0.2604	0.1940	0.2608	0.1682
5.9	0.2156	0.1834	0.2195	0.1624	0.2202	0.1401
6.0	0.1829	0.1531	0.1857	0.1352	0.1869	0.1163
6.1	0.1543	0.1303	0.1579	0.1149	0.1576	0.0986
6.2	0.1323	0.1105	0.1336	0.0973	0.1352	0.0833
6.3	0.1130	0.0954	0.1150	0.0838	0.1156	0.0717
6.4	0.0981	0.0821	0.0986	0.0721	0.1003	0.0617
6.5	0.0849	0.0717	0.0858	0.0630	0.0869	0.0538
6.6	0.0745	0.0626	0.0746	0.0549	0.0763	0.0469
6.7	0.0653	0.0553	0.0657	0.0486	0.0668	0.0414
6.8	0.0579	0.0489	0.0578	0.0429	0.0593	0.0366
6.9	0.0513	0.0436	0.0514	0.0383	0.0525	0.0326
7.0	0.0459	0.0389	0.0457	0.0342	0.0470	0.0291
7.1	0.0411	0.0347	0.0410	0.0305	0.0421	0.0262
7.2	0.0368	0.0314	0.0368	0.0276	0.0380	0.0236
7.3	0.0333	0.0284	0.0330	0.0250	0.0343	0.0212
7.4	0.0302	0.0257	0.0300	0.0226	0.0309	0.0193
7.5	0.0273	0.0235	0.0272	0.0207	0.0282	0.0176
7.6	0.0250	0.0214	0.0249	0.0189	0.0257	0.0160
7.7	0.0229	0.0196	0.0228	0.0173	0.0235	0.0148
7.8	0.0210	0.0181	0.0209	0.0159	0.0216	0.0136
7.9	0.0194	0.0167	0.0193	0.0147	0.0199	0.0125
8.0	0.0179	0.0154	0.0178	0.0135	0.0183	0.0115
8.1	0.0165	0.0143	0.0165	0.0125	0.0170	0.0107
8.2	0.0153	0.0133	0.0153	0.0116	0.0157	0.0099
8.3	0.0142	0.0123	0.0142	0.0108	0.0146	0.0092
8.4	0.0132	0.0114	0.0132	0.0100	0.0135	0.0086
8.5	0.0123	0.0107	0.0123	0.0093	0.0126	0.0080
8.6	0.0115	0.0100	0.0115	0.0087	0.0118	0.0075
8.7	0.0108	0.0094	0.0108	0.0081	0.0110	0.0070
8.8	0.0101	0.0088	0.0101	0.0076	0.0103	0.0066
8.9	0.0095	0.0083	0.0095	0.0071	0.0097	0.0062
9.0	0.0089	0.0078	0.0090	0.0067	0.0091	0.0058
9.1	0.0084	0.0073	0.0084	0.0063	0.0086	0.0055
9.2	0.0079	0.0069	0.0080	0.0060	0.0081	0.0052
9.3	0.0075	0.0066	0.0075	0.0056	0.0077	0.0049
9.4	0.0071	0.0062	0.0071	0.0053	0.0072	0.0046
9.5	0.0067	0.0059	0.0067	0.0051	0.0069	0.0044
9.6	0.0064	0.0056	0.0064	0.0048	0.0065	0.0042
9.7	0.0060	0.0053	0.0061	0.0045	0.0061	0.0039
9.8	0.0057	0.0050	0.0058	0.0043	0.0058	0.0038
9.9	0.0054	0.0048	0.0055	0.0041	0.0056	0.0036

Dimensionless Hydrograph Envelopes for Width ($t_r / t_e = 5.0$)

t/t_e	$\phi=2$ (High)	$\phi=2$ (Low)	$\phi=4$ (High)	$\phi=4$ (Low)	$\phi=6$ (High)	$\phi=6$ (Low)
0.0	0.0000	0.0000	0.0000	0.0000	0.0000	0.0000
0.1	0.0299	0.0125	0.0384	0.0079	0.0451	0.0060
0.2	0.0943	0.0490	0.1147	0.0318	0.1209	0.0200
0.3	0.1717	0.0993	0.2102	0.0637	0.2269	0.0538
0.4	0.2612	0.1681	0.3177	0.1130	0.3570	0.1143
0.5	0.3617	0.2497	0.4251	0.2043	0.4898	0.1941
0.6	0.4747	0.3583	0.5271	0.3037	0.5959	0.2835
0.7	0.5918	0.4804	0.6208	0.4218	0.6793	0.3906
0.8	0.7097	0.6123	0.7151	0.5569	0.7563	0.5229
0.9	0.8119	0.7399	0.8137	0.6942	0.8219	0.6705
1.0	0.8875	0.8384	0.8967	0.8066	0.8937	0.8013
1.1	0.9442	0.9122	0.9576	0.8896	0.9513	0.8898
1.2	0.9838	0.9544	0.9858	0.9420	0.9811	0.9435
1.3	1.0080	0.9812	1.0090	0.9737	1.0070	0.9746
1.4	1.0220	0.9971	1.0220	0.9933	1.0210	0.9937
1.5	1.0290	1.0060	1.0280	1.0040	1.0290	1.0040
1.6	1.0340	1.0100	1.0330	1.0070	1.0360	1.0070
1.7	1.0260	1.0110	1.0240	1.0090	1.0400	1.0070
1.8	1.0190	1.0110	1.0210	1.0100	1.0420	1.0070
1.9	1.0180	1.0110	1.0220	1.0100	1.0430	1.0060
2.0	1.0190	1.0110	1.0220	1.0090	1.0300	1.0060
2.1	1.0190	1.0100	1.0220	1.0090	1.0230	1.0060
2.2	1.0190	1.0100	1.0230	1.0090	1.0230	1.0060
2.3	1.0190	1.0090	1.0230	1.0090	1.0230	1.0060
2.4	1.0190	1.0090	1.0230	1.0090	1.0230	1.0060
2.5	1.0190	1.0090	1.0230	1.0080	1.0230	1.0050
2.6	1.0190	1.0090	1.0230	1.0080	1.0230	1.0050
2.7	1.0190	1.0090	1.0230	1.0080	1.0230	1.0050
2.8	1.0190	1.0090	1.0230	1.0080	1.0230	1.0050
2.9	1.0190	1.0090	1.0230	1.0080	1.0230	1.0050
3.0	1.0190	1.0090	1.0230	1.0080	1.0230	1.0050
3.1	1.0190	1.0090	1.0230	1.0080	1.0230	1.0050
3.2	1.0190	1.0090	1.0230	1.0080	1.0230	1.0050
3.3	1.0190	1.0090	1.0230	1.0080	1.0230	1.0050
3.4	1.0190	1.0090	1.0230	1.0080	1.0230	1.0050
3.5	1.0190	1.0090	1.0230	1.0080	1.0230	1.0050
3.6	1.0190	1.0090	1.0230	1.0080	1.0230	1.0050
3.7	1.0190	1.0090	1.0230	1.0080	1.0230	1.0050
3.8	1.0190	1.0090	1.0230	1.0080	1.0230	1.0050
3.9	1.0190	1.0090	1.0230	1.0080	1.0230	1.0050
4.0	1.0190	1.0090	1.0230	1.0080	1.0230	1.0050
4.1	1.0190	1.0090	1.0230	1.0080	1.0230	1.0050
4.2	1.0190	1.0090	1.0230	1.0080	1.0230	1.0050
4.3	1.0190	1.0090	1.0230	1.0080	1.0230	1.0050
4.4	1.0190	1.0090	1.0230	1.0080	1.0230	1.0050
4.5	1.0190	1.0090	1.0230	1.0080	1.0230	1.0050
4.6	1.0190	1.0090	1.0230	1.0080	1.0230	1.0050
4.7	1.0190	1.0090	1.0230	1.0080	1.0230	1.0050
4.8	1.0190	1.0090	1.0230	1.0080	1.0230	1.0050
4.9	1.0190	1.0090	1.0230	1.0080	1.0230	1.0050

Dimensionless Hydrograph Envelopes for Width ($t_r / t_e = 5.0$) - continued

t/t_e	$\phi=2$ (High)	$\phi=2$ (Low)	$\phi=4$ (High)	$\phi=4$ (Low)	$\phi=6$ (High)	$\phi=6$ (Low)
5.0	1.0190	1.0090	1.0230	1.0080	1.0230	1.0050
5.1	0.8750	0.8325	0.8929	0.8112	0.8986	0.7940
5.2	0.7362	0.6866	0.7635	0.6569	0.7681	0.6273
5.3	0.6185	0.5661	0.6443	0.5357	0.6547	0.5030
5.4	0.5178	0.4691	0.5380	0.4421	0.5551	0.4105
5.5	0.4324	0.3906	0.4506	0.3683	0.4667	0.3403
5.6	0.3609	0.3268	0.3771	0.3090	0.3903	0.2856
5.7	0.3016	0.2735	0.3163	0.2606	0.3259	0.2419
5.8	0.2527	0.2299	0.2655	0.2209	0.2725	0.2063
5.9	0.2126	0.1945	0.2236	0.1875	0.2301	0.1770
6.0	0.1805	0.1654	0.1892	0.1590	0.1933	0.1512
6.1	0.1523	0.1403	0.1590	0.1343	0.1651	0.1310
6.2	0.1307	0.1208	0.1360	0.1154	0.1404	0.1131
6.3	0.1118	0.1038	0.1163	0.0990	0.1213	0.0989
6.4	0.0971	0.0904	0.1005	0.0861	0.1046	0.0858
6.5	0.0841	0.0787	0.0878	0.0749	0.0914	0.0753
6.6	0.0739	0.0692	0.0767	0.0659	0.0798	0.0660
6.7	0.0648	0.0610	0.0678	0.0580	0.0705	0.0585
6.8	0.0576	0.0542	0.0599	0.0516	0.0623	0.0518
6.9	0.0510	0.0482	0.0535	0.0459	0.0556	0.0464
7.0	0.0457	0.0432	0.0477	0.0412	0.0496	0.0415
7.1	0.0410	0.0387	0.0430	0.0370	0.0446	0.0374
7.2	0.0368	0.0347	0.0387	0.0331	0.0402	0.0337
7.3	0.0332	0.0315	0.0348	0.0301	0.0361	0.0304
7.4	0.0301	0.0285	0.0317	0.0273	0.0329	0.0277
7.5	0.0274	0.0259	0.0288	0.0248	0.0300	0.0253
7.6	0.0250	0.0237	0.0263	0.0228	0.0273	0.0230
7.7	0.0229	0.0217	0.0241	0.0209	0.0251	0.0212
7.8	0.0211	0.0199	0.0222	0.0191	0.0230	0.0195
7.9	0.0194	0.0184	0.0204	0.0177	0.0212	0.0179
8.0	0.0179	0.0170	0.0189	0.0163	0.0196	0.0166
8.1	0.0166	0.0157	0.0175	0.0151	0.0181	0.0154
8.2	0.0154	0.0146	0.0162	0.0141	0.0168	0.0143
8.3	0.0143	0.0136	0.0150	0.0131	0.0156	0.0132
8.4	0.0133	0.0126	0.0140	0.0122	0.0145	0.0123
8.5	0.0124	0.0117	0.0131	0.0113	0.0136	0.0115
8.6	0.0116	0.0110	0.0122	0.0106	0.0127	0.0108
8.7	0.0109	0.0103	0.0114	0.0100	0.0118	0.0101
8.8	0.0102	0.0097	0.0107	0.0093	0.0111	0.0095
8.9	0.0096	0.0090	0.0101	0.0087	0.0105	0.0089
9.0	0.0090	0.0085	0.0095	0.0083	0.0098	0.0084
9.1	0.0085	0.0080	0.0090	0.0078	0.0093	0.0079
9.2	0.0080	0.0076	0.0085	0.0073	0.0088	0.0075
9.3	0.0076	0.0072	0.0080	0.0069	0.0083	0.0071
9.4	0.0072	0.0067	0.0076	0.0065	0.0078	0.0067
9.5	0.0068	0.0064	0.0072	0.0062	0.0074	0.0063
9.6	0.0064	0.0061	0.0068	0.0059	0.0070	0.0060
9.7	0.0061	0.0058	0.0064	0.0056	0.0067	0.0057
9.8	0.0058	0.0055	0.0061	0.0053	0.0063	0.0054
9.9	0.0055	0.0052	0.0059	0.0050	0.0060	0.0051

Dimensionless Hydrograph Envelopes for Rainfall Intensity ($t_r / t_e = 5.0$)

t/t_e	$\phi=2$ (High)	$\phi=2$ (Low)	$\phi=4$ (High)	$\phi=4$ (Low)	$\phi=6$ (High)	$\phi=6$ (Low)
0.0	0.0000	0.0000	0.0000	0.0000	0.0000	0.0000
0.1	0.0393	0.0092	0.0584	0.0041	0.0738	0.0020
0.2	0.1020	0.0276	0.1242	0.0057	0.1879	0.0037
0.3	0.2053	0.0622	0.2232	0.0327	0.3452	0.0103
0.4	0.3070	0.1339	0.3856	0.0750	0.4550	0.0366
0.5	0.3998	0.2107	0.5237	0.1117	0.5215	0.1209
0.6	0.4918	0.2956	0.6308	0.2053	0.5736	0.2324
0.7	0.6079	0.4098	0.7147	0.3343	0.6681	0.3606
0.8	0.7173	0.5557	0.7893	0.4850	0.7701	0.4824
0.9	0.8177	0.7045	0.8493	0.6249	0.8545	0.6132
1.0	0.8971	0.8188	0.9210	0.7471	0.9185	0.7006
1.1	0.9556	0.8975	0.9633	0.8583	0.9674	0.8022
1.2	0.9880	0.9505	0.9902	0.9341	1.0010	0.8859
1.3	1.0100	0.9808	1.0220	0.9720	1.0150	0.9522
1.4	1.0240	0.9967	1.0270	0.9934	1.0280	0.9826
1.5	1.0300	1.0040	1.0310	1.0030	1.0300	0.9936
1.6	1.0250	1.0080	1.0350	1.0070	1.0350	1.0000
1.7	1.0200	1.0100	1.0370	1.0070	1.0370	1.0040
1.8	1.0210	1.0110	1.0350	1.0070	1.0260	1.0060
1.9	1.0210	1.0100	1.0250	1.0060	1.0250	1.0080
2.0	1.0210	1.0090	1.0250	1.0040	1.0260	1.0080
2.1	1.0210	1.0090	1.0250	1.0040	1.0260	1.0070
2.2	1.0210	1.0090	1.0250	1.0030	1.0260	1.0070
2.3	1.0210	1.0090	1.0250	1.0030	1.0260	1.0070
2.4	1.0210	1.0090	1.0250	1.0020	1.0260	1.0070
2.5	1.0210	1.0090	1.0250	1.0020	1.0260	1.0070
2.6	1.0210	1.0090	1.0250	1.0020	1.0260	1.0070
2.7	1.0210	1.0090	1.0250	1.0020	1.0260	1.0070
2.8	1.0210	1.0090	1.0250	1.0020	1.0260	1.0070
2.9	1.0210	1.0090	1.0250	1.0020	1.0260	1.0070
3.0	1.0210	1.0090	1.0250	1.0020	1.0260	1.0070
3.1	1.0210	1.0090	1.0250	1.0020	1.0260	1.0070
3.2	1.0210	1.0090	1.0250	1.0020	1.0260	1.0070
3.3	1.0210	1.0090	1.0250	1.0020	1.0260	1.0070
3.4	1.0210	1.0090	1.0250	1.0020	1.0260	1.0070
3.5	1.0210	1.0090	1.0250	1.0020	1.0260	1.0070
3.6	1.0210	1.0090	1.0250	1.0020	1.0260	1.0070
3.7	1.0210	1.0090	1.0250	1.0020	1.0260	1.0070
3.8	1.0210	1.0090	1.0250	1.0020	1.0260	1.0070
3.9	1.0210	1.0090	1.0250	1.0020	1.0260	1.0070
4.0	1.0210	1.0090	1.0250	1.0020	1.0260	1.0070
4.1	1.0210	1.0090	1.0250	1.0020	1.0260	1.0070
4.2	1.0210	1.0090	1.0250	1.0020	1.0260	1.0070
4.3	1.0210	1.0090	1.0250	1.0020	1.0260	1.0070
4.4	1.0210	1.0090	1.0250	1.0020	1.0260	1.0070
4.5	1.0210	1.0090	1.0250	1.0020	1.0260	1.0070
4.6	1.0210	1.0090	1.0250	1.0020	1.0260	1.0070
4.7	1.0210	1.0090	1.0250	1.0020	1.0260	1.0070
4.8	1.0210	1.0090	1.0250	1.0020	1.0260	1.0070
4.9	1.0210	1.0090	1.0250	1.0020	1.0260	1.0070

Dimensionless Hydrograph Envelopes for Rainfall Intensity ($t_r / t_e = 5.0$) - continued

t/t_e	$\phi=2$ (High)	$\phi=2$ (Low)	$\phi=4$ (High)	$\phi=4$ (Low)	$\phi=6$ (High)	$\phi=6$ (Low)
5.0	1.0210	1.0090	1.0250	1.0020	1.0260	1.0070
5.1	0.8906	0.8153	0.9213	0.7878	0.9254	0.7502
5.2	0.7671	0.6626	0.8063	0.6150	0.7935	0.5842
5.3	0.6537	0.5469	0.6873	0.4886	0.6745	0.4771
5.4	0.5511	0.4557	0.5778	0.3958	0.5680	0.4007
5.5	0.4609	0.3821	0.4841	0.3261	0.4740	0.3413
5.6	0.3838	0.3195	0.4028	0.2723	0.3943	0.2924
5.7	0.3195	0.2660	0.3345	0.2298	0.3290	0.2493
5.8	0.2665	0.2232	0.2794	0.1955	0.2764	0.2080
5.9	0.2233	0.1887	0.2356	0.1675	0.2352	0.1750
6.0	0.1881	0.1583	0.1995	0.1430	0.2004	0.1468
6.1	0.1576	0.1353	0.1678	0.1239	0.1693	0.1256
6.2	0.1345	0.1152	0.1434	0.1070	0.1451	0.1072
6.3	0.1144	0.0997	0.1221	0.0931	0.1238	0.0930
6.4	0.0989	0.0861	0.1056	0.0802	0.1072	0.0806
6.5	0.0855	0.0754	0.0911	0.0702	0.0926	0.0708
6.6	0.0750	0.0660	0.0798	0.0613	0.0811	0.0621
6.7	0.0657	0.0584	0.0697	0.0543	0.0709	0.0551
6.8	0.0583	0.0517	0.0617	0.0480	0.0628	0.0489
6.9	0.0518	0.0462	0.0546	0.0429	0.0555	0.0438
7.0	0.0464	0.0413	0.0488	0.0384	0.0496	0.0391
7.1	0.0415	0.0372	0.0436	0.0343	0.0443	0.0350
7.2	0.0372	0.0335	0.0389	0.0311	0.0396	0.0317
7.3	0.0337	0.0302	0.0353	0.0282	0.0358	0.0287
7.4	0.0306	0.0275	0.0319	0.0255	0.0324	0.0259
7.5	0.0277	0.0251	0.0289	0.0234	0.0293	0.0237
7.6	0.0254	0.0229	0.0264	0.0214	0.0268	0.0217
7.7	0.0233	0.0210	0.0242	0.0196	0.0245	0.0199
7.8	0.0213	0.0193	0.0221	0.0181	0.0224	0.0183
7.9	0.0197	0.0178	0.0204	0.0167	0.0207	0.0169
8.0	0.0182	0.0165	0.0189	0.0154	0.0191	0.0156
8.1	0.0168	0.0153	0.0174	0.0143	0.0176	0.0145
8.2	0.0156	0.0142	0.0162	0.0133	0.0163	0.0135
8.3	0.0145	0.0131	0.0150	0.0124	0.0152	0.0125
8.4	0.0135	0.0123	0.0140	0.0115	0.0141	0.0116
8.5	0.0125	0.0115	0.0130	0.0108	0.0131	0.0109
8.6	0.0118	0.0107	0.0121	0.0101	0.0123	0.0102
8.7	0.0110	0.0100	0.0114	0.0095	0.0115	0.0095
8.8	0.0103	0.0094	0.0107	0.0089	0.0108	0.0089
8.9	0.0097	0.0089	0.0100	0.0084	0.0101	0.0084
9.0	0.0091	0.0083	0.0094	0.0079	0.0095	0.0080
9.1	0.0086	0.0078	0.0089	0.0074	0.0089	0.0075
9.2	0.0081	0.0074	0.0084	0.0070	0.0084	0.0071
9.3	0.0076	0.0070	0.0079	0.0066	0.0079	0.0067
9.4	0.0072	0.0066	0.0075	0.0063	0.0075	0.0063
9.5	0.0068	0.0063	0.0071	0.0060	0.0071	0.0060
9.6	0.0065	0.0059	0.0067	0.0056	0.0068	0.0057
9.7	0.0062	0.0057	0.0064	0.0054	0.0064	0.0054
9.8	0.0058	0.0054	0.0060	0.0051	0.0061	0.0051
9.9	0.0055	0.0051	0.0057	0.0049	0.0058	0.0049

Dimensionless Deviation Hydrographs ($t_r / t_e = 0.4$)

t/t_e	Slope $\phi=2$	Slope $\phi=4$	Slope $\phi=6$	Manning's "n" $\phi=2$	Manning's "n" $\phi=4$	Manning's "n" $\phi=6$
0.0	0.0000	0.0000	0.0000	0.0000	0.0000	0.0000
0.1	0.0105	0.0168	0.0222	0.0222	0.0591	0.0719
0.2	0.0212	0.0427	0.0511	0.0538	0.1156	0.1313
0.3	0.0328	0.0675	0.0865	0.0793	0.1531	0.1786
0.4	0.0426	0.0877	0.1231	0.0922	0.1683	0.2151
0.5	0.0390	0.0704	0.1136	0.0666	0.1148	0.1712
0.6	0.0350	0.0585	0.1069	0.0593	0.1005	0.1529
0.7	0.0298	0.0531	0.1002	0.0543	0.0962	0.1368
0.8	0.0252	0.0523	0.0913	0.0487	0.0910	0.1206
0.9	0.0222	0.0514	0.0818	0.0439	0.0833	0.1016
1.0	0.0202	0.0475	0.0726	0.0400	0.0731	0.0820
1.1	0.0183	0.0406	0.0632	0.0360	0.0615	0.0673
1.2	0.0161	0.0329	0.0539	0.0316	0.0513	0.0604
1.3	0.0140	0.0268	0.0460	0.0272	0.0445	0.0589
1.4	0.0134	0.0238	0.0419	0.0238	0.0403	0.0578
1.5	0.0105	0.0210	0.0375	0.0201	0.0383	0.0572
1.6	0.0111	0.0216	0.0374	0.0177	0.0353	0.0537
1.7	0.0083	0.0193	0.0339	0.0153	0.0339	0.0512
1.8	0.0090	0.0197	0.0338	0.0135	0.0305	0.0464
1.9	0.0067	0.0174	0.0302	0.0120	0.0288	0.0433
2.0	0.0072	0.0172	0.0294	0.0105	0.0257	0.0387
2.1	0.0054	0.0151	0.0261	0.0095	0.0240	0.0357
2.2	0.0057	0.0146	0.0249	0.0083	0.0213	0.0319
2.3	0.0044	0.0129	0.0222	0.0076	0.0198	0.0293
2.4	0.0046	0.0123	0.0210	0.0067	0.0177	0.0262
2.5	0.0036	0.0105	0.0185	0.0064	0.0167	0.0245
2.6	0.0029	0.0095	0.0166	0.0058	0.0153	0.0223
2.7	0.0033	0.0095	0.0161	0.0050	0.0134	0.0198
2.8	0.0027	0.0082	0.0144	0.0047	0.0127	0.0185
2.9	0.0023	0.0075	0.0131	0.0044	0.0117	0.0170
3.0	0.0025	0.0074	0.0126	0.0038	0.0104	0.0152
3.1	0.0021	0.0066	0.0114	0.0036	0.0098	0.0143
3.2	0.0018	0.0061	0.0104	0.0034	0.0091	0.0132
3.3	0.0019	0.0059	0.0100	0.0030	0.0082	0.0120
3.4	0.0016	0.0053	0.0091	0.0028	0.0078	0.0113
3.5	0.0015	0.0049	0.0084	0.0027	0.0072	0.0105
3.6	0.0015	0.0048	0.0080	0.0024	0.0066	0.0096
3.7	0.0016	0.0047	0.0077	0.0021	0.0060	0.0087
3.8	0.0013	0.0041	0.0070	0.0021	0.0058	0.0083
3.9	0.0011	0.0038	0.0065	0.0020	0.0055	0.0079
4.0	0.0011	0.0037	0.0062	0.0018	0.0050	0.0073
4.1	0.0012	0.0036	0.0060	0.0016	0.0046	0.0067
4.2	0.0010	0.0033	0.0055	0.0016	0.0045	0.0064
4.3	0.0009	0.0030	0.0051	0.0015	0.0042	0.0061
4.4	0.0009	0.0029	0.0049	0.0014	0.0039	0.0057
4.5	0.0009	0.0029	0.0047	0.0013	0.0037	0.0053
4.6	0.0008	0.0026	0.0044	0.0013	0.0035	0.0051
4.7	0.0007	0.0024	0.0041	0.0012	0.0034	0.0048
4.8	0.0006	0.0023	0.0039	0.0012	0.0032	0.0046
4.9	0.0007	0.0022	0.0037	0.0011	0.0030	0.0043

Dimensionless Deviation Hydrographs ($t_r / t_e = 0.4$)

t/t_e	Width $\phi=2$	Width $\phi=4$	Width $\phi=6$	Rainfall Intensity $\phi=2$	Rainfall Intensity $\phi=4$	Rainfall Intensity $\phi=6$
0.0	0.0000	0.0000	0.0000	0.0000	0.0000	0.0000
0.1	0.0190	0.0435	0.0464	0.0324	0.0589	0.0795
0.2	0.0455	0.0937	0.1092	0.0746	0.1312	0.1616
0.3	0.0745	0.1400	0.1570	0.1170	0.2101	0.2379
0.4	0.0944	0.1787	0.1898	0.1486	0.2694	0.3002
0.5	0.0701	0.1339	0.1583	0.1214	0.2038	0.2353
0.6	0.0562	0.1033	0.1381	0.0975	0.1663	0.1891
0.7	0.0486	0.0885	0.1217	0.0772	0.1529	0.1713
0.8	0.0433	0.0835	0.1125	0.0693	0.1404	0.1655
0.9	0.0403	0.0795	0.1033	0.0704	0.1278	0.1583
1.0	0.0388	0.0748	0.0928	0.0699	0.1163	0.1482
1.1	0.0368	0.0697	0.0831	0.0646	0.1041	0.1335
1.2	0.0337	0.0635	0.0741	0.0564	0.0918	0.1144
1.3	0.0296	0.0561	0.0654	0.0474	0.0800	0.0950
1.4	0.0255	0.0489	0.0568	0.0398	0.0687	0.0786
1.5	0.0208	0.0404	0.0486	0.0319	0.0580	0.0648
1.6	0.0176	0.0347	0.0418	0.0274	0.0493	0.0554
1.7	0.0141	0.0282	0.0354	0.0217	0.0409	0.0463
1.8	0.0121	0.0246	0.0309	0.0192	0.0349	0.0404
1.9	0.0097	0.0201	0.0264	0.0153	0.0289	0.0339
2.0	0.0085	0.0179	0.0234	0.0138	0.0250	0.0299
2.1	0.0069	0.0149	0.0202	0.0111	0.0209	0.0252
2.2	0.0062	0.0135	0.0182	0.0102	0.0183	0.0225
2.3	0.0052	0.0114	0.0159	0.0083	0.0155	0.0192
2.4	0.0047	0.0105	0.0145	0.0077	0.0137	0.0173
2.5	0.0040	0.0090	0.0126	0.0065	0.0121	0.0152
2.6	0.0034	0.0078	0.0113	0.0053	0.0102	0.0129
2.7	0.0032	0.0074	0.0105	0.0052	0.0092	0.0120
2.8	0.0028	0.0065	0.0094	0.0044	0.0082	0.0106
2.9	0.0025	0.0058	0.0085	0.0037	0.0071	0.0092
3.0	0.0024	0.0056	0.0080	0.0036	0.0065	0.0086
3.1	0.0021	0.0049	0.0072	0.0032	0.0059	0.0078
3.2	0.0019	0.0044	0.0066	0.0027	0.0052	0.0069
3.3	0.0018	0.0043	0.0062	0.0027	0.0048	0.0065
3.4	0.0016	0.0038	0.0057	0.0024	0.0044	0.0059
3.5	0.0015	0.0035	0.0053	0.0021	0.0039	0.0053
3.6	0.0014	0.0034	0.0050	0.0020	0.0037	0.0050
3.7	0.0014	0.0033	0.0047	0.0020	0.0035	0.0047
3.8	0.0012	0.0029	0.0043	0.0017	0.0032	0.0043
3.9	0.0011	0.0027	0.0040	0.0015	0.0028	0.0038
4.0	0.0011	0.0026	0.0038	0.0015	0.0027	0.0036
4.1	0.0010	0.0025	0.0036	0.0014	0.0025	0.0035
4.2	0.0009	0.0022	0.0033	0.0013	0.0023	0.0032
4.3	0.0009	0.0021	0.0031	0.0011	0.0021	0.0029
4.4	0.0008	0.0020	0.0030	0.0011	0.0020	0.0028
4.5	0.0008	0.0019	0.0028	0.0011	0.0019	0.0026
4.6	0.0007	0.0018	0.0026	0.0010	0.0018	0.0024
4.7	0.0007	0.0017	0.0025	0.0009	0.0016	0.0022
4.8	0.0006	0.0016	0.0024	0.0008	0.0015	0.0021
4.9	0.0006	0.0015	0.0023	0.0008	0.0014	0.0020

Dimensionless Deviation Hydrographs ($t_r / t_e = 1.0$)

t/t_e	Slope $\phi=2$	Slope $\phi=4$	Slope $\phi=6$	Manning's "n" $\phi=2$	Manning's "n" $\phi=4$	Manning's "n" $\phi=6$
0.0	0.0000	0.0000	0.0000	0.0000	0.0000	0.0000
0.1	0.0024	0.0043	0.0056	0.0050	0.0127	0.0185
0.2	0.0055	0.0098	0.0141	0.0103	0.0208	0.0315
0.3	0.0086	0.0147	0.0230	0.0159	0.0308	0.0430
0.4	0.0107	0.0196	0.0299	0.0201	0.0414	0.0531
0.5	0.0127	0.0247	0.0354	0.0234	0.0494	0.0599
0.6	0.0144	0.0298	0.0417	0.0258	0.0541	0.0639
0.7	0.0144	0.0332	0.0475	0.0262	0.0553	0.0682
0.8	0.0127	0.0331	0.0493	0.0252	0.0539	0.0700
0.9	0.0104	0.0302	0.0468	0.0215	0.0459	0.0614
1.0	0.0078	0.0229	0.0364	0.0172	0.0360	0.0479
1.1	0.0080	0.0172	0.0254	0.0151	0.0280	0.0346
1.2	0.0084	0.0152	0.0207	0.0151	0.0287	0.0337
1.3	0.0083	0.0158	0.0214	0.0149	0.0300	0.0351
1.4	0.0078	0.0162	0.0227	0.0142	0.0296	0.0353
1.5	0.0070	0.0158	0.0229	0.0129	0.0279	0.0343
1.6	0.0061	0.0149	0.0220	0.0116	0.0255	0.0324
1.7	0.0053	0.0136	0.0205	0.0102	0.0230	0.0298
1.8	0.0045	0.0123	0.0188	0.0089	0.0205	0.0271
1.9	0.0039	0.0110	0.0169	0.0078	0.0182	0.0243
2.0	0.0033	0.0091	0.0144	0.0078	0.0172	0.0226
2.1	0.0028	0.0085	0.0136	0.0060	0.0141	0.0192
2.2	0.0023	0.0071	0.0116	0.0058	0.0131	0.0176
2.3	0.0021	0.0067	0.0108	0.0046	0.0109	0.0150
2.4	0.0017	0.0056	0.0093	0.0044	0.0100	0.0137
2.5	0.0016	0.0052	0.0086	0.0036	0.0085	0.0118
2.6	0.0013	0.0045	0.0075	0.0034	0.0078	0.0108
2.7	0.0013	0.0042	0.0070	0.0028	0.0067	0.0094
2.8	0.0010	0.0036	0.0061	0.0026	0.0061	0.0086
2.9	0.0010	0.0034	0.0057	0.0022	0.0053	0.0075
3.0	0.0008	0.0030	0.0051	0.0021	0.0049	0.0069
3.1	0.0008	0.0027	0.0046	0.0018	0.0044	0.0062
3.2	0.0008	0.0026	0.0043	0.0016	0.0038	0.0055
3.3	0.0006	0.0022	0.0039	0.0015	0.0036	0.0051
3.4	0.0006	0.0020	0.0035	0.0014	0.0033	0.0047
3.5	0.0006	0.0019	0.0033	0.0012	0.0029	0.0041
3.6	0.0005	0.0017	0.0030	0.0012	0.0027	0.0039
3.7	0.0005	0.0016	0.0028	0.0010	0.0025	0.0036
3.8	0.0005	0.0015	0.0026	0.0009	0.0022	0.0032
3.9	0.0004	0.0014	0.0024	0.0009	0.0021	0.0030
4.0	0.0004	0.0013	0.0022	0.0008	0.0019	0.0028
4.1	0.0004	0.0012	0.0021	0.0007	0.0018	0.0026
4.2	0.0003	0.0011	0.0019	0.0007	0.0017	0.0024
4.3	0.0003	0.0010	0.0018	0.0007	0.0016	0.0023
4.4	0.0003	0.0010	0.0017	0.0006	0.0015	0.0021
4.5	0.0003	0.0009	0.0016	0.0006	0.0013	0.0019
4.6	0.0002	0.0009	0.0015	0.0005	0.0013	0.0018
4.7	0.0002	0.0008	0.0014	0.0005	0.0012	0.0017
4.8	0.0002	0.0007	0.0013	0.0005	0.0011	0.0016
4.9	0.0002	0.0007	0.0013	0.0004	0.0010	0.0015

Dimensionless Deviation Hydrographs ($t_r / t_e = 1.0$)

t/t_e	Width $\phi=2$	Width $\phi=4$	Width $\phi=6$	Rainfall Intensity $\phi=2$	Rainfall Intensity $\phi=4$	Rainfall Intensity $\phi=6$
0.0	0.0000	0.0000	0.0000	0.0000	0.0000	0.0000
0.1	0.0047	0.0096	0.0102	0.0081	0.0156	0.0170
0.2	0.0105	0.0220	0.0274	0.0210	0.0368	0.0344
0.3	0.0181	0.0361	0.0453	0.0328	0.0551	0.0609
0.4	0.0244	0.0445	0.0580	0.0398	0.0654	0.0836
0.5	0.0274	0.0489	0.0646	0.0429	0.0694	0.0998
0.6	0.0270	0.0496	0.0663	0.0410	0.0706	0.1053
0.7	0.0242	0.0455	0.0633	0.0348	0.0685	0.0951
0.8	0.0202	0.0375	0.0555	0.0292	0.0608	0.0769
0.9	0.0143	0.0279	0.0441	0.0235	0.0478	0.0605
1.0	0.0097	0.0192	0.0298	0.0187	0.0335	0.0455
1.1	0.0146	0.0258	0.0371	0.0263	0.0443	0.0556
1.2	0.0179	0.0313	0.0432	0.0288	0.0482	0.0643
1.3	0.0178	0.0315	0.0431	0.0269	0.0463	0.0635
1.4	0.0160	0.0289	0.0395	0.0233	0.0417	0.0578
1.5	0.0138	0.0252	0.0346	0.0196	0.0361	0.0501
1.6	0.0114	0.0214	0.0294	0.0162	0.0304	0.0424
1.7	0.0093	0.0179	0.0246	0.0133	0.0252	0.0352
1.8	0.0075	0.0148	0.0204	0.0109	0.0206	0.0290
1.9	0.0061	0.0123	0.0169	0.0089	0.0168	0.0240
2.0	0.0052	0.0100	0.0138	0.0081	0.0144	0.0202
2.1	0.0039	0.0084	0.0115	0.0059	0.0111	0.0160
2.2	0.0033	0.0069	0.0094	0.0055	0.0096	0.0135
2.3	0.0026	0.0059	0.0080	0.0040	0.0075	0.0109
2.4	0.0022	0.0049	0.0067	0.0037	0.0065	0.0093
2.5	0.0018	0.0044	0.0059	0.0028	0.0052	0.0076
2.6	0.0015	0.0037	0.0050	0.0026	0.0046	0.0066
2.7	0.0013	0.0033	0.0044	0.0021	0.0038	0.0055
2.8	0.0011	0.0028	0.0038	0.0019	0.0034	0.0048
2.9	0.0010	0.0026	0.0034	0.0015	0.0028	0.0041
3.0	0.0008	0.0022	0.0030	0.0014	0.0025	0.0036
3.1	0.0008	0.0020	0.0027	0.0012	0.0022	0.0032
3.2	0.0007	0.0019	0.0025	0.0010	0.0018	0.0027
3.3	0.0006	0.0016	0.0022	0.0010	0.0017	0.0025
3.4	0.0005	0.0015	0.0020	0.0008	0.0015	0.0022
3.5	0.0005	0.0014	0.0019	0.0007	0.0013	0.0019
3.6	0.0004	0.0012	0.0016	0.0007	0.0012	0.0018
3.7	0.0004	0.0011	0.0015	0.0006	0.0011	0.0016
3.8	0.0004	0.0011	0.0014	0.0005	0.0009	0.0014
3.9	0.0003	0.0010	0.0013	0.0005	0.0009	0.0013
4.0	0.0003	0.0009	0.0012	0.0004	0.0008	0.0012
4.1	0.0003	0.0009	0.0011	0.0004	0.0007	0.0011
4.2	0.0003	0.0008	0.0010	0.0004	0.0007	0.0010
4.3	0.0002	0.0007	0.0009	0.0004	0.0006	0.0009
4.4	0.0002	0.0007	0.0009	0.0003	0.0006	0.0009
4.5	0.0002	0.0006	0.0008	0.0003	0.0005	0.0008
4.6	0.0002	0.0006	0.0008	0.0003	0.0005	0.0007
4.7	0.0002	0.0005	0.0007	0.0003	0.0005	0.0007
4.8	0.0002	0.0005	0.0007	0.0002	0.0004	0.0006
4.9	0.0002	0.0005	0.0007	0.0002	0.0004	0.0006

Dimensionless Deviation Hydrographs ($t_r / t_e = 5.0$)

t/t_e	Slope $\phi=2$	Slope $\phi=4$	Slope $\phi=6$	Manning's "n" $\phi=2$	Manning's "n" $\phi=4$	Manning's "n" $\phi=6$
0.0	0.0000	0.0000	0.0000	0.0000	0.0000	0.0000
0.1	0.0021	0.0041	0.0047	0.0047	0.0103	0.0160
0.2	0.0052	0.0102	0.0122	0.0097	0.0207	0.0267
0.3	0.0080	0.0163	0.0205	0.0138	0.0310	0.0410
0.4	0.0108	0.0210	0.0298	0.0180	0.0407	0.0524
0.5	0.0134	0.0250	0.0386	0.0214	0.0483	0.0596
0.6	0.0146	0.0287	0.0455	0.0232	0.0530	0.0638
0.7	0.0141	0.0318	0.0493	0.0234	0.0532	0.0652
0.8	0.0124	0.0329	0.0490	0.0223	0.0498	0.0634
0.9	0.0107	0.0317	0.0462	0.0185	0.0396	0.0520
1.0	0.0082	0.0256	0.0368	0.0137	0.0287	0.0380
1.1	0.0066	0.0199	0.0294	0.0095	0.0183	0.0240
1.2	0.0058	0.0154	0.0236	0.0075	0.0097	0.0119
1.3	0.0104	0.0173	0.0226	0.0098	0.0092	0.0096
1.4	0.0060	0.0096	0.0123	0.0075	0.0068	0.0067
1.5	0.0030	0.0046	0.0061	0.0061	0.0056	0.0053
1.6	0.0012	0.0017	0.0033	0.0040	0.0048	0.0046
1.7	0.0006	0.0012	0.0030	0.0028	0.0033	0.0041
1.8	0.0009	0.0019	0.0032	0.0026	0.0031	0.0039
1.9	0.0012	0.0024	0.0036	0.0019	0.0032	0.0040
2.0	0.0014	0.0026	0.0039	0.0018	0.0034	0.0041
2.1	0.0015	0.0028	0.0041	0.0018	0.0034	0.0042
2.2	0.0015	0.0028	0.0041	0.0019	0.0035	0.0043
2.3	0.0015	0.0029	0.0042	0.0019	0.0035	0.0043
2.4	0.0015	0.0029	0.0042	0.0019	0.0035	0.0043
2.5	0.0015	0.0029	0.0042	0.0019	0.0035	0.0043
2.6	0.0015	0.0029	0.0042	0.0020	0.0035	0.0043
2.7	0.0015	0.0029	0.0042	0.0020	0.0035	0.0043
2.8	0.0015	0.0029	0.0042	0.0020	0.0035	0.0043
2.9	0.0015	0.0029	0.0042	0.0020	0.0035	0.0043
3.0	0.0015	0.0029	0.0042	0.0020	0.0035	0.0043
3.1	0.0015	0.0029	0.0042	0.0020	0.0035	0.0043
3.2	0.0015	0.0029	0.0042	0.0020	0.0035	0.0043
3.3	0.0015	0.0029	0.0042	0.0020	0.0035	0.0043
3.4	0.0015	0.0029	0.0042	0.0020	0.0035	0.0043
3.5	0.0015	0.0029	0.0042	0.0020	0.0035	0.0043
3.6	0.0015	0.0029	0.0042	0.0020	0.0035	0.0043
3.7	0.0015	0.0029	0.0042	0.0020	0.0035	0.0043
3.8	0.0015	0.0029	0.0042	0.0020	0.0035	0.0043
3.9	0.0015	0.0029	0.0042	0.0020	0.0035	0.0043
4.0	0.0015	0.0029	0.0042	0.0020	0.0035	0.0043
4.1	0.0015	0.0029	0.0042	0.0020	0.0035	0.0043
4.2	0.0015	0.0029	0.0042	0.0020	0.0035	0.0043
4.3	0.0015	0.0029	0.0042	0.0020	0.0035	0.0043
4.4	0.0015	0.0029	0.0042	0.0020	0.0035	0.0043
4.5	0.0015	0.0029	0.0042	0.0020	0.0035	0.0043
4.6	0.0015	0.0029	0.0042	0.0020	0.0035	0.0043
4.7	0.0015	0.0029	0.0042	0.0020	0.0035	0.0043
4.8	0.0015	0.0029	0.0042	0.0020	0.0035	0.0043
4.9	0.0015	0.0029	0.0042	0.0020	0.0035	0.0043

Dimensionless Deviation Hydrographs ($t_r / t_e = 5.0$) - continued

t/t_e	Slope $\phi=2$	Slope $\phi=4$	Slope $\phi=6$	Manning's "n" $\phi=2$	Manning's "n" $\phi=4$	Manning's "n" $\phi=6$
5.0	0.0015	0.0029	0.0042	0.0020	0.0035	0.0043
5.1	0.0049	0.0103	0.0151	0.0072	0.0175	0.0224
5.2	0.0064	0.0127	0.0185	0.0107	0.0243	0.0321
5.3	0.0066	0.0134	0.0197	0.0120	0.0268	0.0355
5.4	0.0061	0.0132	0.0193	0.0119	0.0269	0.0357
5.5	0.0053	0.0126	0.0182	0.0111	0.0256	0.0343
5.6	0.0045	0.0116	0.0168	0.0100	0.0236	0.0320
5.7	0.0038	0.0106	0.0153	0.0089	0.0214	0.0292
5.8	0.0032	0.0095	0.0138	0.0078	0.0191	0.0264
5.9	0.0028	0.0085	0.0123	0.0068	0.0170	0.0236
6.0	0.0024	0.0071	0.0102	0.0070	0.0159	0.0218
6.1	0.0020	0.0066	0.0098	0.0052	0.0132	0.0184
6.2	0.0016	0.0055	0.0082	0.0052	0.0121	0.0169
6.3	0.0015	0.0052	0.0078	0.0040	0.0102	0.0144
6.4	0.0012	0.0044	0.0066	0.0039	0.0093	0.0131
6.5	0.0011	0.0041	0.0062	0.0031	0.0080	0.0113
6.6	0.0009	0.0035	0.0054	0.0030	0.0073	0.0103
6.7	0.0009	0.0033	0.0051	0.0024	0.0063	0.0090
6.8	0.0007	0.0028	0.0044	0.0023	0.0058	0.0082
6.9	0.0007	0.0026	0.0041	0.0019	0.0051	0.0072
7.0	0.0006	0.0023	0.0037	0.0018	0.0046	0.0066
7.1	0.0006	0.0021	0.0033	0.0016	0.0042	0.0059
7.2	0.0006	0.0020	0.0032	0.0014	0.0036	0.0052
7.3	0.0004	0.0017	0.0028	0.0013	0.0034	0.0049
7.4	0.0004	0.0016	0.0026	0.0012	0.0031	0.0044
7.5	0.0005	0.0015	0.0024	0.0010	0.0028	0.0040
7.6	0.0003	0.0013	0.0022	0.0010	0.0026	0.0037
7.7	0.0004	0.0012	0.0020	0.0009	0.0024	0.0034
7.8	0.0004	0.0012	0.0019	0.0008	0.0021	0.0031
7.9	0.0003	0.0011	0.0018	0.0008	0.0020	0.0029
8.0	0.0003	0.0010	0.0016	0.0007	0.0019	0.0027
8.1	0.0003	0.0010	0.0016	0.0006	0.0017	0.0025
8.2	0.0002	0.0009	0.0014	0.0006	0.0016	0.0023
8.3	0.0002	0.0008	0.0013	0.0006	0.0015	0.0022
8.4	0.0002	0.0007	0.0012	0.0005	0.0014	0.0020
8.5	0.0002	0.0007	0.0012	0.0005	0.0013	0.0018
8.6	0.0002	0.0007	0.0011	0.0005	0.0012	0.0018
8.7	0.0002	0.0006	0.0010	0.0004	0.0011	0.0017
8.8	0.0002	0.0006	0.0010	0.0004	0.0011	0.0015
8.9	0.0002	0.0006	0.0009	0.0004	0.0010	0.0014
9.0	0.0001	0.0005	0.0009	0.0004	0.0009	0.0014
9.1	0.0001	0.0005	0.0008	0.0003	0.0009	0.0013
9.2	0.0001	0.0005	0.0008	0.0003	0.0008	0.0012
9.3	0.0001	0.0004	0.0007	0.0003	0.0008	0.0011
9.4	0.0001	0.0004	0.0007	0.0003	0.0007	0.0011
9.5	0.0001	0.0004	0.0007	0.0003	0.0007	0.0010
9.6	0.0001	0.0004	0.0006	0.0003	0.0007	0.0010
9.7	0.0001	0.0004	0.0006	0.0002	0.0006	0.0009
9.8	0.0001	0.0003	0.0006	0.0002	0.0006	0.0009
9.9	0.0001	0.0003	0.0006	0.0002	0.0006	0.0008

Dimensionless Deviation Hydrographs ($t_r / t_e = 5.0$)

t/t_e	Width $\phi=2$	Width $\phi=4$	Width $\phi=6$	Rainfall Intensity $\phi=2$	Rainfall Intensity $\phi=4$	Rainfall Intensity $\phi=6$
0.0	0.0000	0.0000	0.0000	0.0000	0.0000	0.0000
0.1	0.0045	0.0080	0.0101	0.0070	0.0128	0.0156
0.2	0.0101	0.0200	0.0239	0.0189	0.0267	0.0357
0.3	0.0155	0.0306	0.0393	0.0298	0.0463	0.0568
0.4	0.0194	0.0403	0.0511	0.0363	0.0674	0.0732
0.5	0.0223	0.0476	0.0603	0.0387	0.0830	0.0814
0.6	0.0241	0.0507	0.0653	0.0390	0.0863	0.0809
0.7	0.0236	0.0494	0.0634	0.0373	0.0776	0.0746
0.8	0.0211	0.0442	0.0550	0.0329	0.0636	0.0644
0.9	0.0170	0.0368	0.0430	0.0266	0.0492	0.0525
1.0	0.0117	0.0259	0.0292	0.0188	0.0345	0.0379
1.1	0.0089	0.0189	0.0204	0.0133	0.0228	0.0262
1.2	0.0084	0.0151	0.0154	0.0103	0.0155	0.0184
1.3	0.0122	0.0163	0.0166	0.0130	0.0147	0.0161
1.4	0.0072	0.0088	0.0089	0.0081	0.0086	0.0085
1.5	0.0038	0.0046	0.0056	0.0051	0.0068	0.0060
1.6	0.0025	0.0036	0.0054	0.0030	0.0064	0.0060
1.7	0.0017	0.0034	0.0059	0.0025	0.0065	0.0060
1.8	0.0018	0.0038	0.0062	0.0027	0.0065	0.0060
1.9	0.0020	0.0042	0.0058	0.0030	0.0059	0.0062
2.0	0.0022	0.0044	0.0052	0.0032	0.0059	0.0064
2.1	0.0023	0.0046	0.0050	0.0033	0.0059	0.0065
2.2	0.0024	0.0046	0.0050	0.0034	0.0060	0.0066
2.3	0.0024	0.0047	0.0051	0.0034	0.0060	0.0066
2.4	0.0024	0.0047	0.0051	0.0034	0.0060	0.0066
2.5	0.0024	0.0047	0.0052	0.0034	0.0060	0.0066
2.6	0.0024	0.0047	0.0052	0.0034	0.0061	0.0066
2.7	0.0024	0.0047	0.0052	0.0034	0.0061	0.0066
2.8	0.0024	0.0047	0.0052	0.0034	0.0061	0.0066
2.9	0.0024	0.0047	0.0052	0.0034	0.0061	0.0066
3.0	0.0024	0.0047	0.0052	0.0034	0.0061	0.0066
3.1	0.0024	0.0047	0.0052	0.0034	0.0061	0.0066
3.2	0.0024	0.0047	0.0052	0.0034	0.0061	0.0066
3.3	0.0024	0.0047	0.0052	0.0034	0.0061	0.0066
3.4	0.0024	0.0047	0.0052	0.0034	0.0061	0.0066
3.5	0.0024	0.0047	0.0052	0.0034	0.0061	0.0066
3.6	0.0024	0.0047	0.0052	0.0034	0.0061	0.0066
3.7	0.0024	0.0047	0.0052	0.0034	0.0061	0.0066
3.8	0.0024	0.0047	0.0052	0.0034	0.0061	0.0066
3.9	0.0024	0.0047	0.0052	0.0034	0.0061	0.0066
4.0	0.0024	0.0047	0.0052	0.0034	0.0061	0.0066
4.1	0.0024	0.0047	0.0052	0.0034	0.0061	0.0066
4.2	0.0024	0.0047	0.0052	0.0034	0.0061	0.0066
4.3	0.0024	0.0047	0.0052	0.0034	0.0061	0.0066
4.4	0.0024	0.0047	0.0052	0.0034	0.0061	0.0066
4.5	0.0024	0.0047	0.0052	0.0034	0.0061	0.0066
4.6	0.0024	0.0047	0.0052	0.0034	0.0061	0.0066
4.7	0.0024	0.0047	0.0052	0.0034	0.0061	0.0066
4.8	0.0024	0.0047	0.0052	0.0034	0.0061	0.0066
4.9	0.0024	0.0047	0.0052	0.0034	0.0061	0.0066

Dimensionless Deviation Hydrographs ($t_r / t_e = 5.0$) - continued

t/t_e	Width $\phi=2$	Width $\phi=4$	Width $\phi=6$	Rainfall Intensity $\phi=2$	Rainfall Intensity $\phi=4$	Rainfall Intensity $\phi=6$
5.0	0.0024	0.0047	0.0052	0.0034	0.0061	0.0066
5.1	0.0087	0.0189	0.0233	0.0160	0.0298	0.0321
5.2	0.0113	0.0234	0.0296	0.0195	0.0389	0.0387
5.3	0.0119	0.0235	0.0302	0.0191	0.0394	0.0371
5.4	0.0112	0.0213	0.0279	0.0172	0.0358	0.0327
5.5	0.0098	0.0184	0.0243	0.0149	0.0307	0.0277
5.6	0.0083	0.0153	0.0204	0.0125	0.0255	0.0230
5.7	0.0068	0.0126	0.0168	0.0104	0.0209	0.0189
5.8	0.0055	0.0102	0.0137	0.0086	0.0170	0.0155
5.9	0.0044	0.0083	0.0111	0.0070	0.0137	0.0126
6.0	0.0039	0.0067	0.0090	0.0065	0.0119	0.0110
6.1	0.0028	0.0055	0.0073	0.0047	0.0090	0.0084
6.2	0.0024	0.0045	0.0060	0.0044	0.0079	0.0074
6.3	0.0018	0.0038	0.0050	0.0032	0.0061	0.0057
6.4	0.0016	0.0031	0.0041	0.0030	0.0054	0.0051
6.5	0.0012	0.0027	0.0036	0.0023	0.0042	0.0040
6.6	0.0011	0.0023	0.0030	0.0021	0.0038	0.0036
6.7	0.0009	0.0020	0.0027	0.0016	0.0030	0.0029
6.8	0.0008	0.0017	0.0023	0.0015	0.0027	0.0026
6.9	0.0006	0.0016	0.0021	0.0012	0.0023	0.0022
7.0	0.0006	0.0014	0.0019	0.0011	0.0021	0.0020
7.1	0.0005	0.0012	0.0017	0.0009	0.0018	0.0018
7.2	0.0005	0.0012	0.0016	0.0007	0.0015	0.0015
7.3	0.0004	0.0010	0.0014	0.0008	0.0014	0.0013
7.4	0.0003	0.0009	0.0013	0.0006	0.0012	0.0012
7.5	0.0003	0.0009	0.0012	0.0005	0.0010	0.0010
7.6	0.0003	0.0008	0.0011	0.0005	0.0010	0.0010
7.7	0.0003	0.0007	0.0010	0.0005	0.0009	0.0009
7.8	0.0003	0.0007	0.0009	0.0004	0.0008	0.0008
7.9	0.0002	0.0006	0.0008	0.0004	0.0007	0.0007
8.0	0.0002	0.0006	0.0008	0.0003	0.0006	0.0007
8.1	0.0002	0.0005	0.0007	0.0003	0.0006	0.0006
8.2	0.0002	0.0005	0.0007	0.0003	0.0005	0.0005
8.3	0.0002	0.0004	0.0006	0.0003	0.0005	0.0005
8.4	0.0001	0.0004	0.0006	0.0002	0.0005	0.0005
8.5	0.0001	0.0004	0.0006	0.0002	0.0004	0.0004
8.6	0.0001	0.0004	0.0005	0.0002	0.0004	0.0004
8.7	0.0001	0.0003	0.0005	0.0002	0.0004	0.0004
8.8	0.0001	0.0003	0.0005	0.0002	0.0003	0.0003
8.9	0.0001	0.0003	0.0004	0.0002	0.0003	0.0003
9.0	0.0001	0.0003	0.0004	0.0002	0.0003	0.0003
9.1	0.0001	0.0003	0.0004	0.0002	0.0003	0.0003
9.2	0.0001	0.0003	0.0004	0.0001	0.0003	0.0003
9.3	0.0001	0.0003	0.0004	0.0001	0.0002	0.0002
9.4	0.0001	0.0002	0.0004	0.0001	0.0002	0.0002
9.5	0.0001	0.0002	0.0003	0.0001	0.0002	0.0002
9.6	0.0001	0.0002	0.0003	0.0001	0.0002	0.0002
9.7	0.0001	0.0002	0.0003	0.0001	0.0002	0.0002
9.8	0.0001	0.0002	0.0003	0.0001	0.0002	0.0002
9.9	0.0001	0.0002	0.0003	0.0001	0.0002	0.0002

Values of R_s for various values of t_r / t_e

t_r / t_e	Slope	Manning's "n"	Width	Rainfall Intensity	Slope-Manning's "n"
0.4	0.0615	0.1133	0.1165	0.1872	0.1410
0.6	0.0546	0.1106	0.0919	0.1467	0.1348
0.8	0.0478	0.0887	0.0820	0.1454	0.1039
1.0	0.0385	0.0826	0.0752	0.1212	0.0947
1.1	0.0361	0.0686	0.0715	0.1156	0.0769
1.2	0.0412	0.0591	0.0584	0.0979	0.0708
1.3	0.0320	0.0640	0.0558	0.0881	0.0740
1.4	0.0295	0.0598	0.0581	0.0953	0.0659
1.5	0.0317	0.0565	0.0473	0.0779	0.0642
1.8	0.0235	0.0479	0.0438	0.0730	0.0575
2.0	0.0204	0.0368	0.0389	0.0635	0.0507
2.5	0.0191	0.0332	0.0361	0.0497	0.0386
3.0	0.0145	0.0271	0.0287	0.0424	0.0296
4.0	0.0122	0.0212	0.0211	0.0328	0.0263
5.0	0.0095	0.0200	0.0167	0.0289	0.0212

Values of V^* for various values of t_r / t_e

t_r / t_e	Slope	Manning's "n"	Width	Rainfall Intensity	Slope-Manning's "n"
0.4	0.0220	0.0411	0.0428	0.0675	0.0510
0.6	0.0200	0.0410	0.0329	0.0519	0.0495
0.8	0.0178	0.0326	0.0292	0.0550	0.0385
1.0	0.0137	0.0294	0.0275	0.0440	0.0350
1.1	0.0128	0.0249	0.0264	0.0424	0.0286
1.2	0.0150	0.0217	0.0212	0.0353	0.0257
1.3	0.0120	0.0233	0.0205	0.0320	0.0270
1.4	0.0107	0.0221	0.0214	0.0351	0.0240
1.5	0.0113	0.0208	0.0177	0.0280	0.0239
1.8	0.0087	0.0173	0.0159	0.0269	0.0209
2.0	0.0073	0.0134	0.0140	0.0238	0.0186
2.5	0.0069	0.0122	0.0131	0.0184	0.0141
3.0	0.0053	0.0097	0.0102	0.0155	0.0106
4.0	0.0045	0.0077	0.0077	0.0121	0.0095
5.0	0.0034	0.0070	0.0062	0.0106	0.0076

Values of C_v for various values of t_r / t_e

t_r / t_e	Slope	Manning's "n"	Width	Rainfall Intensity	Slope-Manning's "n"
0.4	0.3587	0.3627	0.3674	0.3606	0.3619
0.6	0.3670	0.3708	0.3586	0.3534	0.3670
0.8	0.3722	0.3682	0.3558	0.3786	0.3701
1.0	0.3568	0.3556	0.3662	0.3629	0.3694
1.1	0.3543	0.3627	0.3698	0.3670	0.3719
1.2	0.3650	0.3663	0.3636	0.3603	0.3629
1.3	0.3746	0.3644	0.3671	0.3636	0.3652
1.4	0.3633	0.3692	0.3687	0.3682	0.3646
1.5	0.3554	0.3675	0.3736	0.3598	0.3716
1.8	0.3704	0.3613	0.3624	0.3687	0.3633
2.0	0.3563	0.3652	0.3606	0.3754	0.3674
2.5	0.3620	0.3677	0.3613	0.3694	0.3646
3.0	0.3635	0.3575	0.3564	0.3648	0.3575
4.0	0.3715	0.3625	0.3630	0.3696	0.3629
5.0	0.3587	0.3504	0.3730	0.3669	0.3595

Dimensionless Peak Distributions for Slope

Probability	t_r/t_e=0.3	t_r/t_e=0.4	t_r/t_e=0.8	t_r/t_e=1.0	t_r/t_e=1.3	t_r/t_e=2.0
0.0196	0.9199	0.9428	0.9138	0.9449	0.9792	0.9973
0.0392	0.9493	0.9541	0.9175	0.9481	0.9824	0.9980
0.0588	0.9586	0.9544	0.9194	0.9574	0.9827	0.9994
0.0784	0.9668	0.9568	0.9216	0.9590	0.9827	1.0000
0.0980	0.9686	0.9570	0.9261	0.9627	0.9830	1.0000
0.1176	0.9774	0.9639	0.9286	0.9643	0.9840	1.0010
0.1373	0.9799	0.9656	0.9321	0.9672	0.9841	1.0010
0.1569	0.9822	0.9701	0.9338	0.9678	0.9845	1.0010
0.1765	0.9839	0.9707	0.9338	0.9678	0.9850	1.0010
0.1961	0.9886	0.9765	0.9350	0.9694	0.9852	1.0020
0.2157	0.9966	0.9786	0.9365	0.9697	0.9852	1.0020
0.2353	0.9977	0.9797	0.9476	0.9716	0.9864	1.0020
0.2549	0.9998	0.9801	0.9481	0.9727	0.9878	1.0020
0.2745	1.0000	0.9802	0.9489	0.9730	0.9889	1.0020
0.2941	1.0050	0.9817	0.9516	0.9746	0.9890	1.0030
0.3137	1.0080	0.9847	0.9550	0.9750	0.9892	1.0030
0.3333	1.0120	0.9861	0.9560	0.9755	0.9894	1.0030
0.3529	1.0180	0.9870	0.9575	0.9770	0.9895	1.0030
0.3725	1.0210	0.9898	0.9622	0.9772	0.9896	1.0030
0.3922	1.0230	0.9965	0.9652	0.9772	0.9903	1.0030
0.4118	1.0240	0.9979	0.9656	0.9773	0.9908	1.0030
0.4314	1.0250	0.9997	0.9662	0.9774	0.9914	1.0030
0.4510	1.0260	1.0000	0.9664	0.9783	0.9916	1.0030
0.4706	1.0270	1.0030	0.9671	0.9788	0.9922	1.0030
0.4902	1.0270	1.0040	0.9685	0.9790	0.9929	1.0040
0.5098	1.0270	1.0050	0.9689	0.9809	0.9929	1.0040
0.5294	1.0370	1.0060	0.9778	0.9817	0.9936	1.0040
0.5490	1.0390	1.0110	0.9788	0.9823	0.9941	1.0040
0.5686	1.0400	1.0140	0.9792	0.9825	0.9941	1.0040
0.5882	1.0460	1.0180	0.9798	0.9838	0.9942	1.0050
0.6078	1.0520	1.0190	0.9824	0.9851	0.9945	1.0050
0.6275	1.0540	1.0200	0.9843	0.9853	0.9946	1.0050
0.6471	1.0550	1.0280	0.9858	0.9862	0.9951	1.0050
0.6667	1.0580	1.0290	0.9870	0.9866	0.9953	1.0060
0.6863	1.0590	1.0330	0.9871	0.9877	0.9954	1.0060
0.7059	1.0600	1.0340	0.9879	0.9879	0.9956	1.0060
0.7255	1.0600	1.0350	0.9915	0.9888	0.9960	1.0070
0.7451	1.0610	1.0410	0.9917	0.9891	0.9962	1.0070
0.7647	1.0680	1.0450	0.9931	0.9908	0.9965	1.0080
0.7843	1.0720	1.0470	0.9954	0.9921	0.9967	1.0080
0.8039	1.0790	1.0480	0.9967	0.9928	0.9973	1.0090
0.8235	1.0850	1.0540	0.9979	0.9935	0.9977	1.0090
0.8431	1.0980	1.0570	0.9984	0.9952	0.9979	1.0090
0.8627	1.0980	1.0640	1.0000	0.9956	0.9984	1.0100
0.8824	1.1030	1.0680	1.0010	0.9973	0.9987	1.0100
0.9020	1.1030	1.0800	1.0040	0.9977	0.9990	1.0140
0.9216	1.1110	1.0850	1.0040	0.9994	1.0000	1.0150
0.9412	1.1260	1.0940	1.0050	0.9997	1.0010	1.0160
0.9608	1.1940	1.1200	1.0050	1.0000	1.0010	1.0160
0.9804	1.2310	1.1340	1.0140	1.0010	1.0010	1.0190

Dimensionless Peak Distributions for Manning's "n"

Probability	t_r/t_e=0.3	t_r/t_e=0.4	t_r/t_e=0.8	t_r/t_e=1.0	t_r/t_e=1.3	t_r/t_e=2.0
0.0196	1.0000	0.9377	0.9469	0.9787	0.9819	0.9942
0.0392	1.0310	0.9544	0.9628	0.9822	0.9833	0.9951
0.0588	1.0560	0.9825	0.9629	0.9831	0.9852	0.9962
0.0784	1.0860	0.9924	0.9630	0.9853	0.9874	0.9966
0.0980	1.0860	1.0000	0.9689	0.9857	0.9901	0.9977
0.1176	1.0930	1.0110	0.9704	0.9861	0.9904	0.9986
0.1373	1.1060	1.0180	0.9859	0.9872	0.9905	0.9988
0.1569	1.1080	1.0230	0.9871	0.9876	0.9919	0.9989
0.1765	1.1180	1.0360	0.9882	0.9891	0.9925	0.9998
0.1961	1.1370	1.0370	0.9882	0.9903	0.9925	1.0000
0.2157	1.1540	1.0370	0.9887	0.9939	0.9932	1.0000
0.2353	1.1580	1.0420	0.9891	0.9956	0.9945	1.0000
0.2549	1.1610	1.0460	0.9892	0.9985	0.9948	1.0010
0.2745	1.1620	1.0580	0.9912	1.0000	0.9951	1.0020
0.2941	1.1620	1.0640	0.9992	1.0010	0.9964	1.0020
0.3137	1.1680	1.0650	1.0000	1.0010	0.9971	1.0020
0.3333	1.1730	1.0720	1.0020	1.0010	0.9973	1.0030
0.3529	1.1730	1.0910	1.0030	1.0050	0.9984	1.0030
0.3725	1.1780	1.0910	1.0070	1.0050	0.9986	1.0030
0.3922	1.1830	1.0930	1.0100	1.0070	1.0000	1.0030
0.4118	1.1850	1.0940	1.0120	1.0070	1.0000	1.0040
0.4314	1.1880	1.0960	1.0130	1.0080	1.0010	1.0040
0.4510	1.1950	1.1060	1.0140	1.0110	1.0020	1.0050
0.4706	1.2050	1.1090	1.0160	1.0110	1.0020	1.0060
0.4902	1.2110	1.1120	1.0210	1.0110	1.0020	1.0060
0.5098	1.2160	1.1170	1.0250	1.0120	1.0020	1.0060
0.5294	1.2160	1.1190	1.0250	1.0190	1.0020	1.0060
0.5490	1.2160	1.1310	1.0250	1.0230	1.0030	1.0070
0.5686	1.2220	1.1370	1.0270	1.0230	1.0040	1.0070
0.5882	1.2220	1.1440	1.0280	1.0240	1.0040	1.0080
0.6078	1.2230	1.1520	1.0290	1.0270	1.0050	1.0090
0.6275	1.2260	1.1570	1.0350	1.0270	1.0050	1.0090
0.6471	1.2320	1.1690	1.0440	1.0280	1.0050	1.0090
0.6667	1.2320	1.1810	1.0500	1.0330	1.0060	1.0100
0.6863	1.2330	1.1920	1.0510	1.0350	1.0070	1.0100
0.7059	1.2490	1.1940	1.0520	1.0360	1.0070	1.0110
0.7255	1.2530	1.1960	1.0530	1.0370	1.0070	1.0110
0.7451	1.2550	1.2090	1.0590	1.0400	1.0070	1.0110
0.7647	1.2580	1.2110	1.0590	1.0410	1.0080	1.0120
0.7843	1.2600	1.2210	1.0600	1.0410	1.0080	1.0120
0.8039	1.2920	1.2260	1.0600	1.0410	1.0090	1.0120
0.8235	1.3010	1.2490	1.0710	1.0420	1.0090	1.0120
0.8431	1.3610	1.2630	1.0780	1.0440	1.0090	1.0130
0.8627	1.3810	1.2650	1.0790	1.0450	1.0100	1.0130
0.8824	1.4100	1.2650	1.0890	1.0470	1.0100	1.0140
0.9020	1.4440	1.2790	1.0980	1.0480	1.0110	1.0140
0.9216	1.4600	1.3110	1.1100	1.0510	1.0110	1.0140
0.9412	1.4950	1.3250	1.1180	1.0520	1.0110	1.0160
0.9608	1.5180	1.3980	1.1260	1.0550	1.0120	1.0180
0.9804	1.7510	1.4120	1.1400	1.0680	1.0130	1.0180

Dimensionless Peak Distributions for Width

Probability	t_r/t_e=0.3	t_r/t_e=0.4	t_r/t_e=0.8	t_r/t_e=1.0	t_r/t_e=1.3	t_r/t_e=2.0
0.0196	0.9540	0.9194	0.8650	0.9514	0.9763	0.9947
0.0392	0.9684	0.9497	0.9151	0.9517	0.9764	0.9955
0.0588	0.9836	0.9666	0.9218	0.9536	0.9781	0.9962
0.0784	0.9943	0.9708	0.9230	0.9556	0.9817	0.9970
0.0980	1.0000	0.9754	0.9269	0.9645	0.9837	0.9972
0.1176	1.0050	0.9821	0.9279	0.9656	0.9868	0.9978
0.1373	1.0050	0.9903	0.9379	0.9716	0.9894	0.9983
0.1569	1.0080	0.9921	0.9436	0.9748	0.9903	1.0000
0.1765	1.0080	0.9961	0.9464	0.9791	0.9908	1.0010
0.1961	1.0170	1.0000	0.9512	0.9791	0.9911	1.0010
0.2157	1.0260	1.0040	0.9538	0.9795	0.9917	1.0010
0.2353	1.0280	1.0100	0.9580	0.9831	0.9921	1.0020
0.2549	1.0310	1.0140	0.9585	0.9836	0.9927	1.0020
0.2745	1.0410	1.0180	0.9674	0.9850	0.9928	1.0040
0.2941	1.0480	1.0200	0.9679	0.9882	0.9930	1.0040
0.3137	1.0520	1.0220	0.9689	0.9890	0.9931	1.0040
0.3333	1.0630	1.0310	0.9703	0.9898	0.9932	1.0050
0.3529	1.0690	1.0380	0.9715	0.9904	0.9937	1.0060
0.3725	1.0700	1.0520	0.9725	0.9929	0.9939	1.0060
0.3922	1.0710	1.0520	0.9734	0.9935	0.9941	1.0060
0.4118	1.0710	1.0540	0.9832	0.9946	0.9951	1.0070
0.4314	1.0770	1.0670	0.9927	0.9950	0.9958	1.0070
0.4510	1.0790	1.0680	0.9944	0.9952	0.9959	1.0070
0.4706	1.0900	1.0760	0.9962	0.9956	0.9961	1.0080
0.4902	1.0910	1.0830	0.9967	0.9959	0.9967	1.0080
0.5098	1.0950	1.0920	0.9972	0.9965	0.9975	1.0090
0.5294	1.0990	1.0980	0.9974	0.9974	0.9982	1.0090
0.5490	1.1040	1.1040	0.9980	0.9977	0.9982	1.0100
0.5686	1.1070	1.1040	1.0000	0.9985	0.9984	1.0110
0.5882	1.1240	1.1100	1.0000	0.9993	0.9987	1.0110
0.6078	1.1280	1.1120	1.0010	1.0000	0.9991	1.0110
0.6275	1.1400	1.1140	1.0020	1.0000	0.9992	1.0110
0.6471	1.1440	1.1250	1.0060	1.0010	0.9995	1.0130
0.6667	1.1460	1.1260	1.0070	1.0010	1.0000	1.0130
0.6863	1.1530	1.1380	1.0140	1.0020	1.0010	1.0130
0.7059	1.1810	1.1460	1.0140	1.0030	1.0020	1.0130
0.7255	1.2010	1.1500	1.0170	1.0040	1.0020	1.0130
0.7451	1.2200	1.1540	1.0180	1.0060	1.0020	1.0140
0.7647	1.2360	1.1660	1.0260	1.0060	1.0030	1.0140
0.7843	1.2520	1.1830	1.0290	1.0060	1.0030	1.0140
0.8039	1.2580	1.1850	1.0300	1.0070	1.0040	1.0140
0.8235	1.2650	1.1940	1.0320	1.0090	1.0050	1.0150
0.8431	1.2760	1.2080	1.0410	1.0110	1.0050	1.0150
0.8627	1.2810	1.2140	1.0420	1.0120	1.0050	1.0160
0.8824	1.2960	1.2150	1.0540	1.0130	1.0060	1.0180
0.9020	1.3040	1.2290	1.0590	1.0160	1.0070	1.0200
0.9216	1.3040	1.2580	1.0610	1.0220	1.0070	1.0210
0.9412	1.3110	1.2600	1.0650	1.0260	1.0070	1.0210
0.9608	1.3840	1.3150	1.0710	1.0270	1.0150	1.0210
0.9804	1.5180	1.4390	1.0940	1.0300	1.0180	1.0220

Dimensionless Peak Distributions for Rainfall Intensity

Probability	t_r/t_e=0.3	t_r/t_e=0.4	t_r/t_e=0.8	t_r/t_e=1.0	t_r/t_e=1.3	t_r/t_e=2.0
0.0196	0.9732	0.8662	0.8088	0.8606	0.9518	0.9942
0.0392	1.0000	0.9132	0.8216	0.8942	0.9678	0.9953
0.0588	1.0270	0.9466	0.8599	0.8955	0.9701	0.9967
0.0784	1.0340	0.9470	0.8733	0.9005	0.9725	0.9984
0.0980	1.0440	0.9718	0.8814	0.9127	0.9749	0.9985
0.1176	1.0740	1.0000	0.8935	0.9310	0.9751	0.9986
0.1373	1.0770	1.0130	0.8951	0.9362	0.9756	0.9998
0.1569	1.0780	1.0150	0.8954	0.9379	0.9761	0.9999
0.1765	1.0890	1.0170	0.8961	0.9449	0.9854	1.0000
0.1961	1.1130	1.0240	0.9051	0.9508	0.9856	1.0000
0.2157	1.1170	1.0280	0.9056	0.9520	0.9868	1.0000
0.2353	1.1700	1.0300	0.9263	0.9561	0.9874	1.0030
0.2549	1.1860	1.0500	0.9350	0.9580	0.9876	1.0040
0.2745	1.1920	1.0620	0.9370	0.9604	0.9880	1.0050
0.2941	1.2080	1.0710	0.9403	0.9618	0.9882	1.0050
0.3137	1.2140	1.0740	0.9430	0.9620	0.9907	1.0060
0.3333	1.2190	1.0770	0.9517	0.9680	0.9907	1.0060
0.3529	1.2240	1.0810	0.9541	0.9684	0.9916	1.0070
0.3725	1.2260	1.0970	0.9584	0.9691	0.9918	1.0090
0.3922	1.2290	1.0970	0.9597	0.9730	0.9933	1.0090
0.4118	1.2330	1.1050	0.9711	0.9733	0.9941	1.0100
0.4314	1.2370	1.1110	0.9736	0.9739	0.9943	1.0120
0.4510	1.2500	1.1140	0.9788	0.9759	0.9959	1.0130
0.4706	1.2750	1.1230	0.9831	0.9815	0.9963	1.0130
0.4902	1.2820	1.1310	0.9833	0.9835	0.9977	1.0130
0.5098	1.2830	1.1460	0.9841	0.9892	0.9988	1.0130
0.5294	1.3250	1.1490	0.9877	0.9902	0.9988	1.0160
0.5490	1.3410	1.1580	0.9903	0.9908	0.9990	1.0160
0.5686	1.3410	1.1610	1.0000	0.9977	0.9993	1.0160
0.5882	1.3610	1.1720	1.0010	1.0000	1.0000	1.0170
0.6078	1.3700	1.1870	1.0030	1.0000	1.0000	1.0170
0.6275	1.3710	1.1880	1.0090	1.0040	1.0000	1.0170
0.6471	1.4010	1.1950	1.0110	1.0040	1.0000	1.0180
0.6667	1.4070	1.2020	1.0150	1.0080	1.0010	1.0190
0.6863	1.4170	1.2100	1.0220	1.0130	1.0010	1.0190
0.7059	1.4330	1.2140	1.0240	1.0150	1.0030	1.0190
0.7255	1.4380	1.2200	1.0250	1.0190	1.0050	1.0210
0.7451	1.4390	1.2350	1.0370	1.0200	1.0060	1.0220
0.7647	1.4390	1.2430	1.0370	1.0230	1.0060	1.0220
0.7843	1.4410	1.2610	1.0380	1.0240	1.0060	1.0230
0.8039	1.4440	1.2650	1.0410	1.0240	1.0070	1.0230
0.8235	1.4650	1.3040	1.0640	1.0250	1.0070	1.0230
0.8431	1.4780	1.3050	1.0820	1.0280	1.0080	1.0260
0.8627	1.5120	1.3070	1.0910	1.0320	1.0120	1.0260
0.8824	1.5830	1.3320	1.1400	1.0320	1.0140	1.0270
0.9020	1.6070	1.3390	1.1450	1.0350	1.0150	1.0270
0.9216	1.6130	1.4520	1.1600	1.0480	1.0160	1.0280
0.9412	1.6230	1.7380	1.1630	1.0570	1.0170	1.0280
0.9608	1.6720	1.7720	1.2120	1.0570	1.0220	1.0280
0.9804	1.7880	2.0370	1.2450	1.0690	1.0360	1.0500